

**DEVELOPMENT AND ANALYSIS OF
DUAL FREQUENCY MICROSTRIP ANTENNAS**

Thesis submitted by
MANJU PAULSON

*In partial fulfilment of the
requirements for the degree of
Doctor of Philosophy
under the Faculty of Technology*

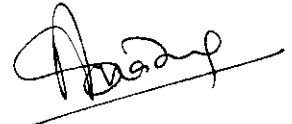
**DEPARTMENT OF ELECTRONICS
COCHIN UNIVERSITY OF SCIENCE AND TECHNOLOGY
COCHIN 682 022, INDIA**

MAY 2002

Dedicated to my daughter

CERTIFICATE

This is to certify that this thesis entitled “**DEVELOPMENT AND ANALYSIS OF DUAL FREQUENCY MICROSTRIP ANTENNAS**” is a bona fide record of the research work carried out by Ms. Manju Paulson, under my supervision in the Department of Electronics, Cochin University of Science and Technology. The result presented in this thesis or parts of it have not been presented for any other degree.



Dr. C. K. Aanandan
(Supervising Teacher)
Reader

Cochin 682 022
31st May 2002

Department of Electronics
Cochin University of Science and Technology

DECLARATION

I hereby declare that the work presented in this thesis entitled “**DEVELOPMENT AND ANALYSIS OF DUAL FREQUENCY MICROSTRIP ANTENNAS**” is based on the original work done by me under the supervision of **Dr. C. K. Aanandan** in the Department of Electronics, Cochin University of science and Technology, and that no part thereof has been presented for any other degree.

COCHIN 682 022

31st MAY 2002

Manju Paulson
MANJU PAULSON

ACKNOWLEDGEMENTS

I would like to express my sincere gratitude and indebtedness to Dr. C.K. Aanandan, Reader, Department of Electronics, Cochin University of Science and Technology whose valuable guidance and constant encouragement were indispensable for the progress and completion of the thesis. It has been really a great privilege to work under him.

Let me thank Dr. K. G. Balakrishnan, Professor & Head, Department of Electronics, Cochin University of Science and Technology for his wholehearted support during my research work.

I am also happy to express my sincere thanks to former Heads of The Department, Prof. P.R.S. Pillai and Prof. C. S. Sridhar (presently, Principal, SBMS Institute of Technology, Bangalore) for their support and interest shown in my work.

I would like to thank Prof. K. G. Nair, Director, STIC, CUSAT, for his valuable support and suggestions for the successful completion of my research work.

I am obliged to Dr. P. Mohanan, Professor, Department of Electronics, for his constant encouragement and information imparted. I also thank him for his timely suggestions and discussions, which helped me to complete significant part of my work.

It is with great pleasure I thank my colleague and friend Ms. Sona O Kundukulam, Research Scholar, Dept. of Electronics, for her cooperation for the successful completion of some of the combined investigations.

In the course of my work I have been enjoying a Junior Research fellowship of Cochin University of Science and Technology and Senior Research Fellowship of Council of Scientific and Industrial Research, Govt.. of India. The financial supports provided are gratefully acknowledged.

I also take this opportunity to record my sincere thanks to Prof. K. Vasudevan and Prof. K.T. Mathew for their consistent support and cooperation extended. I would also like to express my sincere thanks to all the teaching staff in Department of Electronics, CUSAT for their wholehearted support and encouragements.

In this context I also remember the supports of Dr. Jacob George, Corning Inc., USA, Dr. Joe Jacob, Research Associate, Dept. of Electronics, CUSAT, Dr. Sebastian Mathew. Lecturer, K.E. College, Mannanam, Dr. V. P. Joseph, Sr. Lecturer, Christ College, Irinjalakuda, Prof. V. P. Devassia, Model Engg. College, Thrikkakara, Dr. Thomaskutty Mathew, M. G. University Regional Centre, Edapilly, Mr. Cyriac M. Odackal, Lecturer, Dept. of Electronics, Dr. K. K. Narayanan, Lecturer, SD College Alappuzha and Mr. Paul V John, Scientist, STIC for the successful completion of my Ph.D programme.

My words are boundless to thank my colleagues in the department, Mr. Biju Kumar, Mr. Binoy G.S., Mr. Mani T.K., Ms. Mini M.G., Ms. Mridula. M, Ms. Binu Paul, Ms. Sree Devi, Ms. Latha Kumari, Mr. Shabeer Ali, Dr. C. P. Anil Kumar, Mr. Sajith N Pai, Mr. Prakash Kumar, Mr. Binu George, Mr. Anil Lonappan, Mr. Jayaram, Dr. Jaimon Yohannan; Librarians Dr. Beena C., Dept. of Physics, Mr. Suresh, Department of Electronics, all other office/technical staff of Department of Electronics and all my well wishers for their co-operation and help extended to me during my work.

MANJU PAULSON

Contents

Chapter 1

| | |
|---|-----------|
| INTRODUCTION | 1 |
| 1.1 PRINTED STRUCTURES | 2 |
| 1.2 WAVES IN MICROSTRIP STRUCTURES | 2 |
| 1.3 MICROSTRIP ANTENNA | 4 |
| 1.3.1 Radiation Fields of Microstrip Antennas | 4 |
| 1.3.2 Advantages and Disadvantages | 6 |
| 1.3.3 Applications | 6 |
| 1.4 EXCITATION TECHNIQUES | 7 |
| 1.4.1 Coaxial Feed | 7 |
| 1.4.2 Microstrip Feed | 8 |
| 1.4.3 Proximity Coupled Feed | 8 |
| 1.4.4 Aperture Coupled Feed | 8 |
| 1.5 SUBSTRATE MATERIALS | 10 |
| 1.6 MICROSTRIP ANTENNA CONFIGURATIONS | 11 |
| 1.6.1 Microstrip Patch Antennas | 11 |
| 1.6.2 Microstrip Travelling Wave Antennas | 11 |
| 1.6.3 Microstrip Slot Antennas | 11 |
| 1.7 BASIC CHARACTERISTICS OF RECTANGULAR PATCHES | 13 |
| 1.7.1 Magnetic Current Distribution | 13 |
| 1.7.2 Radiation Pattern | 13 |
| 1.7.3 Directivity and Gain | 15 |
| 1.8 SIMULATION TECHNIQUES | 15 |
| 1.9 OUTLINE OF THE PRESENT WORK | 15 |
| 1.10 CHAPTER ORGANIZATION | 16 |

Chapter 2

| | |
|--|-----------|
| BRIEF REVIEW OF THE PAST WORK | 18 |
| 2.1 DEVELOPMENT OF MICROSTRIP ANTENNAS | 19 |
| 2.2 COMPACT DUAL FREQUENCY MICROSTRIP ANTENNAS | 23 |
| 2.3 BROADBAND MICROSTRIP ANTENNA | 30 |

Chapter 3

| | |
|---|-----------|
| METHODOLOGY :- EXPERIMENTAL SETUP, MEASUREMENT AND SIMULATION TECHNIQUES | 36 |
| 3.1 BASIC FACILITIES USED | 37 |
| 3.1.1 Network Analyzer | 37 |
| 3.1.2 Anechoic Chamber | 37 |
| 3.2 FABRICATION OF MICROSTRIP ANTENNA | 39 |
| 3.2.1 Fast Fabrication Process | 39 |
| 3.2.2 Excitation Techniques | 39 |
| 3.3 MEASUREMENT OF RETURN LOSS, RESONANT FREQUENCY AND BANDWIDTH | 41 |
| 3.4 MEASUREMENT OF RADIATION PATTERN | 41 |
| 3.5 MEASUREMENT OF GAIN | 43 |
| 3.6 MEASUREMENT OF AXIAL RATIO FOR CIRCULARLY POLARIZED FREQUENCY BAND | 45 |
| 3.7 MEASUREMENT OF RETURN LOSS AND RADIATION PATTERN USING IE3D SIMULATION SOFTWARE | 45 |

Chapter 4

| | |
|---|-----------|
| EXPERIMENTAL RESULTS AND OBSERVATIONS | 52 |
| 4.1 ARROW SHAPED COAXIALLY FED PATCH ANTENNA FOR DUAL FREQUENCY OPERATION | 53 |
| 4.1.1 GEOMETRY | 53 |
| 4.1.2 EXCITATION TECHNIQUES | 53 |
| 4.1.3 RESONANT MODES OF THE ARROW SHAPED ANTENNA | 55 |

| | | |
|---------|--|----|
| 4.1.3.1 | Variation with Intruding Triangle Height ' W_{cd} ' of the Patch | 55 |
| 4.1.3.2 | Variation with Protruding Triangle Height ' W_{cp} ' of the Patch | 55 |
| 4.1.3.3 | Resonant Frequency Variation With Length ' L ' Of the Patch | 59 |
| 4.1.3.4 | Effect of Patch Width ' W ' | 59 |
| 4.1.3.5 | Effect of Varying Height ' h ' And Permittivity ' ϵ_r ' of the Substrate | 59 |
| 4.1.4 | IE3D SIMULATION | 63 |
| 4.1.5 | TYPICAL ANTENNA DESIGN AND STUDY ON ITS CHARACTERISTICS | 67 |
| 4.1.5.1 | Impedance Bandwidth | 67 |
| 4.1.5.2 | Radiation Pattern | 67 |
| 4.1.5.3 | Gain | 70 |
| 4.1.5.4 | Compactness | 70 |
| 4.1.6 | FREQUENCY RATIO TUNING | 72 |
| 4.2 | ELECTROMAGNETICALLY COUPLED ARROW SHAPED MICROSTRIP ANTENNA | 73 |
| 4.2.1 | POLARIZATION DIVERSITY | 74 |
| 4.2.1.1 | Circularly Polarized Radiator-Antenna Design and Experimental Results | 77 |
| 4.2.1.2 | Dual Frequency Design: One Linear Polarization and Other Circular Polarization | 81 |
| 4.3 | SLOT LOADED ARROW SHAPED MICROSTRIP ANTENNA | 85 |
| 4.3.1 | ARROW SHAPED ANTENNA WITH A SINGLE RECTANGULAR SLOT | 85 |
| 4.3.1.1 | Antenna Geometry | 86 |
| 4.3.1.2 | Experimental Results | 86 |
| 4.3.1.3 | Discussion on the Resonant Modes and its Variation with Different Antenna Parameters | 90 |
| 4.3.2 | ARROW SHAPED ANTENNA WITH SLOTS ON ITS RADIATING EDGES | 93 |
| 4.3.2.1 | Antenna Geometry | 93 |
| 4.3.2.2 | Typical Antenna Design And Experimental Results | 94 |
| 4.3.3 | ARROW SHAPED ANTENNA WITH SLOTS ON ITS NON RADIATING EDGES FOR BANDWIDTH ENHANCEMENT | 98 |
| 4.3.3.1 | Antenna Geometry | 99 |
| 4.3.3.2 | Antenna Design and Experimental Results | 99 |

| | |
|--|------------|
| 4.3.3.3 Discussion on the Effect of Various Slot Parameters on Resonant Mode Frequencies | 100 |
| 4.4 DUAL PORT ARROW SHAPED ANTENNA | 108 |
| 4.4.1 ANTENNA DESIGN AND EXPERIMENTAL RESULTS | 108 |
| Chapter 5 | |
| THEORETICAL INTERPRETATION AND DESIGN EQUATIONS | 114 |
| 5.1 INTRODUCTION | 115 |
| 5.2 RESONANT FREQUENCIES OF A RECTANGULAR MICROSTRIP PATCH | 115 |
| 5.3 RESONANT FREQUENCIES OF ARROW SHAPED MICROSTRIP PATCH | 121 |
| 5.3.1 COAXIALLY FED ARROW SHAPED MICROSTRIP ANTENNA | 121 |
| 5.3.1.1 Comparison Between Theoretical And Experimental Results | 124 |
| 5.3.2 ELECTROMAGNETICALLY COUPLED DUAL PORT ARROW SHAPED MICROSTRIP ANTENNA | 131 |
| 5.4 VERIFICATION OF RESONANT MODES USING IE3D | 135 |
| 5.5 MODE VERIFICATION FOR SLOTTED GEOMETRIES | 138 |
| Chapter 6 | |
| CONCLUSIONS | 142 |
| Appendix A | |
| DUAL FREQUENCY DUAL PORT CRESCENT SHAPED MICROSTRIP ANTENNA | 148 |
| Appendix B | |
| COMPACT CIRCULAR SIDED MICROSTRIP ANTENNA | 154 |
| Appendix C | |
| DRUM SHAPED ANTENNA FOR DUAL FREQUENCY DUAL POLARIZATION OPERATION AND CIRCULAR POLARIZATION | 161 |
| REFERENCES | 169 |
| INDEX | 185 |
| LIST OF PUBLICATIONS OF THE CANDIDATE | 187 |
| RESUME OF THE CANDIDATE | 189 |

Antennas are like electronic eyes and ears; our links to the world and the space beyond. In a wireless communication system they act as interface between space and circuitry. Although some antennas like the dipole and loop have changed little since Hertz invented them, many new types have been developed and resulted in an antenna family of great diversity. The recent explosion in commercial applications involving RF and microwave systems is fueling customer demand for small, low-cost, easy-to-use systems. Microstrip antennas are thin printed-circuit antennas that allow transmission and reception of electromagnetic energy using a planar structure.

The concept of microstrip radiators was first proposed by Deschamps as early as 1953. Howell and Munson developed the first practical antennas in the early 1970's. Microstrip antennas due to the diverse range of applications are now established as a separate topic in their own right within the broad field of microwave antennas.

Microstrip antennas popularity stems from the fact that the structure is "planar" in configuration and enjoys all the advantages of printed circuit technology. It is essentially a printed circuit board with all the power dividers, matching networks, phasing circuits and radiators, photo etched on one side of the board. The other side of the board is a metallic ground plane and thus the system can be directly attached to a metallic surface on an aircraft or missile.

The future demand for microstrip antennas is expected to escalate because of market growth in mobile satellite communications, cellular telephone networks, direct broadcast television, wireless local area networks and intelligent vehicle highway systems.

1.1 PRINTED STRUCTURES

The need to replace bulky, heavy and difficult to manufacture waveguide structures was one of the main motivations for the endeavors, which lead to the invention of printed structures. Printed structures are made of one or several dielectric layers with metallic traces printed on. Early structures back in the 1950's were essentially triplate or strip lines with one thin metallic strip enclosed by two dielectric layers with metallisations on the outside as shown in Figure 1.1 (a). Subsequently, other line structures were invented: microstrip lines (Figure 1.1(b)) where one of the dielectric layers was removed, slotlines (Figure 1.1(c)) where only one side of the dielectric is metallised and coplanar wave-guides as a symmetric slotline (Figure 1.1(d)). Other enclosed lines are the suspended line (Figure 1.1(e)), the inverted line (Figure 1.1(f)), and the finline (Figure 1.1(g)). Each type has its own advantages and disadvantages; today the most widely used type is probably the microstrip line. This line is comparatively easy to manufacture and has a low weight.

1.2 WAVES IN MICROSTRIP STRUCTURES

Depending on the actual structure, four wave types can exist in a planar structure: space waves, surface waves, leaky waves, and guided waves as shown in Figure 1.2. If the structure is to be used as an antenna, most of the energy has to be converted into space wave. For transmission lines, most of the energy should be held in a guided wave. The other two wave types, the surface and the leaky wave represent mostly losses. Guided waves (A) are confined in the dielectric layer between two metallisations. Space Waves (B) are transmitted upward in an angle θ_{sw} between 0 and $\Pi/2$. Leaky Waves (C) originate from waves transmitted from the top layer to the ground plane at an angle θ_{lw} smaller than the critical angle $\theta_{lim} = \sin^{-1}(1/\epsilon_r)$. After being reflected from the ground plane, they are partially reflected by the dielectric-air interface, but some energy leaks out of the substrate (hence leaky waves). Surface waves (D), are waves directed slightly downward

from the top layer at an angle θ_{sw} larger than θ_{lim} . They are totally reflected by the dielectric-air interface (total reflection condition). The fields are trapped in the dielectric layer (the waves in optical fibres are the best known surface waves), however can cause unwanted interaction (crosstalk) or degradation of the radiation pattern by being diffracted and reflected at the edges of the dielectric layer.

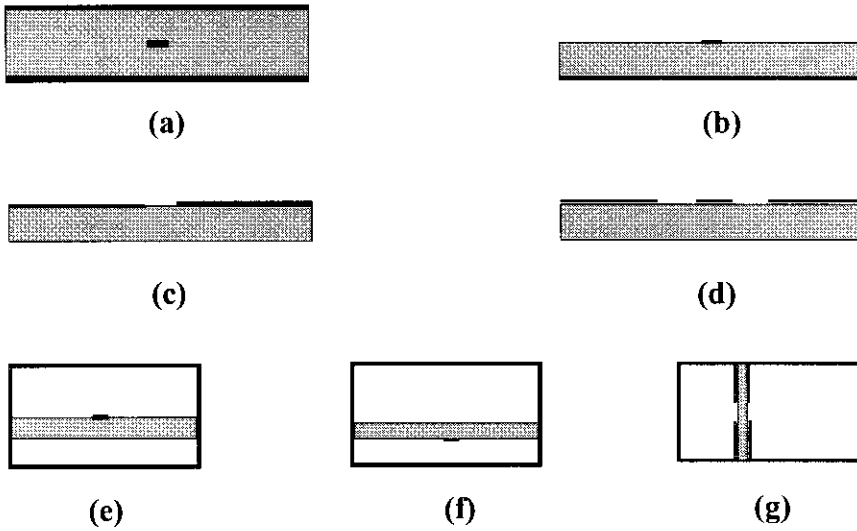


Figure 1.1 Various printed line types (a) Stripline (b) Microstrip line (c) Slotline (d) Coplanar line (e) Suspended line (f) Inverted line (g) Finline

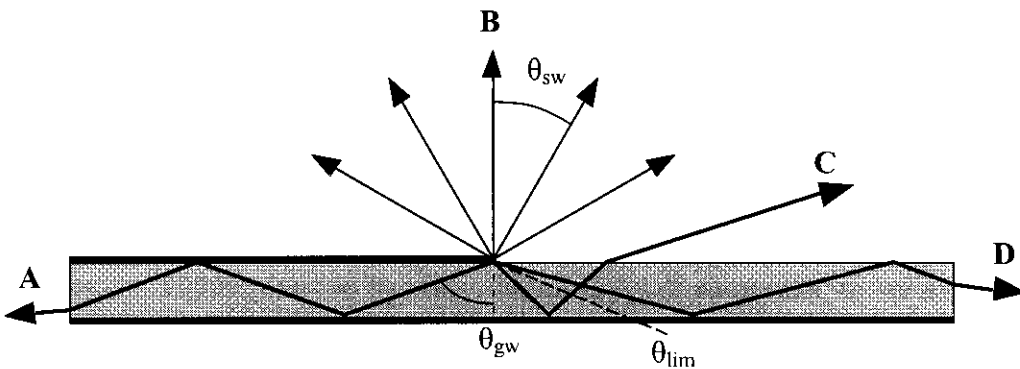


Figure 1.2 Waves in Microstrip structures (A) Guided Waves (B) Space Waves (C) Leaky Waves (D) Surface Waves

1.3 MICROSTRIP ANTENNA

Microstrip antenna consists of a planar radiating structure over a ground plane separated by an electrically thin layer of dielectric substrate as shown in Figure 1.3. The patch conductors can assume virtually any shape but conventional shapes are generally used to simplify analysis and performance prediction. The dielectric constant ϵ_r of the substrate should be low so as to enhance the fringe fields, which account for the radiation.

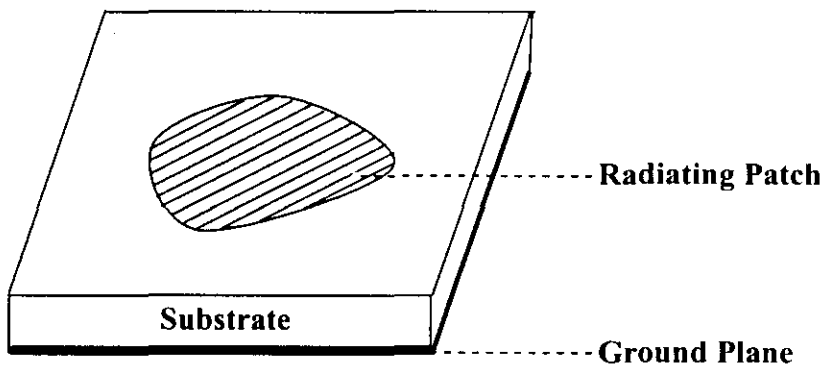


Figure 1.3 Microstrip Antenna Configurations

1.3.1 Radiation fields of microstrip antennas

Radiation from microstrip antennas can be understood by considering the simple case of a rectangular microstrip patch spaced a small fraction of a wavelength above a ground plane as shown in Figure 1.4 (a). Assuming no variations of the electric field along the width and thickness of the microstrip structure, the electric field configuration of the radiator can be represented as shown in Figure 1.4 (b). The fields vary along the patch length, which is about half a wavelength ($\lambda/2$). Radiation is mainly due to the fringing fields at the open circuited edges of the

patch. The fields at the end can be resolved into normal and tangential components with respect to the ground plane. Since the patch is $\lambda/2$ long the normal components are out of phase and the far field produced by them cancels in the broad side direction. The tangential components are in phase and the resulting fields combine to give maximum radiated field normal to the surface of the structure. Therefore the patch may be represented by two slots half wavelength apart excited in phase and radiating in the half space above the ground plane.

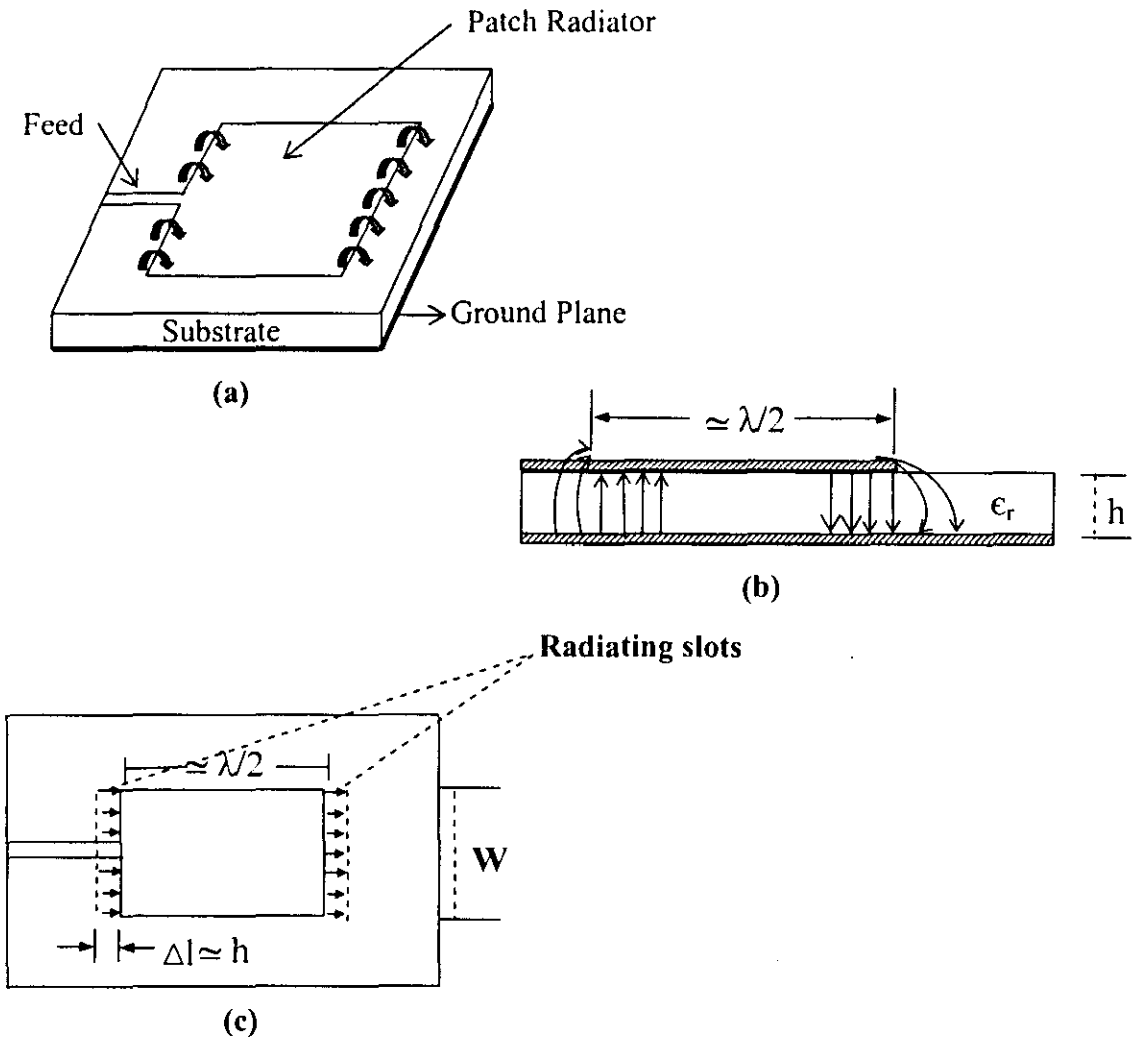


Figure 1.4 (a) Rectangular Microstrip Patch Antenna (b) Side View (c) Top View

1.3.2 Advantages and Disadvantages

Microstrip antennas are compatible with microwave integrated circuits. The solid state circuits such as oscillators, phase shifters etc. and the feedlines and matching networks can be directly added to the antenna structure. They have low weight and low volume. Their low profile planar nature helps to make these antennas conformal with the body of the systems such as rockets, satellites and missiles so that they can be mounted without much alteration to the parent body. Linear and circular polarizations are possible by adjusting the antenna parameters, feeding networks or by placing shorting pins at appropriate points. Dual frequency microstrip antenna can be easily produced by cutting slots or stubs, using shorting pins, loading of reactive components etc.

Microstrip antennas suffer from some drawbacks, which limit their application in certain specified areas. The most serious disadvantage is the narrow impedance bandwidth, which is only of the order of a few percent. The power handling capacity is lower than that of conventional microwave antennas; the gain is very low; the isolation between the radiator and the feed element is also poor.

1.3.3 Applications

Some notable applications for which microstrip antennas have been developed include:

- Satellite Communication
- Doppler Radars
- Missile Telemetry
- Remote sensing
- Biomedical Radiator
- Phased Array Radars

Present applications of this technology are growing most rapidly in the commercial sector also. While specifications for defense and space application antennas typically emphasize maximum performance with little constraint on cost, commercial applications demand low cost components, often at the expense of reduced electrical performance. Some of the commercial systems that presently use microstrip antennas are listed in the table below:

| Application | Frequency |
|--------------------------------|---------------------------------|
| Global Positioning System | 1575 MHz and 1227 MHz |
| Paging | 931-932 MHz |
| Cellular Phone | 824-849 MHz and 869.895 MHz |
| Personal Communication Systems | 1.85-1.99 GHz and 2.18-2.20 GHz |
| GSM | 890-915 MHz and 935-960 MHz |
| Wireless Local Area networks | 2.40-2.48 GHz and 5.4 GHz |
| Cellular Video | 28 GHz |
| Direct Broadcast Satellite | 11.7-12.5 GHz |
| Automatic Toll Collection | 905 MHz and 5-6 GHz |
| Collision Avoidance Radar | 60 GHz, 77 GHz, and 94 GHz |
| Wide Area Computer Networks | 60 GHz |

1.4 EXCITATION TECHNIQUES

The feed has the task to couple the electromagnetic wave propagating on a transmission line to the radiating element as efficiently as possible. The antenna input impedance is greatly controlled by the location of the feed point. The variation of feed location may produce a small shift in resonant frequency, but radiation pattern remains unaltered.

1.4.1 Coaxial feed

Here the outer conductor is connected to the ground plane and the centre conductor is connected to the patch as shown in Figure 1.5 (a). Due to the non-

monolithic structure, however, the fabrication is more difficult than with planar feeding methods. Furthermore, the spurious radiation of the probe is in some cases unacceptable.

1.4.2 Microstrip feed

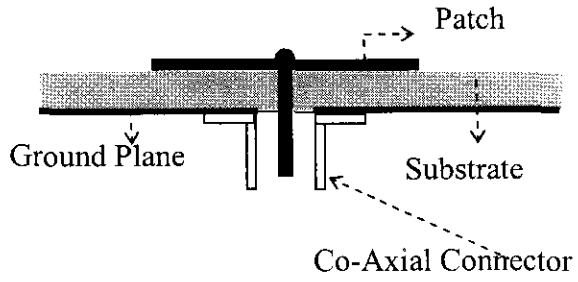
Easier to fabricate than the coaxial feed, the edge (Figure 1.5 (b)) and the inset feed (Figure 1.5 (c)) has the advantage that the whole antenna including the feed is one piece, the structure is monolithic. Especially at high frequencies, the spurious radiation from the feed line can degrade the radiation efficiency and the radiation pattern. The inset feed allows some control over the impedance, at the cost of increased spurious radiation.

1.4.3 Proximity Coupled feed

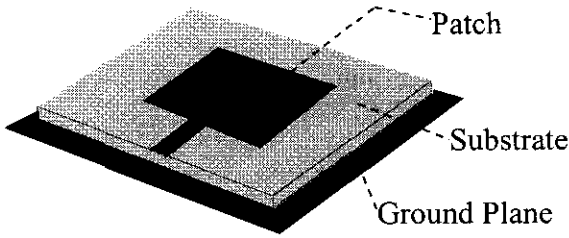
This feed is also called electromagnetic (EM) coupled feed, as the EM energy is coupled by placing the feed and the radiating element in close interaction with no conducting connection. This is achieved by placing an additional substrate with the radiating element on top of the feed line as shown in Figure 1.5 (d). By doing so, the spurious radiation of the feed can be reduced so that the radiation pattern is less affected by the feed.

1.4.4 Aperture Coupled feed

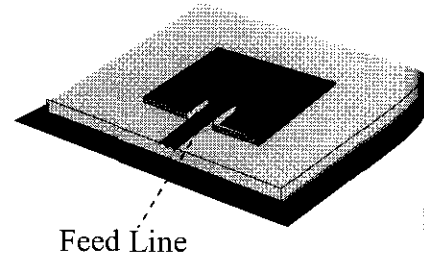
The spurious radiation of the feed can be completely shielded by using an aperture coupled antenna. The antenna is mounted on the other side of the ground plane of the feed; the EM energy is coupled through an aperture to the patch as shown in Figure 1.5 (e).



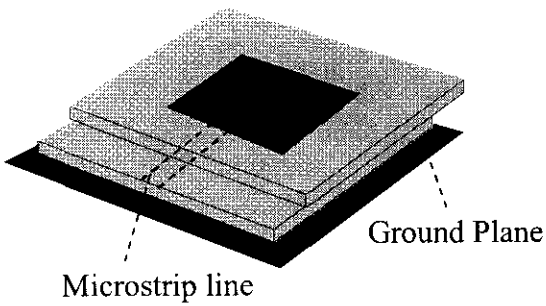
(a) Coaxial feed



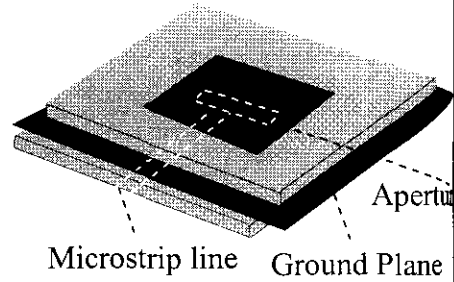
(b) Microstrip edge feed



(c) Microstrip Inset Feed



(d) Proximity Coupling



(e) Aperture Coupling

Figure 1.5 Microstrip antenna feeding

1.5 SUBSTRATE MATERIALS

Choice of the substrate materials depends on the application. Conformal antennas require flexible substrates; low frequency antennas require high dielectric constant substrates to reduce the size of the antenna.

Substrate choice and evaluation is an essential part of the design procedure. Properties like dielectric constant (ϵ_r) and loss tangent ($\tan \delta$) and their variation with temperature and frequency, dimensional stability with processing, thickness uniformity of the substrate, thermal coefficient and temperature range must be involved in these considerations.

A large range of substrate materials is available in the market with dielectric constants ranging from 1.17 to 25 and loss tangents from 0.0001 to 0.004. Earlier microstrip antennas used plastic substrates or in some cases alumina, but in recent years the use of low permittivity substrate is most common. This reduces the surface wave effects but feeder radiation is then more difficult to suppress.

The substrate dielectric constant, loss tangent and dimensions are functions of temperature. So in the design of antennas for use in high speed missiles, rockets etc., the changes in ϵ_r and $\tan \delta$ with temperature should be known. This is important because the bandwidth is narrow. Dielectric constant and loss tangent also vary with frequency. The change in ϵ_r is very small but $\tan \delta$ varies much with frequency. So, for higher frequencies substrate with low losses are developed.

Substrate technology thus offers a challenge to material manufacturers to create low-cost high-performance stable substrates.

1.6 MICROSTRIP ANTENNA CONFIGURATIONS

Microstrip antennas can be divided into three basic categories: microstrip patch antennas, microstrip traveling wave antennas, and microstrip slot antennas. Their characteristics are discussed below.

1.6.1 Microstrip Patch Antennas

A microstrip patch antenna consists of a conducting patch of any planar geometry on one side of a dielectric substrate backed by a ground plane on the other side. Various microstrip patch configurations are shown in Figure 1.6.

1.6.2 Microstrip Traveling Wave Antennas

Microstrip Traveling Wave Antennas consists of chain shaped periodic conductors or an ordinary long TEM line which also supports a TE mode, on a substrate backed by a ground plane. The open end of the TEM line is terminated in a matched resistive load. As antenna supports traveling waves, their structures may be designed so that the main beam lies in any direction from broadside to endfire. Various configurations are shown in Figure 1.7.

1.6.3 Microstrip Slot Antennas

Microstrip slot antenna comprises of a slot in the ground plane fed by a microstrip line. The slot may have the shape of a rectangle, a circle or an annulus as shown in the Figure 1.8.

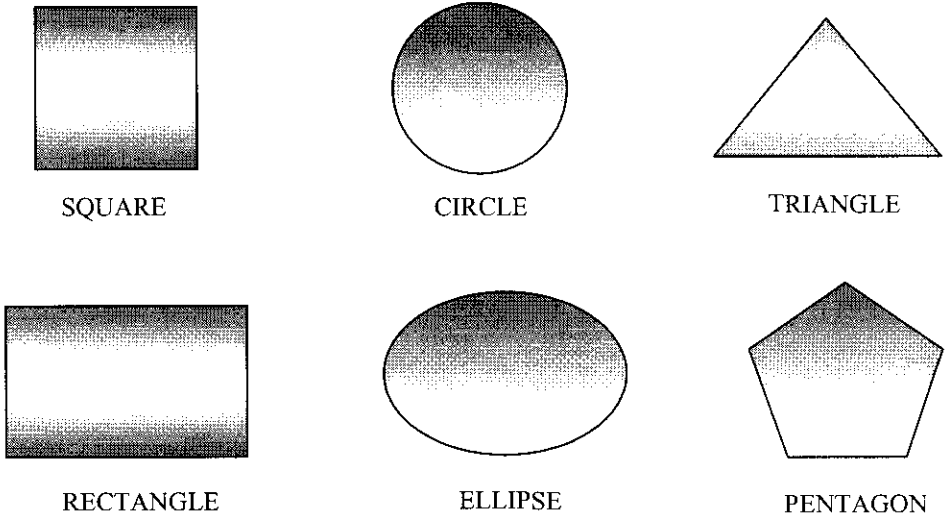


Figure 1.6 Microstrip Patch Antennas

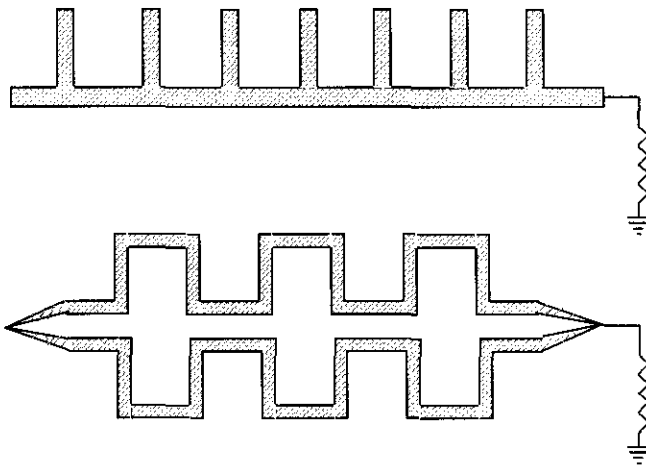


Figure 1.7 Microstrip Traveling Wave Antennas

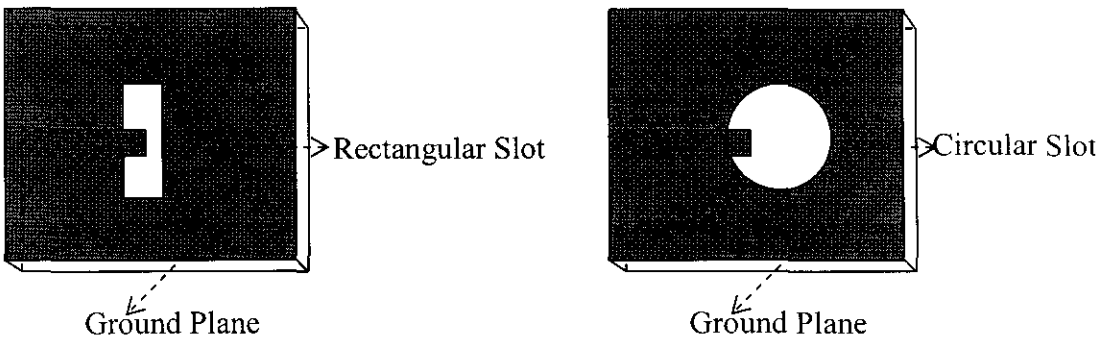


Figure 1.8 Microstrip Slot Antennas

1.7 BASIC CHARACTERISTICS OF RECTANGULAR PATCHES

Rectangular geometry can be analyzed by straightforward application of the cavity model. It is characterized by length 'a' and width 'b'.

The electric field of a resonant mode in the cavity under the patch is given by

$$E_z = E_0 \cos(m\pi x/a) \cos(n\pi y/b) \quad \text{where } m, n = 0, 1, 2 \dots \quad (1)$$

The resonant frequency is

$$f_{mn} = k_{mn}c/2\pi\sqrt{\epsilon_r} \quad \text{where } (k_{mn})^2 = (m\pi/a)^2 + (n\pi/b)^2 \quad (2)$$

To account for the fringing field at the perimeter of the patch effective length and width is to be calculated as explained in the chapter on theoretical investigations.

1.7.1 Magnetic current distribution

The electric field and magnetic surface current distributions on the sidewall for TM_{10} , TM_{01} , and TM_{20} modes are illustrated in Figure 1.9. For TM_{10} mode, the magnetic currents are constant and in phase along 'b' and out of phase along 'a'. For this reason 'b' edge is known as radiating edge since it contributes predominantly to the radiation. For TM_{01} mode, 'a' is regarded as the radiating edge along which the magnetic currents are constant and in phase.

1.7.2 Radiation Pattern

The modes of general interest are TM_{10} and TM_{01} modes. These modes have broadside radiation patterns. The two are orthogonal to each other. TM_{10} and TM_{01} modes can be utilized to operate the rectangular patch as a dual frequency antenna also. Most of the other modes like TM_{11} have maxima off broadside.

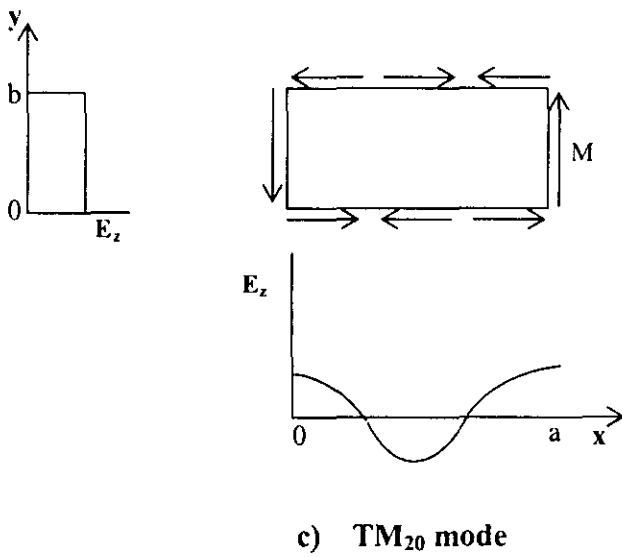
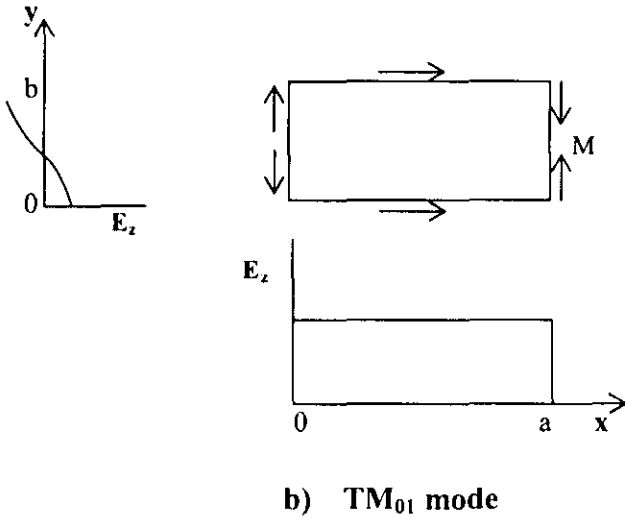
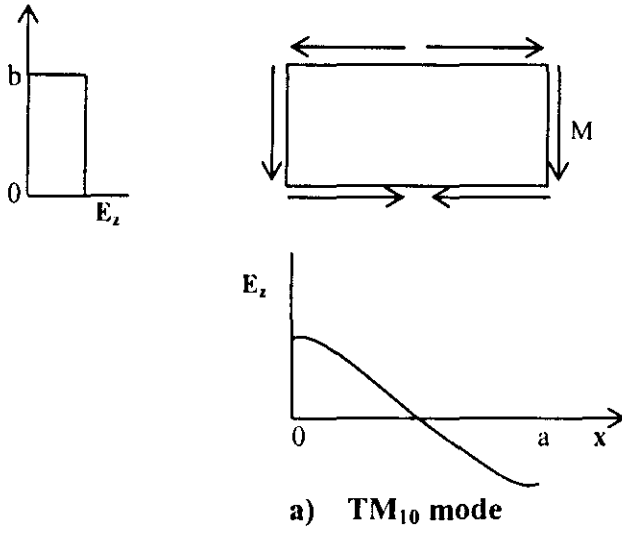


Figure 1.9 Electric Field and magnetic surface current distributions in walls for different modes of a rectangular microstrip patch antenna

1.7.3 Directivity and gain

Directivity of TM_{03} mode is largest and that of TM_{10} mode the smallest. It is not sensitive to substrate thickness and permittivity. The gain on the other hand increases with resonant frequency.

1.8 SIMULATION TECHNIQUES

Electromagnetic Simulation is a new technology to yield high accuracy analysis and design of complicated microwave and RF printed circuit. IE3D is an integrated full wave electromagnetic simulation and optimization package for the analysis and design of three dimensional microstrip antennas. Its primary formulation is based on an integral equation obtained through the use of Green's functions. The field and current distributions from the simulated structure are also accessible to the users using this package. FIDELITY is a finite difference time domain (FDTD) based full-wave electromagnetic simulator. Its basic principle is to use finite difference to represent the differentials in the Maxwells equations. The final algebraic equations for FDTD are in the time-marching style.

Through out the work presented in the thesis, the IE3D simulation results are used for optimizing the various antenna dimensions for a desired resonance frequency.

1.9 OUTLINE OF THE PRESENT WORK

The fast developments in the area of communication demands compact dual frequency microstrip antennas suitable for use in MMICs, satellite mobile communication, personal communication systems etc. In this thesis, theoretical and experimental investigations towards the development of a new compact dual frequency arrow shaped microstrip antenna are presented. The theoretical

investigations carried out resulted in the formulation of simple relations for calculating resonance frequencies, which made the analysis of the geometry easier.

Polarization diversity attained by changing the antenna dimensions is one of the important results obtained for these configurations. Various slot-loaded techniques for exciting new modes are explained with experimental and simulated results. Method for improving the bandwidth by cutting a pair of slots on the non-radiating edges is also presented in detail. Dual port geometry developed for arrow shaped antenna, which avoids cross talk between the frequencies of opposite polarizations is also discussed in this thesis.

1.10 CHAPTER ORGANISATION

In chapter 2, a brief review of the previous work in the area of microstrip antennas is presented with emphasis on compact microstrip antennas, broadband and dual frequency antennas.

In chapter 3, the methodology adopted for the development and analysis of the new patch antenna is presented. The fabrication techniques used in the antenna design is briefly explained. The facilities and techniques used for the measurement of different antenna characteristics like resonant frequency, return loss, radiation pattern, axial ratio etc. are also described.

The important observations and results of the experimental investigations carried out for the different antenna configurations are described in chapter 4. Chapter 5 explains in detail, the development of empirical relations for the design of this antenna. The resonance frequency calculations for single and dual port geometry are also included in this chapter.

The conclusions drawn from experimental and theoretical investigations are presented in chapter 6. Some possible applications of the newly developed antenna along with scope of further work are also described.

The work done by the author in related fields is incorporated as three appendices in this thesis. In Appendix A, dual frequency dual port crescent shaped microstrip antenna is presented. Appendix B discusses on compact circular sided microstrip antenna. Appendix C presents drum shaped antenna for dual frequency dual polarized operation and circular polarization.

CHAPTER 2

BRIEF REVIEW OF THE PAST WORK

Historical perspective of the experimental and theoretical studies on the microstrip antenna during the past few decades is explained in this chapter. The relevant research works in this field are reviewed with emphasis given to compact, dual frequency and broadband microstrip antennas.

2.1 DEVELOPMENT OF MICROSTRIP ANTENNAS

Microstrip antenna was conceived by Deschamps [11] in 1953 in USA. In 1955, Gulton and Bassinot [12] in France patented a 'flat' aerial that can be used in the UHF region. Lewin [13] studied the radiation from the discontinuities in stripline.

The concept of microstrip radiator was not active until the early 1970's, when there was an immediate need for low profile conformal antennas on the emerging new generation missiles. The first microstrip radiator was constructed by Byron [14] in the early 1970's. This antenna was a conducting strip, several wavelength long and half wavelength wide separated from a ground plane by a dielectric strip. The strip was fed at periodic intervals using co-axial connectors along the radiating edges and was used as an array. Munson [15] in 1974 demonstrated new class of microstrip wrap around antennas suitable for missiles using microstrip radiator and microstrip feed networks on the same substrate.

The basic rectangular and circular microstrip antennas were designed by Howell [16]. Design procedures were presented for circularly polarized antennas and for dual frequency antennas from UHF through C band. The bandwidth obtained was very narrow and was found to be depending on permittivity and thickness of the substrate.

Sanford [17] presented the use of conformal microstrip array for L-band communication from KC-135 aircraft to the ATS-6 satellite. Weinschel [18] reported a practical pentagonal antenna in 1975.

Mathematical modeling by applying transmission line analogies was first proposed independently by Munson [15] and Derneryd [19, 20]. This model gives the interpretation for the radiation mechanism and provides expressions for the radiation fields, radiation resistance, input impedance etc. Here the radiating

edges were considered as narrow slots radiating into half space and separated by a half wave length.

Radiation mechanism of an open circuited microstrip termination was studied by James and Wilson [21]. Theoretical and experimental pattern analysis of different radiating elements showed that they are similar to slot radiators.

A more accurate method was suggested by Lo *et al.* [22, 23, 24] in their cavity model. In this model the patch, and the section of the ground plane located below it, is joined by a magnetic wall under the edge of the patch. The antenna parameters of different patch geometries with arbitrary feed points can be calculated using this approach.

Agarwal and Bailey [25] proposed the wire grid model for the evaluation of microstrip antenna characteristics. In this model, the microstrip radiating structure is modeled as a fine grid of wire segments. This method is useful for the design of microstrip antennas of different geometries like circular disc, circular segment and triangular patches.

Carver and Coffey [26, 27, 28] formulated the modal expansion model, which is similar to cavity model. The patch is considered as a thin cavity with leaky magnetic walls. The impedance boundary conditions are imposed on the four walls and the stored and radiated energy were investigated in terms of complex wall admittances. The calculation of wall admittance is given by Hammerstad [29] and more accurately by Alexopolus *et al.* [30].

Newman *et al.* [31, 32] proposed the method of moments for the numerical analysis of microstrip antennas. They used the Richmond's reaction method in connection with the method of moments for calculating the unknown surface currents flowing on the walls forming the microstrip patch, ground plane and magnetic walls.

Hammer *et al.* [33] developed an aperture model for calculating the radiation fields of microstrip antenna. This model accounts radiation from all the edges of the patch and can give the radiation field and the radiation resistance of any mode in a microstrip resonator antenna.

Mink [34] developed a circular microstrip antenna, which operates at a substantially low frequency compared to a circular patch antenna of the same size.

R. Chadha and K. C. Gupta [35] developed Green's function of circular sector, annular ring and annular sector shaped segments in microwave planar circuits and microstrip antennas.

Mosig and Gardiol [36] developed a vector potential approach and applied the numerical techniques to evaluate the fields produced by microstrip antennas of any shape.

Kuester *et al.* [37] reported a thin substrate approximation applied to microstrip antennas. The formulae obtained were found to be useful in simplifying the expression for the microstrip antenna parameters considerably.

The design of a microstrip antenna covered with a dielectric layer was reported by Bahl *et al.* [38]. They suggested appropriate corrections to be considered in calculating the resonant frequency of a microstrip antenna coated with a protective dielectric layer.

N. G. Alexopolus *et al.* [39], discussed a dyadic Green's function technique for calculating the field radiated by a Hertzian dipole printed on a grounded substrate.

Lo and Richards [40] applied the perturbation model approach to the design of circularly polarized microstrip antenna. Critical dimensions needed to produce circular polarization from nearly circular patches were determined by trial and error method.

Elaborate work on the design of microstrip antenna feeds was done by Henderson and James [41, 42]. A canonical transition model was developed to estimate the unwanted radiation loss from the transitions between the feed point and the incoming coaxial line or triplate line.

A technique for controlling the operating frequency and polarization of microstrip antenna was reported by Schaubert *et al.* [43]. The control is achieved by placing shorting posts within the antenna boundary.

A full wave analysis of a circular disc conductor printed on a dielectric substrate backed by a ground plane was presented by Araki and Itoh [44]. The method was based on Galerkin's method applied in the Hankel transform domain.

Itoh and Menzel [45] suggested a method for analyzing the characteristics of open microstrip disk antenna. This method provided a number of unique and convenient features both in analytical and numerical phase.

Electric Probe measurements on Microstrip were proposed by J. S. Dahelle and A. L. Cullen [46]. Here the electric field of microstrip is determined using a field probe.

Long *et al.* [47, 48] measured the driving point impedance of a printed circuit antenna consisting of a circular disc separated by a dielectric from a ground plane.

Shen [49] analysed the elliptical microstrip patch and showed that the radiation from this antenna is circularly polarized in a narrow band when the eccentricity of the ellipse is small.

Microstrip disc antenna has been analysed by Derneryd [50], by calculating the radiation conductance, antenna efficiency, and quality factor associated with the circular disc antenna.

Microstrip antenna on ferrite substrate is reported by Das and Choudhary [51]. The resonant frequency and resonating length of a rectangular microstrip patch on ferromagnetic substrate were derived. It was found that the size of the radiator can be reduced by constructing them on ferrite substrate since the ferrite has both dielectric and magnetic properties.

Kerr [52] investigated the rectangular and circular patches with a central diagonal slot. He obtained circularly polarized radiation with a very good axial ratio over 120° segments of the radiation pattern. The bandwidth achieved was nearly 2 percent.

Wilkinson [53] discussed the radiation from microstrip dipoles. He described a structure with one arm of the dipole on one side of the substrate and other arm on the opposite side and spacing the substrate dipole one quarter wavelength from a ground plane.

2.2 COMPACT DUAL FREQUENCY MICROSTRIP ANTENNAS

Miniaturisation in the personal communication systems demands design and development of compact dual frequency microstrip antennas. The review of these type antennas is presented in this section.

Mohamed A Sultan and Vijay K Tripathi [54] proposed mode features of an annular sector microstrip antenna.

J. L. Volakis and J. M. Jin [55] proposed techniques for lowering the resonant frequency of the rectangular patch antenna by placing a perturbation below the patch. They obtained thirty percent decrease in resonant frequency.

E. K. N. Yung *et al.* [56] obtained frequency reduction of the patch antenna by loading dielectric resonator. They also observed that the resonant frequency decreases with the position of the DR on the antenna.

V. Palanisamy and R. Garg [57] proposed H-shaped microstrip antenna, which requires very less area, compared to the rectangular patch antenna.

G. Kossiavas *et al.* [58] presented C- shaped microstrip radiating element, which is much smaller than the conventional circular and square elements operating in the UHF and L-bands.

Supriyo Dey *et al.* [59] modified the geometry of an ordinary microstrip circular patch antenna by putting two sectoral slots shunted by conducting strips to get reduced resonant frequency. They were able to achieve 19% reduction in resonant frequency by this method.

Y. Hwang [60] demonstrated a planar inverted F antenna loaded with a high permittivity material suitable for mobile communication handsets.

S. Dey *et al.* [61] proposed the design of a compact low-cost wide band circularly polarized antenna suitable for personal communication applications. The configuration consists of four shorted rectangular patches.

M. G. Douglas and R. H. Johnston [62] demonstrated the U patch antenna. This may be used as an alternative to the half wave square patch antenna, but it requires only one quarter of the surface area of the square half wave antenna.

Double C- patch antennas having different aperture shapes were experimentally studied by Mohamed Sanad [63]. He achieved size reduction through shorting the zero potential plane of the antenna as well as through varying the length and width of the apertures.

Jacob George *et al.* [64] proposed a broadband low profile microstrip circular patch antenna. Four sectoral slots are cut on the circular patch antenna with a uniform intersectoral angle 90° and a slot angle 8° .

R. Waterhouse [65] presented a probe fed circular microstrip antenna, which incorporates a sectoral shorting pin. The presence of the shorting pin significantly reduced the overall size of the antenna.

M. Sanad [66] developed a compact microstrip antenna suitable for application in cellular phones. It consists of a driven element and five small parasitic patches distributed in two stacked layers.

K. L. Wong and S.C. Pan [67] loaded a triangular microstrip antenna with a shorting pin and observed significant reduction in antenna size at a given operating frequency.

Experimental details of a single fed dual frequency compact microstrip antenna are presented by K. L. Wong and W. S. Chen [68]. This new rectangular microstrip antenna provides a frequency ratio greater than three between the two operating frequency.

Compact broadband microstrip antenna is experimentally demonstrated by K. L. Wong and Y.F. Lin [69] through chip resistor loading. The impedance matching can be achieved by adjusting the coupling-slot size or by the position or size of the slot.

C. L. Tang *et al.* [70] proposed a dual frequency compact microstrip circular patch antenna. The antenna configuration utilizes a single probe feed and a single shorting pin. The frequency ratio of the two operating frequencies is tunable in the range of 2.55-3.83.

R. B. Waterhouse [71] demonstrated broadband operation of shorted circular patches by coupling annular ring to it. K.L. Wong and J. Y. Wu [72] produced circular polarization from a shorted square patch antenna.

K. L. Wong and K. P. Yang [73] demonstrated a new design of single feed, dual-frequency rectangular microstrip antenna with a cross slot of equal length. Here the two frequencies are orthogonally polarized and the ratio between them depends on the aspect ratio of the patch.

J. H. Lu *et al.* [74] have put forward the design of compact slot coupled triangular microstrip antennas with a shorting pin or chip resistor loading. They achieved the desired matching for TM_{10} mode by adjusting the coupling slot size.

S. K. Satpathy *et al.* [75] presented shorted versions of semi circular and 90° sectoral microstrip antennas. This antenna provided a size reduction of four times without any significant change in performance.

The implementation of compact and broadband rectangular microstrip antenna having enhanced gain is described by C. Y. Huang *et al.* [76]. They used chip resistor loading for bandwidth enhancement and placement of superstartes for gain enhancement.

A. S. Vaello and D. S. Hernandez [77] presented a bow-tie antenna similar to the drum shaped antenna for dual frequency operation. The antenna requires much lesser patch area compared to conventional patch antennas and have similar radiation characteristics.

C. Salvador *et al.* [78] proposed dual frequency planar antenna at S and X bands. The structure consists of an S-band cross patch with four square patches printed in empty spaces among the arms of the cross.

H. Iwasaki [79] demonstrated proximity coupled linearly polarized patch antenna for dual frequency use. The geometry consists of a circular patch antenna having perturbation segments fed by two perpendicular microstrip lines. The antenna also provided high isolation between transmit and receive ports.

H. Nakano and K. Vichien [80] proposed dual-frequency square patch antenna with rectangular notch. The resonant frequencies and return loss are studied as a function of the rectangular notch depth.

K. L. Wong and K. P. Yang [81] demonstrated a modified planar inverted F antenna (PIFA), which is more compact, and has larger bandwidth compared to simple PIFA.

J. George *et al.* [82] proposed compact drum shaped antenna, which provided an area reduction greater than 60 percent, compared to an equivalent rectangular patch antenna.

D. Singh *et al.* [83] studied a quarter wave length, H-shaped miniaturized microstrip antenna for MMIC applications. The antenna occupies only one tenth of the substrate area of a half wave length patch antenna.

T. Huynh *et al.* [84] studied the cross polarization characteristics of rectangular patch antennas. They concluded that the cross polarization component increases with resonant frequency and substrate thickness. K. F. Lee *et al.* [85] determined the cross polarization characteristics of circular patch antennas.

F. Carrez and J. Vindevoghel [86] proposed a compact two port microstrip antenna which operates in the X-band. The compactness was achieved using mutual coupling and parasitic coupling techniques.

Compact two layer rectangular patch antenna has been designed by R. Chair *et al.* [87]. Compared with a basic single layer patch antenna with the same projection area, the resonant frequency is reduced by 39% and bandwidth is enhanced by 5%.

Z. D. Liu and P. S. Hall [88] proposed dual-band inverted F-antenna for hand held portable telephones.

Very compact double C- Patch antenna is studied by L. Zaid *et al.* [89]. The antenna consisted of two stacked C- patch elements connected together with a vertical conducting plane.

Compact dual band dual polarization rectangular microstrip patch antenna is proposed by E. Lee *et al.* [90]. This antenna generated two distinct frequencies with different polarization: a monopolar mode for terrestrial cellular communication and a circularly polarized, upward oriented pattern for satellite mobile.

J. George *et al.* [91] developed a dual frequency drum shaped microstrip antenna using a shorting pin. This new configuration gives a large variation in frequency ratio of the two operating frequency, without increasing the overall size of the antenna.

G. P. Srivastava *et al.* [92], designed a dual band microstrip patch antenna for operation at 3.0 GHz by using a cross load on top of the radiator. The frequency difference is small enough and can be tuned by changing the length of the cross line.

Kin-Lu Wong and Ming-Huang Chen [93] designed a small slot coupled circularly polarized circular microstrip antenna with a modified cross slot cut in the patch and a bent tuning stub aligned along the patch boundary. For CP operation the above antenna has a size reduction of ~ 80 % compared to regular size CP design.

Jui-Han Lu *et al.* [94], proposed a compact CP design for a single feed equilateral triangular microstrip antenna with inserted spur lines at the patch edges. The resonant frequency is significantly lowered by increasing the spur-line length.

Kin- Lu Wong and Wen-Shan Chen [95] designed slot-loaded bow-tie microstrip antenna for dual frequency operation. A pair of narrow slots were embedded close to the radiating edges of the patch and obtained the frequency ratio tunable in the range 2 to 3.

Kin- Lu Wong and Jian – Yi Wu [96] designed compact circularly polarized square microstrip antenna. The design is achieved by cutting slits in the square patch.

Kin- Lu Wong and Jia-Yi Sze [97] proposed a dual frequency slotted rectangular microstrip antenna. By embedding a pair of properly bent slots close to the non radiating edges of the patch two operating frequencies of same polarization plane is obtained. It is found that a new resonant mode TM_{60} is excited between TM_{10} and TM_{20} mode of the simple unslotted patch antenna.

The dual frequency rectangular microstrip antenna with a pair of step slots close to the non radiating edges is proposed and experimentally studied by Jui-Han Lu [98]. The two operating frequencies have same polarization plane and similar broadside radiation characteristics.

D. Sanchez –Hernandez [99] proposed dual-band circularly polarized microstrip antenna with a single feed. This is obtained by using two spur-line band-stop filters within the perimeter of a microstrip patch antenna with optimum feed point location and aspect ratio.

A planar dual-band internal antenna for handsets which operates in ~ 0.9 and 1.8 GHz bands is proposed by N. Chiba *et al.* [100]. Good dual band operation was obtained for frequency ratios in the range 1.3 - 2.7 .

K. M. Luk *et al.* [101] proposed folded rectangular patch antenna. Compared with a conventional patch antenna resonant frequency is reduced by 37% and the cross polarization level is ~ -20 dB.

Kin-Lu-Wong and Yi-Fang-Lin [102] proposed a CP design of microstrip antenna using a tuning stub. It is also demonstrated that, by applying this CP design method to a circular microstrip patch with a cross slot having equal slot lengths, a compact circularly polarized antenna can be implemented.

2.3 BROAD BAND MICROSTRIP ANTENNA

Some of the researchers worldwide, started working towards overcoming the inherent disadvantage of narrow impedance bandwidth and came out with interesting results.

Schaubert and Farrar [103] reported that the use of parasitic elements can improve the bandwidth of the rectangular microstrip antenna.

Wood [104] suggested a method of doubling the bandwidth of rectangular patch antennas. He used two capacitively excited $\lambda/4$ short circuit parasitic elements placed parallel to the radiating edges. Here the driven and the parasite together give two resonances.

C.K. Aanandan and K.G. Nair [105] developed a compact broadband microstrip antenna configuration. The system uses a number of parasitic elements, which are gap coupled to a driven patch. They achieved a bandwidth of 6% without deteriorating the radiation pattern.

Poddar *et al.* [106] obtained considerable improvement in bandwidth by constructing the patch antenna on stepped and wedge shaped dielectric substrate.

Demeryd and Karlsson [107] constructed a broadband microstrip antenna by using a thicker substrate of low dielectric constant.

Construction of conical microstrip antenna was reported by Das and Chatterjee [108]. Here, the circular patch antenna is modified by slightly depressing the patch configuration conically into the substrate. This conical antenna has a much larger bandwidth than that of an identical circular patch antenna.

Jeddari [109] calculated the resonant frequency and bandwidth of conically depressed microstrip antennas.

Pandharipande and Verma [110] presented a novel feeding scheme for the excitation of patch array which gives broader bandwidth. The feed network consists of a stripline power divider using hybrid rings and the coupling from stripline to feed point is achieved by thin metal probe.

Bhatnagar *et al.* [111] obtained large bandwidth in triangular microstrip antennas using two parasitic resonators directly coupled to the non radiating edges and a third one gap coupled to the radiating edge.

Bhatnagar *et al.* [112] proposed a stacked configuration of triangular microstrip antennas to obtain larger bandwidth.

Wood [113] suggested the use of circular and spiral microstrip lines as a compact and wideband circularly polarized microstrip antennas.

Hall *et al.* [114] reported the concepts of multilayer substrate antennas to achieve broader bandwidth. These type of antennas constructed on alumina substrates give a bandwidth which is 16 times that of a standard patch antenna at the expense of an increase in overall antenna height.

Sabban [115] constructed a stacked two layer microstrip antenna. It has a bandwidth of 15% for VSWR 2:1. This antenna has been used as an element for 64 element Ku band array.

Hori and Nakagima [116] designed a broadband circularly polarized microstrip antenna for public radio communication system.

Prior and Hall [117] showed that the addition of a short circuited ring to a microstrip disc antenna will double the bandwidth of the disc, with some reduction in gain.

K. M. Luk *et al.* [118] designed broadband rectangular microstrip patch antenna using an L- shaped probe. By this technique an impedance bandwidth of 35% with an average gain of 7.5 dBi are achieved.

M. Deepukumar *et al.* [119] developed dual port microstrip antenna geometry for dual frequency operation. The structure consists of the intersection of two circles of the same radius with their centres displaced by a small fraction of a wavelength. This antenna provided wide impedance bandwidth and excellent isolation between its ports.

Y. Kim *et al.* [120] designed a wide band microstrip antenna with dual frequency dual polarization operation. To widen the bandwidth at both frequencies a parasitic element is stacked above a fed element. The measured bandwidths for 15 dB return loss at dual frequencies are 9.02 and 12.4 % respectively.

W. K. Lo *et al.* [121] designed a circularly polarized patch antenna array using proximity coupled L- strip line feed. By placing a cross slot with unequal slot lengths on the circular patch, circular polarization can be excited. The impedance and the axial ratio bandwidth are 78 and 16.15%.

Chih – Yu Huang *et al.* [122] designed a compact rectangular microstrip antenna with enhanced gain and wider bandwidth by loading a high permittivity superstrate layer and a 1 ohm chip resistor. The proposed one has an operating bandwidth about six times that of a conventional patch antenna.

Kin-Lu Wong and Jian-Yi Wu [123] designed circularly polarized square microstrip antenna fed along a diagonal with a pair of suitable chip resistors. The proposed patch provided a wider bandwidth for circular polarization about two times that of a similar design with a pair of shorting posts.

Y. X. Guo *et al.* [124] proposed a rectangular microstrip antenna with two U-shaped slots on the patch. Using a foam layer of thickness $\sim 9\%$ wavelength as supporting substrate, an impedance bandwidth of 44% is achieved.

K. M. Luk *et al.* [125] designed a rectangular U- slot patch antenna proximity fed by an L- shaped probe. Using a foam layer of thickness $\sim 7\%$ wavelength as a supporting substrate

R. B. Waterhouse [126] developed a stacked shorted patch for broadband operation. This proposed patch provided an impedance bandwidth greater than 30%.

Experimental investigations on hybrid coupled circular microstrip antenna are presented by K.P. Ray and G. Kumar [127]. Three circular patches with different radii with a small gap between them constitute the antenna geometry. Shorting strips of different widths were used to adjust the coupling between the central fed patch and two parasitic patches, yielding dual-band, triple-band and broadband operation.

Kin-Lu Wong and Jen-Yea Jan [128] proposed a broadband design for a circular microstrip antenna with reactive loading integrated with a circular patch. Here the bandwidth obtained is ~ 3.2 times that of a conventional circular microstrip antenna.

B. L. Ooi and C. L. Lee [129] proposed broadband rectangular air-filled stacked U- slot patch antenna. For a height of 10% of the designed wavelength, the stacked U-slot patch antenna with an offset L- shaped probe produces an impedance bandwidth of 44.4%.

Chih-Yu Hang *et al.* [130] designed broadband slot coupled microstrip antenna using an inclined nonlinear coupling slot for circular polarization. This nonlinear slot, end loaded with two V- slots, significantly broadens the CP bandwidth to about 2.1 times that obtained using a single inclined coupling slot.

Kin- Lu Wong and Wen-Hsiu Hsu [131] demonstrated broadband design of a triangular microstrip antenna with U-shaped slot. The design gives a bandwidth ~ 1.8 times that of corresponding simple triangular patch antenna.

Jia-Yi Sze and Kin Lu Wong [132] proposed rectangular antenna having a tooth brush shaped antenna for broadband operation. The new mode generated has the same polarization as TM_{10} mode. The two resonance frequency combines to give broadband operation.

The use of annular ring antenna instead of circular patch to achieve larger bandwidth was reported by Chew [133].

CHAPTER 3

METHODOLOGY:-EXPERIMENTAL SETUP, MEASUREMENT AND SIMULATION TECHNIQUES

This chapter gives the description of the basic facilities used for the investigation. The techniques employed for the fabrication of the microstrip antennas are explained. The experimental setup and measurement procedures used for the study of various antenna characteristics are also described in this chapter. Finally the chapter concludes with the various simulation techniques used for the optimisation of antenna geometry.

3.1 BASIC FACILITIES USED

A brief description of the different types of equipment and facilities used for the measurement of antenna characteristics is given in this section.

3.1.1 Network Analyzer

A network analyzer is an equipment incorporating swept-frequency measurements to completely characterize the complex network parameters at a faster rate without degradation of accuracy. A vector network analyzer measures both the magnitude and phase of the scattering parameters. Schematic diagram of the network analyzer is shown in Figure 3.1. The experiments presented in this thesis were conducted using HP 8510C network analyzer. The synthesized source (HP 83651B), which uses an open loop YIG tuned source, provides the RF stimulus. It can sweep in a wide range of frequencies, 45 MHz to 50 GHz. The source can operate in ramp and step sweep mode. The step mode provides the highest accuracy, although at reduced measurement speed. The source is fed to the S-parameter test set. Here the different scattering parameters are separated and down converted to 20MHz and fed to the IF detector. The detected signal is processed and fed to the display unit for output. All the devices are connected using GPIB interface called the system bus.

3.1.2 Anechoic Chamber

The radiation measurements are performed inside a microwave anechoic chamber. This is an indigenously built reflection free chamber or microwave dark room. An anechoic chamber is an artificially simulated free-space environment in which e.m. wave propagation studies can be performed without any interaction from other objects. This is a large room, the interior surface of which is covered with absorbing materials of e.m. energy with good absorption at the frequencies of interest. To avoid any possible interaction with outer environment, a metallic

lining is also put on the exterior. The test antenna is mounted on a turntable, which is kept in the quiet zone of the chamber. The turntable is controlled remotely from the control room.

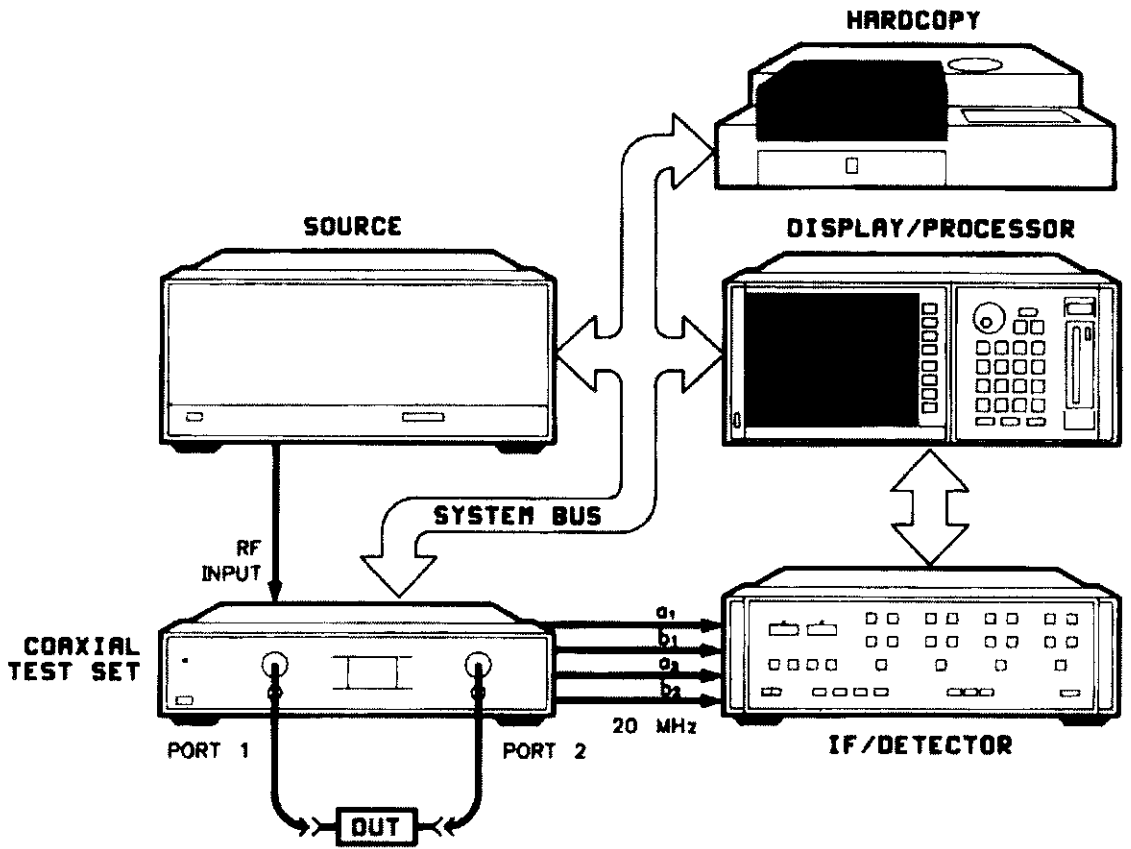


Figure 3.1 Schematic diagram of the HP 8510C network Analyser

3.2 FABRICATION OF MICROSTRIP ANTENNA

For the fabrication of microstrip antennas, photolithographic technique or fast fabrication process can be employed. In the work presented here, the second method is used which is reasonably accurate at low frequencies.

3.2.1 Fast Fabrication Process

The different steps in this process are shown in Figure 3.2. Here the copper clad substrate is cleaned thoroughly (a) and the drawing of the antenna is made on one side (b). The entire top and bottom metallization regions are covered with transparent cellophane tape (c). The tape is then selectively removed from the top metallization layer (d) by means of a sharp cutting tool in such a manner that the tape over the antenna geometry is unaltered. The exposed metallization regions (e) are etched out. After the etching process, tape is removed from both the surfaces and cleaned (f). Now the antenna is ready for testing.

This method is very fast and simple compared to the photolithographic technique. The validity of this technique has been established by fabricating conventional rectangular patch antennas.

3.2.2 Excitation Techniques

In the present work, coaxial feeding or electromagnetic coupling using microstrip feed line are employed. Coaxial feeding is done using an SMA connector with its outer conductor connected to the ground plane and the inner conductor soldered to the patch antenna. Electromagnetic coupling is done using a 50 ohm microstrip feed line etched on a separate substrate and kept below the patch as explained on excitation techniques in chapter 1.

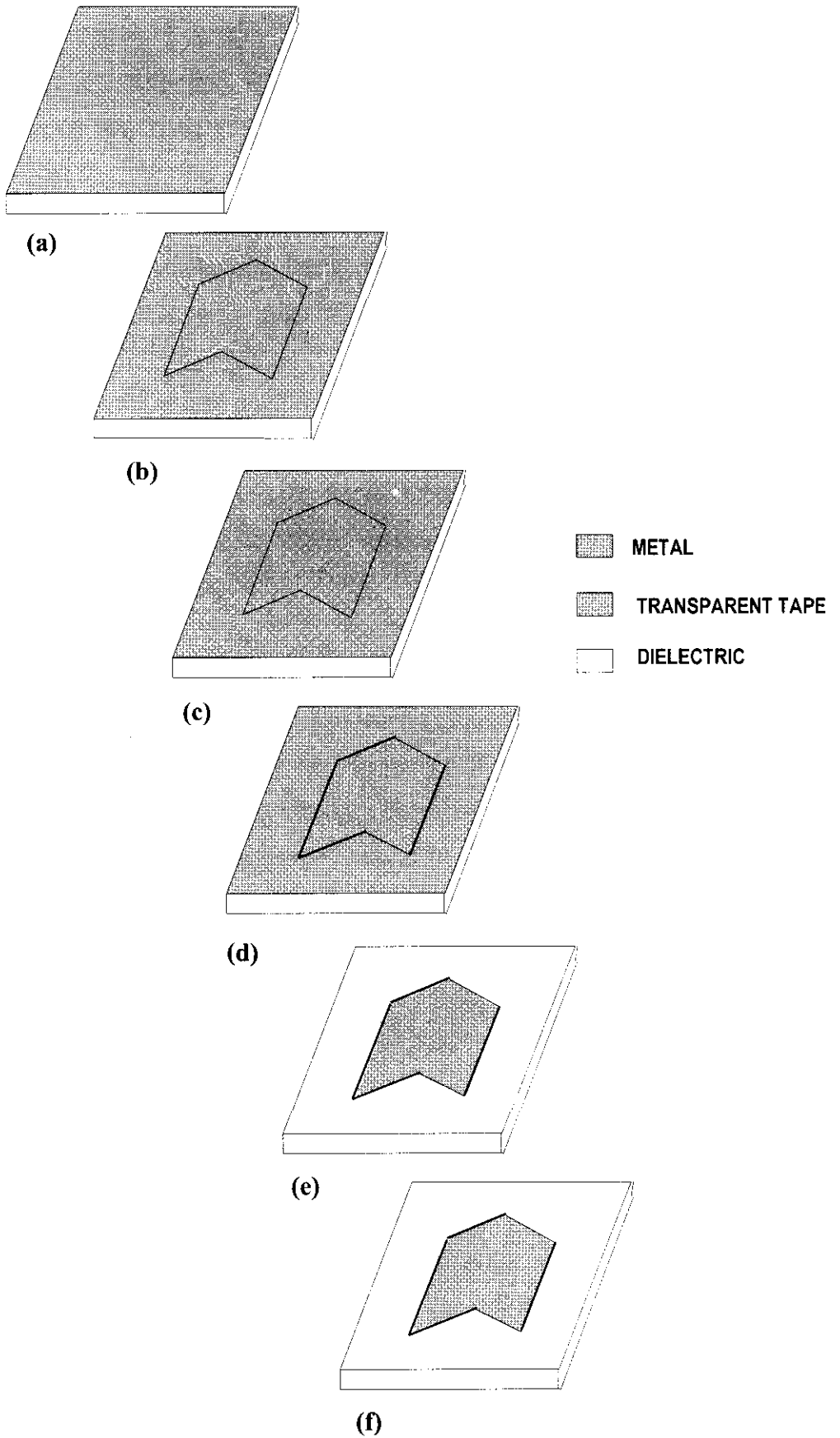


Figure 3.2 Different steps in the fabrication process

3.3 MEASUREMENT OF RETURN LOSS, RESONANT FREQUENCY AND BANDWIDTH

The HP 8510C network analyzer is used for the measurement. The experimental setup for the automatic measurement controlled by an IBM PC interfaced to the network analyzer is shown in Figure 3.3.

Network Analyzer is calibrated for Port 1. The test antenna is connected to the Port 1 of the S-parameter test set. The measured S_{11} LOGMAG data in the network analyzer is acquired and stored in ASCII format in the computer using MERL Soft (The software for antenna studies developed by the microwave group of the Department of Electronics)

The stored return loss data in ASCII format is analyzed for bandwidth and resonant frequency. The resonant frequencies of the antenna are determined from the dip of the return loss curve for that particular mode. The bandwidth can be directly obtained from the return loss data by noting the range of frequencies over which the return loss greater than or equal to 10 dB.

3.4 MEASUREMENT OF RADIATION PATTERN

The copolar and cross-polar E-Plane and H-plane radiation patterns of the test antenna are measured by keeping the antenna inside an anechoic chamber in the receiving mode. The experimental arrangement is shown in Figure 3.4. A wide-band ridged horn is used as the transmitter.

HP 8510C Network Analyzer, interfaced to an IBM PC, is used for the pattern measurement. The PC is also attached to a STIC 310C position controller. The test antenna is mounted on the antenna positioner and kept inside the chamber. The test antenna and the standard transmitting antenna are connected to Port 2 and Port 1 respectively of the network analyzer.

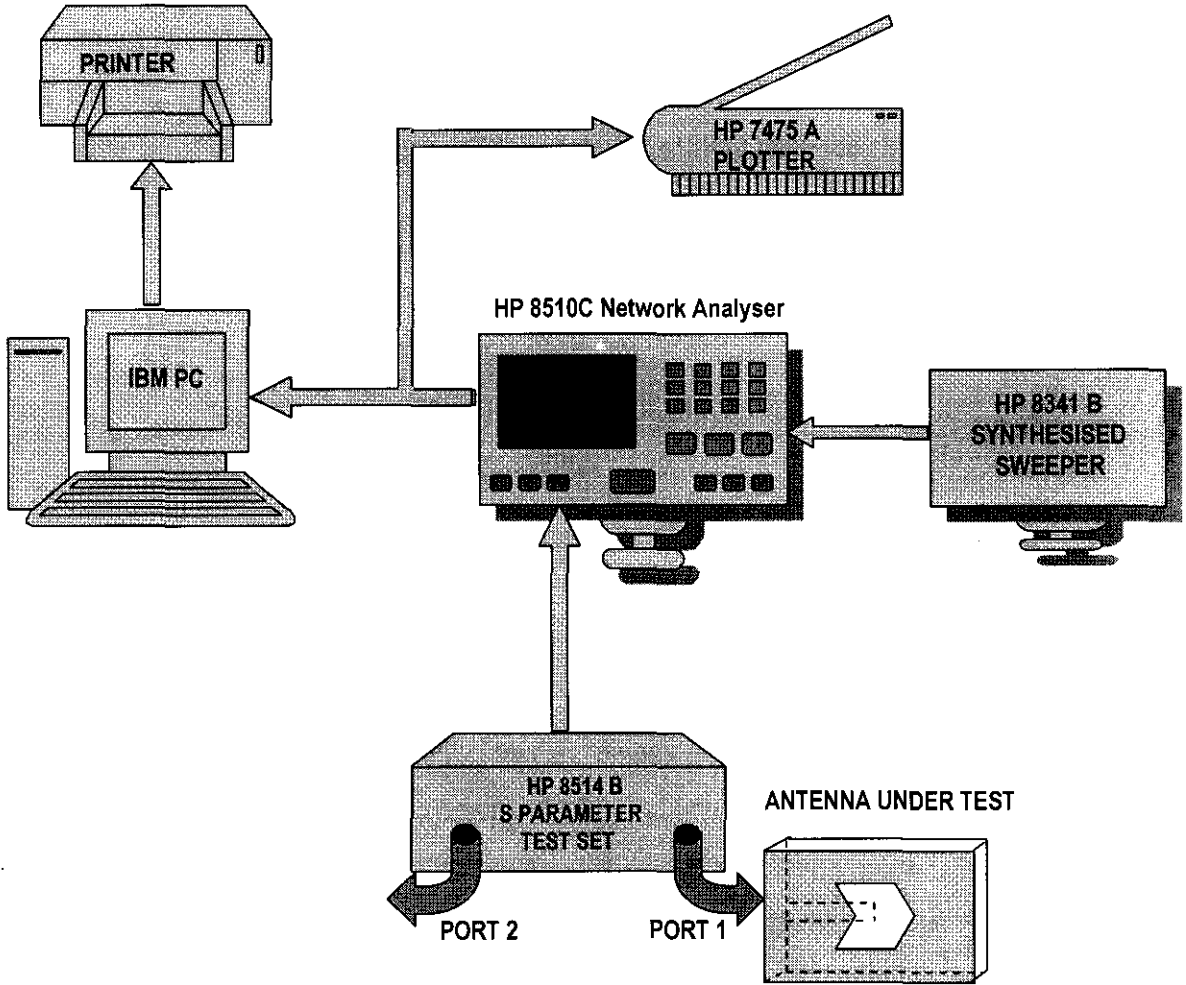


Figure 3.3 Experimental setup for the measurement of return loss

The radiation patterns of the antenna at multiple frequency points can be measured in a single rotation of the test antenna positioner by using MERL Soft. The positioner will stop at each step angle and take S_{21} measurements in the entire band of interest till it reaches the stop angle. The entire measured data are stored in ASCII format and can be used for further processing like analysis and plotting. The different pattern characteristics like half power beam width, cross-polar level etc. are obtained after the analysis of the stored patterns.

3.5 MEASUREMENT OF GAIN

The setup for the measurement of gain is the same as that used for pattern measurement. The relative measurement of gain of the new antenna is made with a standard rectangular patch antenna operating at the same frequency and fabricated on the same substrate.

The standard rectangular microstrip antenna is kept inside the chamber and connected to Port 2 of the Network Analyzer. Port 1 is connected to the transmitting antenna. The antenna is bore-sighted and a THRU RESPONSE calibration is performed in the Network Analyzer and stored in the CAL set. This will act as the reference gain response. The standard antenna is now replaced by the corresponding arrow shaped antenna and the plot displayed on the Network Analyzer will directly give the relative gain of the new antenna.

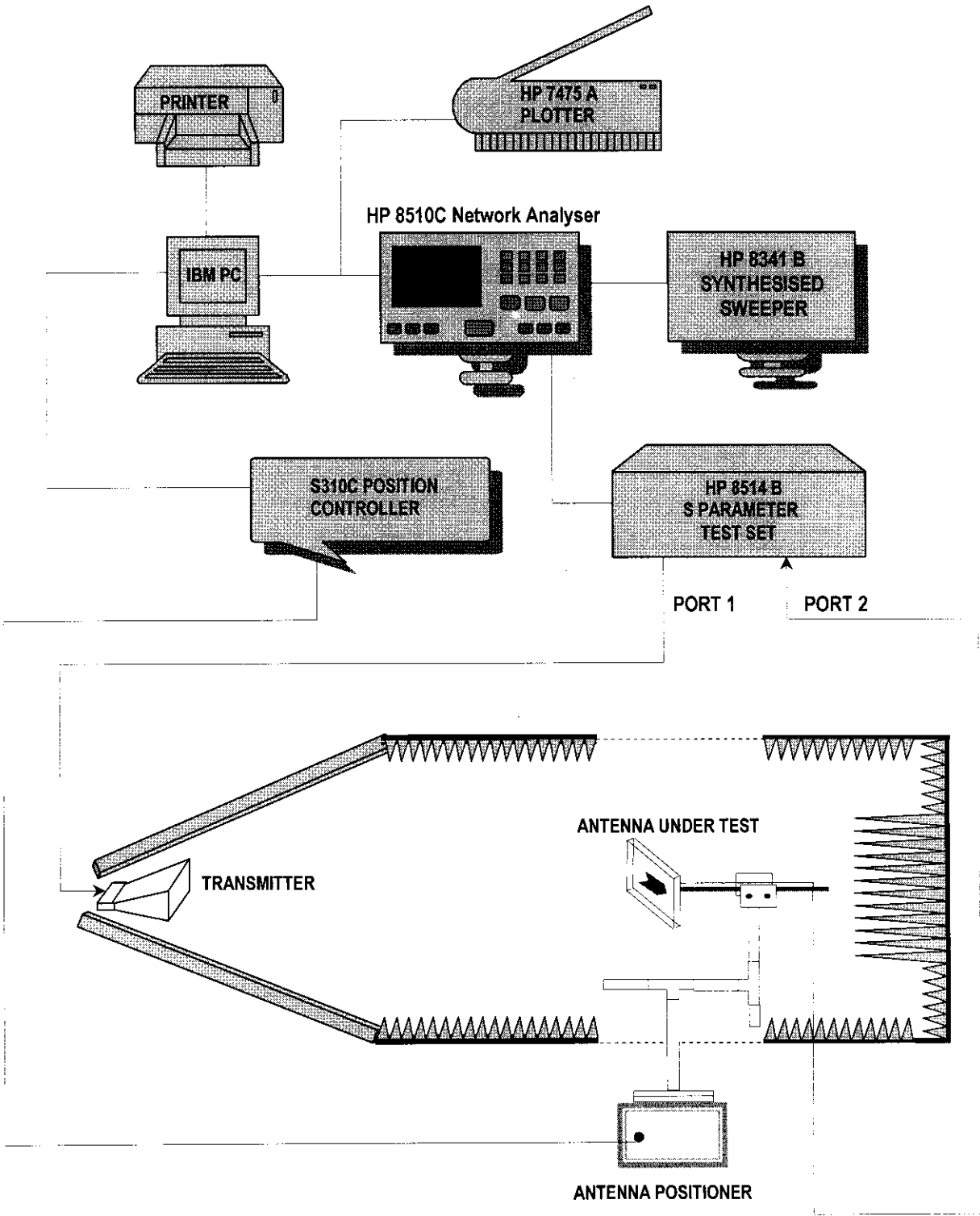


Figure 3.4 Experimental setup for the measurement of radiation pattern

3.6 MEASUREMENT OF AXIAL RATIO FOR CIRCULARLY POLARISED FREQUENCY BAND

The set up is the same as that for pattern measurement. Test antenna connected to Port 2 is kept stationary. The transmitting antenna connected to Port 1 is rotated in its own axis and the maximum and the minimum of the power received are noted. For a particular frequency, the difference between the maximum and the minimum of the power gives the axial ratio.

$$\text{Axial Ratio} = \text{Maximum Power in dB} - \text{Minimum Power in dB}$$

This is repeated for all the frequency points at regular intervals in the band and the graph is plotted. The 3dB axial ratio bandwidth can be obtained from the graph.

3.7 MEASUREMENT OF RETURN LOSS AND RADIATION PATTERN USING IE3D SIMULATION SOFTWARE

IE3D is an integrated full wave electromagnetic simulation and optimisation package for the analysis and design of 3-dimensional microstrip antennas

IE3D consists of a layout editor **MGRID**, the schematic editor **MODUA**, current display post processor **CURVIEW**, and a radiation pattern post processor **PATTERNVIEW**.

On the IE3D, a circuit is described as a set of polygons, and a polygon is described as a set of vertices. This section explains the construction and analysis procedure step by step.

First select the **MGRID** window. Select **NEW** in **FILE** menu. Before entering polygon, circuit initial parameters like the length unit, layout parameters, the

substrate parameters, the metallic strip parameters and the discretization parameters are edited and selected properly. Now the polygon is entered as a set of vertices using the mouse. Polygon is formed and colored for identification as shown in Figure 3.5. Second step is to define the port. The simulation engine will not run without any port on a structure. Port is defined inside or on the polygon edges. This is done by selecting **DEFINE PORT** in **PORT** menu. As the third step Select **SAVE** in **FILE** menu. Now a file having '.geo' extension will be created. Select item **GRIDDING** in menu **PROCESS**. This process is not necessary for simulation. In the IE3D, they adopt triangular and rectangular mixed meshing scheme and apply the non-uniform grid basis function on it. The gridding performed on the arrow shaped microstrip antenna is shown in Figure 3.6.

Now the circuit is constructed. The next step is to perform electromagnetic simulation. Select **SET SIMULATION** in **PROCESS** menu. The simulation setup dialog window as shown in Figure 3.7 appears. Enter start frequency, stop frequency and the no. of frequencies. To find frequency responses Adaptive Intelli-Fit option is to be enabled for fast and accurate response. To calculate the current distribution and field distribution check it in the simulation setup window. In that cases uncheck Adaptive Intelli- Fit. After completing Select **OK** to continue. The IE3D simulation engine (IE3D.exe) is invoked to perform the simulation. IE3D will finish the simulation in a few seconds. . Then it will automatically invoke the **MODUA** window to display the parameters. This window reads the data and display the S_{11} or S_{21} or S_{22} on the smith chart as shown in Figure 3.8. If we want the frequency response in other format, we can do it by selecting **DEFINE DISPLAY DATA** or **DEFINE DISPLAY GRAPH** in **CONTROL** menu. Some of the graphs are shown in Figure 3.8.

As explained before, if we check the radiation pattern file and current distribution file in the simulation setup dialog box, files having '.cur' and '.pat' extension will be created. On **CURVIEW** we can display the 3D view of a discretized

structure, field and the current distribution on the structure. With the help of the window **PATTERNVIEW** we can compare the radiation patterns at different frequencies from different files. The radiation pattern and the current distribution as obtained from IE3D simulation is shown in Figure 3.9 and Figure 3.10

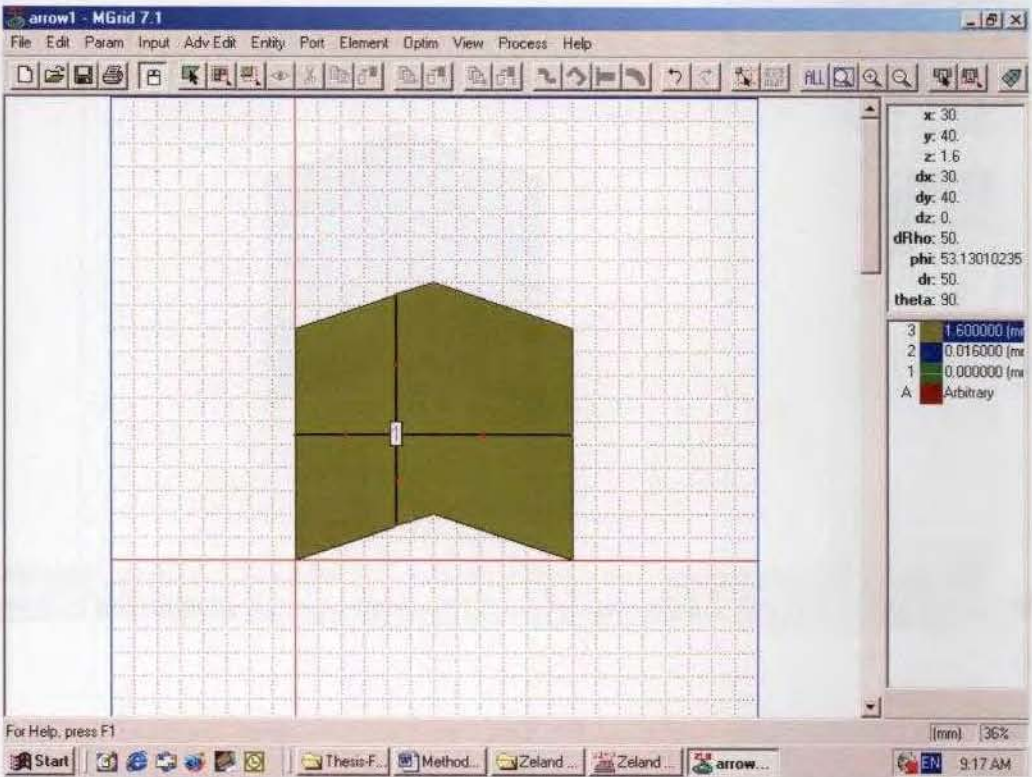


Figure 3.5 Figure showing IE3D MGRID window with arrow shaped polygon with a coaxial feed.

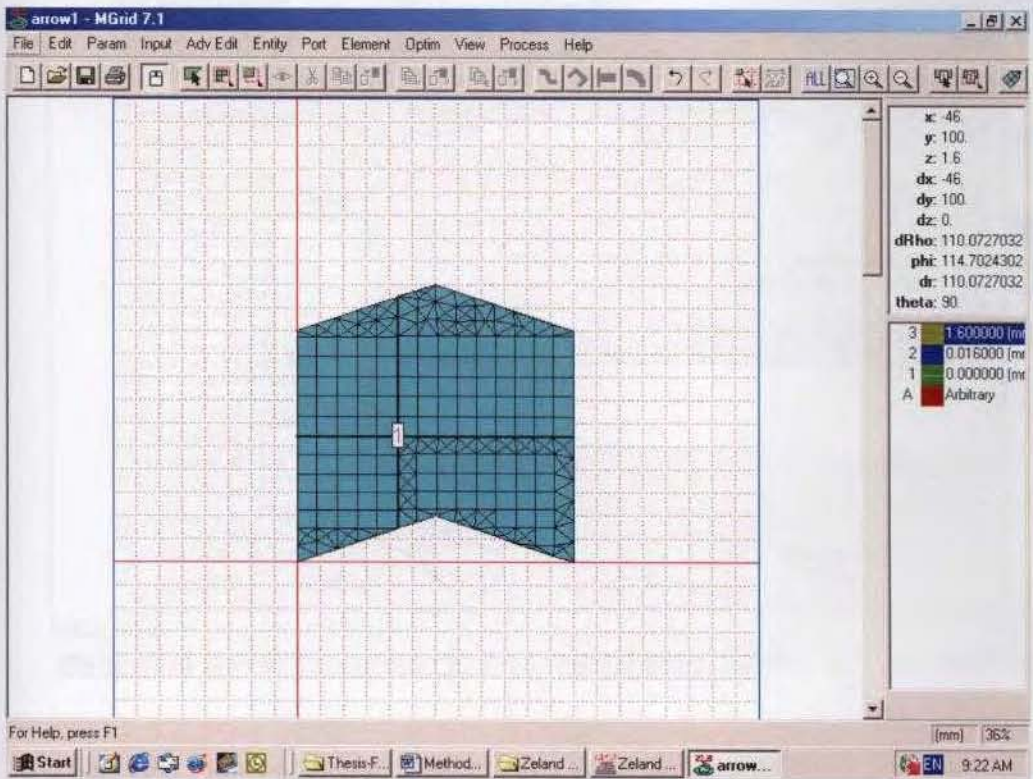


Figure 3.6 Figure showing the gridding performed on the arrow shaped microstrip antenna using triangular and rectangular mixed meshing scheme.

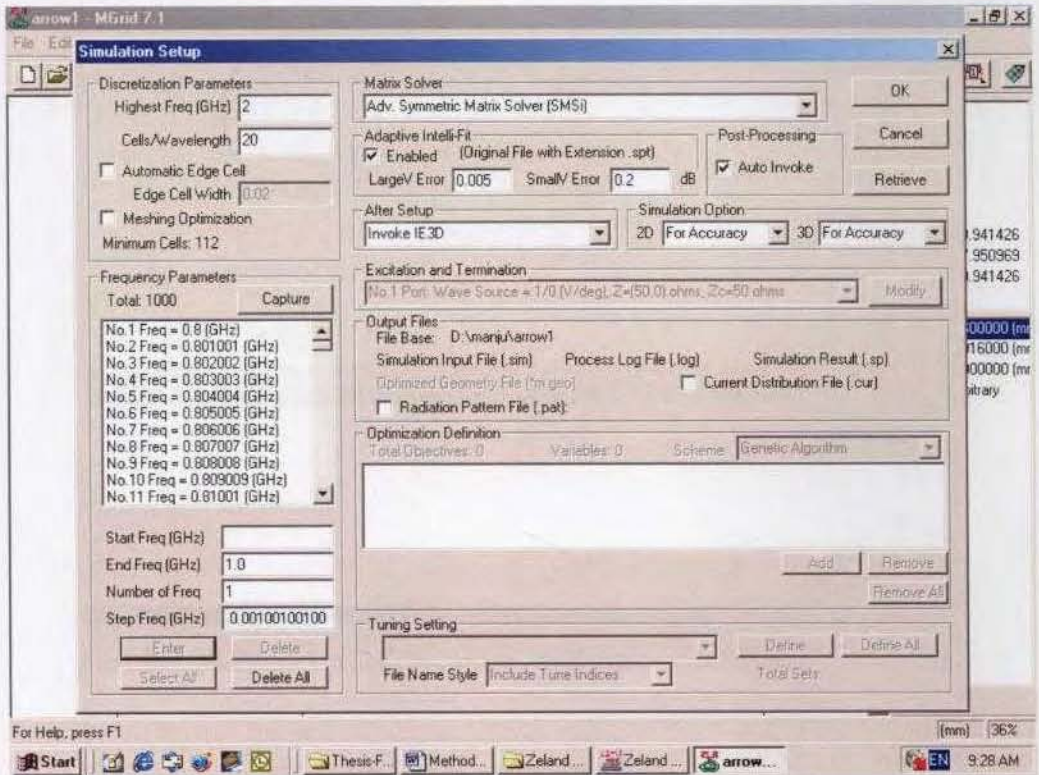


Figure 3.7 Figure showing the simulation setup dialog window

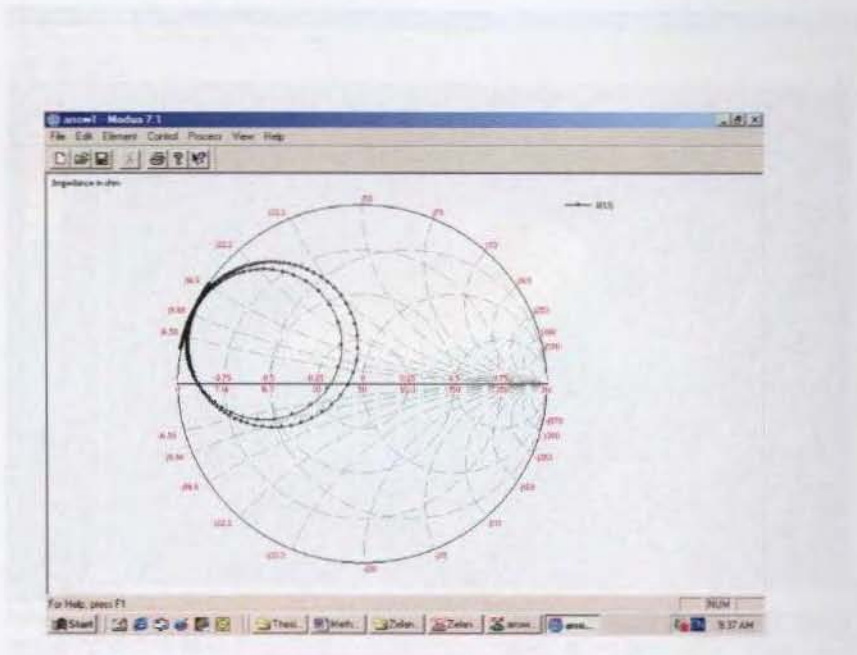


Figure 3.7 Figure showing the Smith chart plot after simulation in the IE3D MODUA window.

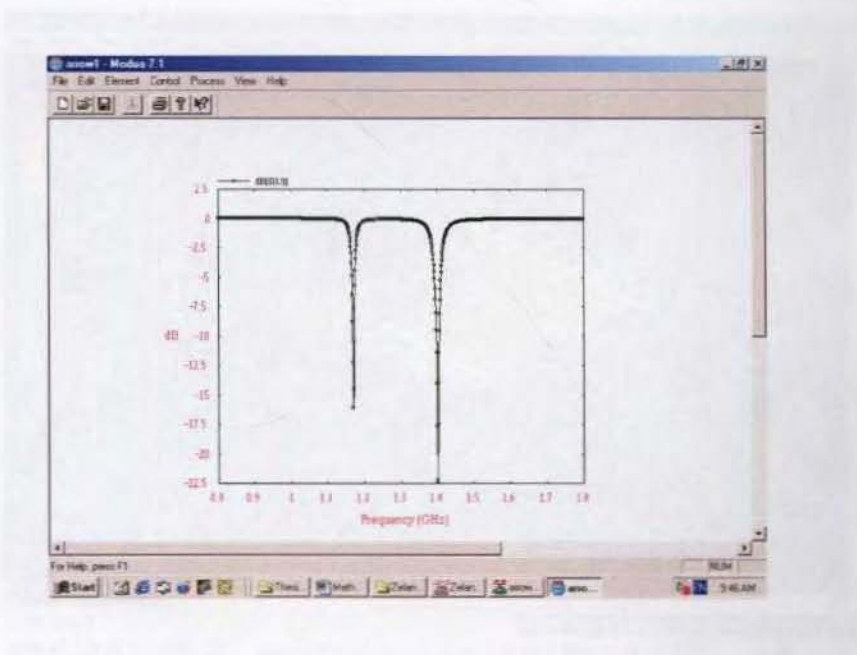


Figure 3.8 Figure showing the smith chart and return loss graph after simulation in the IE3D MODUA window.

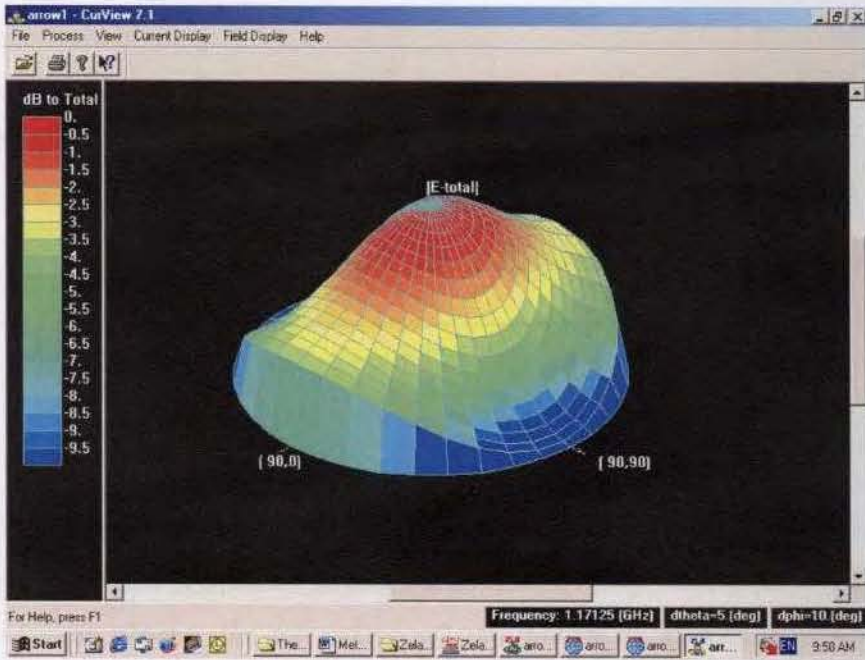


Figure 3.9 Figure showing the 3D radiation pattern in the Curview window

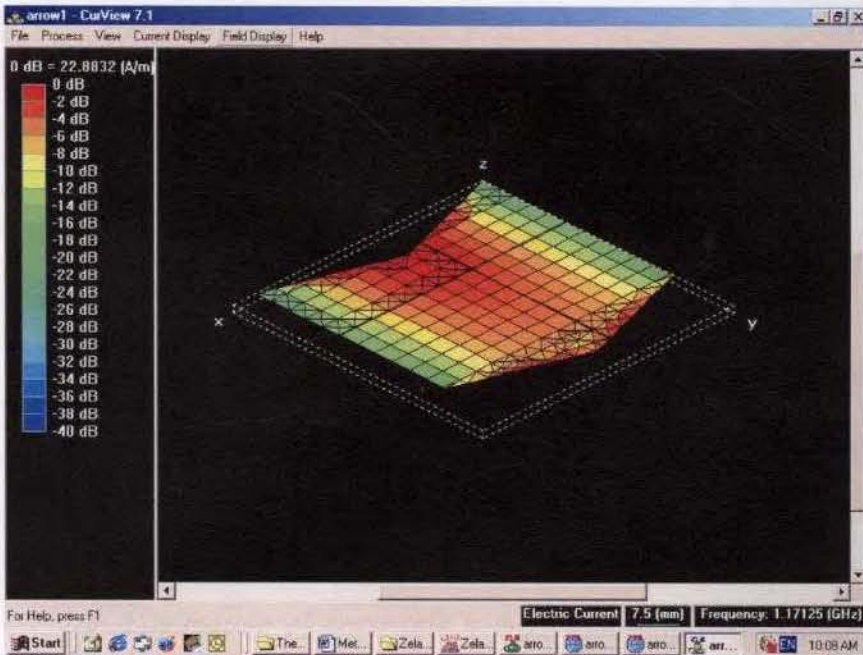


Figure 3.10 Figure showing the 3D average current density in the IE3D CURVIEW window.

CHAPTER 4

EXPERIMENTAL RESULTS AND OBSERVATIONS

This chapter gives the results obtained from the experiments carried out on compact dual frequency arrow shaped microstrip antennas. Dual band patch antennas obtains the advantage of simultaneously operating in more than one frequency bands which find applications in mobile satellite communication systems, personal communication systems, air-borne and space borne radar systems, global positioning systems etc. Miniaturization in the present world of communication demands more and more compact antennas. The experimental results and observations include

- ❖ Dual frequency excitation from arrow shaped co-axially fed microstrip antenna.*
- ❖ Generation of different polarization by trimming antenna parameters.*
- ❖ Excitation of additional resonances using single and double slots.*
- ❖ Improving the bandwidth by loading slots near non-radiating edges of the antenna.*
- ❖ Elimination of cross talk using isolated feeding ports to excite dual frequency antennas.*

4.1 ARROW SHAPED CO-AXIALLY FED PATCH ANTENNA FOR DUAL FREQUENCY OPERATION

4.1.1 GEOMETRY

The antenna geometry developed for attaining dual frequency operation is having the shape of an 'arrow'. The arrow shaped antenna shown in Figure 4.1(a) consists of patch of width 'W' and slanted lengths ' S_1 ' and ' S_2 ' etched on a substrate of thickness 'h' and dielectric constant ' ϵ_r '. The structure can be considered to be obtained from a rectangular patch of width 'W' and length 'L' by removing a triangle of height ' W_{cd} ' (intruding) and adding a triangle of height ' W_{cp} ' (protruding) as shown in Figure 4.1 (b). The different parameters of this patch are varied and their effects in the radiation characteristics are studied in detail.

4.1.2 EXCITATION TECHNIQUES

Coaxial feeding technique as explained earlier is used to couple microwave energy to the antenna. Feed point can be located on the edges or within the patch. Since the antenna resonates at two frequencies one corresponding to the width and the other corresponding to the slanted lengths, the feed point is placed inside the patch. The feed location inside the patch is properly selected to obtain good impedance match at both the resonances. The feed point location $F_p(x_0, y_0)$ inside the patch is shown in Figure 4.1 (c). Here (0, 0) is the geometric centre of the patch. The feed position is symmetrical about the 'Y' axis but unsymmetrical about the 'X' axis.

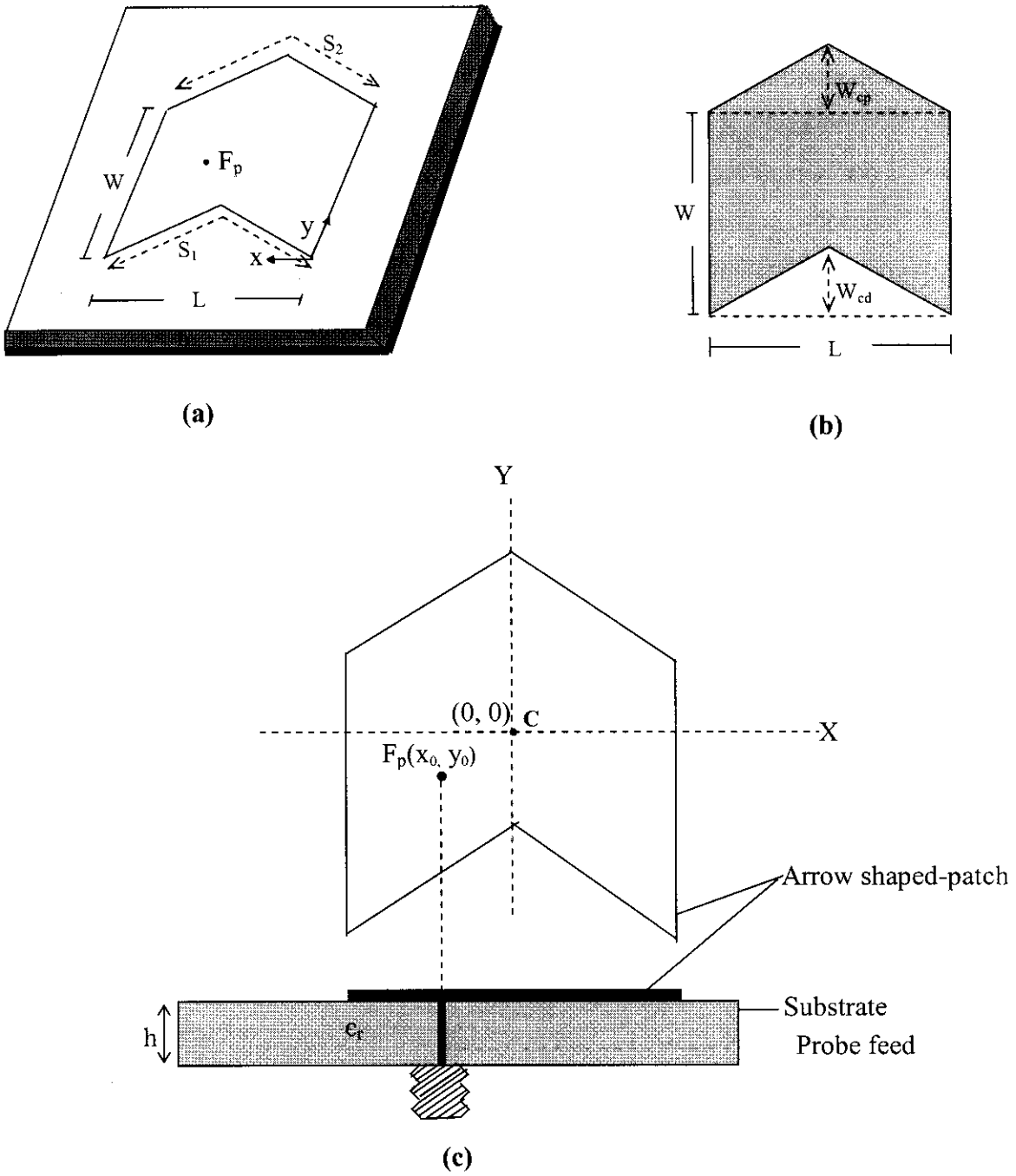


Figure 4.1 (a) Arrow shaped microstrip antenna (b) Patch Geometry
(c) Coaxial feeding

4.1.3 RESONANT MODES OF THE ARROW SHAPED ANTENNA

Resonant frequencies and their dependence on different antenna parameters are the important characteristics to be studied in detail. For a rectangular patch antenna, the resonant frequencies of TM_{10} and TM_{01} modes are determined by its length and width. In the arrow shaped patch, the resonances are obtained by width (TM_{01} mode) and slanted lengths (TM_{10} mode). The effective resonating length for TM_{10} mode depends on slanted lengths which can be modified by changing ' W_{cd} ' and ' W_{cp} '. In the case of TM_{01} mode, the effective resonating length is mainly the width ' W ' of the patch. The variation in resonances obtained by changing the antenna parameters is described in the following sections.

4.1.3.1 Variation with intruding triangle height ' W_{cd} ' of the patch

Variation of TM_{10} and TM_{01} mode frequencies with W_{cd} of the antenna is shown in Table 4.1. As W_{cd} increases the slanted length S_1 increases and hence TM_{10} mode frequency (f_{10}) decreases at a rapid rate for a small change in W_{cd} . TM_{01} mode frequency (f_{01}) remains almost constant since ' W ' is not affected by the changes. This is clearly demonstrated in Figure 4.2.

4.1.3.2 Variation with protruding triangle height ' W_{cp} ' of the patch

Table 4.2 shows the variation of TM_{10} and TM_{01} mode frequencies with W_{cp} of the antenna. The results show that the variation of W_{cp} slightly affects both the frequencies.

Table 4.1 Variation of TM_{10} and TM_{01} mode frequencies with intruding triangle height ' W_{cd} '

| L (cm) | W (cm) | W_{cp} (cm) | W_{cd} (cm) | h (cm) | ϵ_r | Frequency f_{01} (GHz) | Frequency f_{10} (GHz) |
|-----------|-----------|------------------|------------------|-----------|--------------|-----------------------------|-----------------------------|
| 3 | 5 | 1 | 1 | 0.16 | 4.28 | 1.432 | 2.164 |
| | | | 2 | | | 1.528 | 1.770 |
| | | | 3 | | | 1.605 | 1.412 |
| | | | 4 | | | 1.612 | 1.139 |
| | | | 5 | | | 1.600 | 0.932 |
| 4 | 5 | 1 | 1 | 0.16 | 4.28 | 1.424 | 1.691 |
| | | | 2 | | | 1.516 | 1.481 |
| | | | 3 | | | 1.582 | 1.242 |
| | | | 4 | | | 1.587 | 1.032 |
| | | | 5 | | | 1.579 | 0.850 |
| 5 | 5 | 1 | 1 | 0.16 | 4.28 | 1.387 | 1.412 |
| | | | 2 | | | 1.509 | 1.248 |
| | | | 3 | | | 1.560 | 1.080 |
| | | | 4 | | | 1.559 | 0.920 |
| | | | 5 | | | 1.545 | 0.761 |
| 6 | 5 | 1 | 1 | 0.16 | 4.28 | 1.401 | 1.171 |
| | | | 2 | | | 1.492 | 1.075 |
| | | | 3 | | | 1.529 | 0.956 |
| | | | 4 | | | 1.52 | 0.830 |
| | | | 5 | | | 1.509 | 0.692 |
| 7 | 5 | 1 | 1 | 0.16 | 4.28 | 1.393 | 1.016 |
| | | | 2 | | | 1.467 | 0.943 |
| | | | 3 | | | 1.488 | 0.851 |
| | | | 4 | | | 1.474 | 0.745 |
| | | | 5 | | | 1.465 | 0.622 |

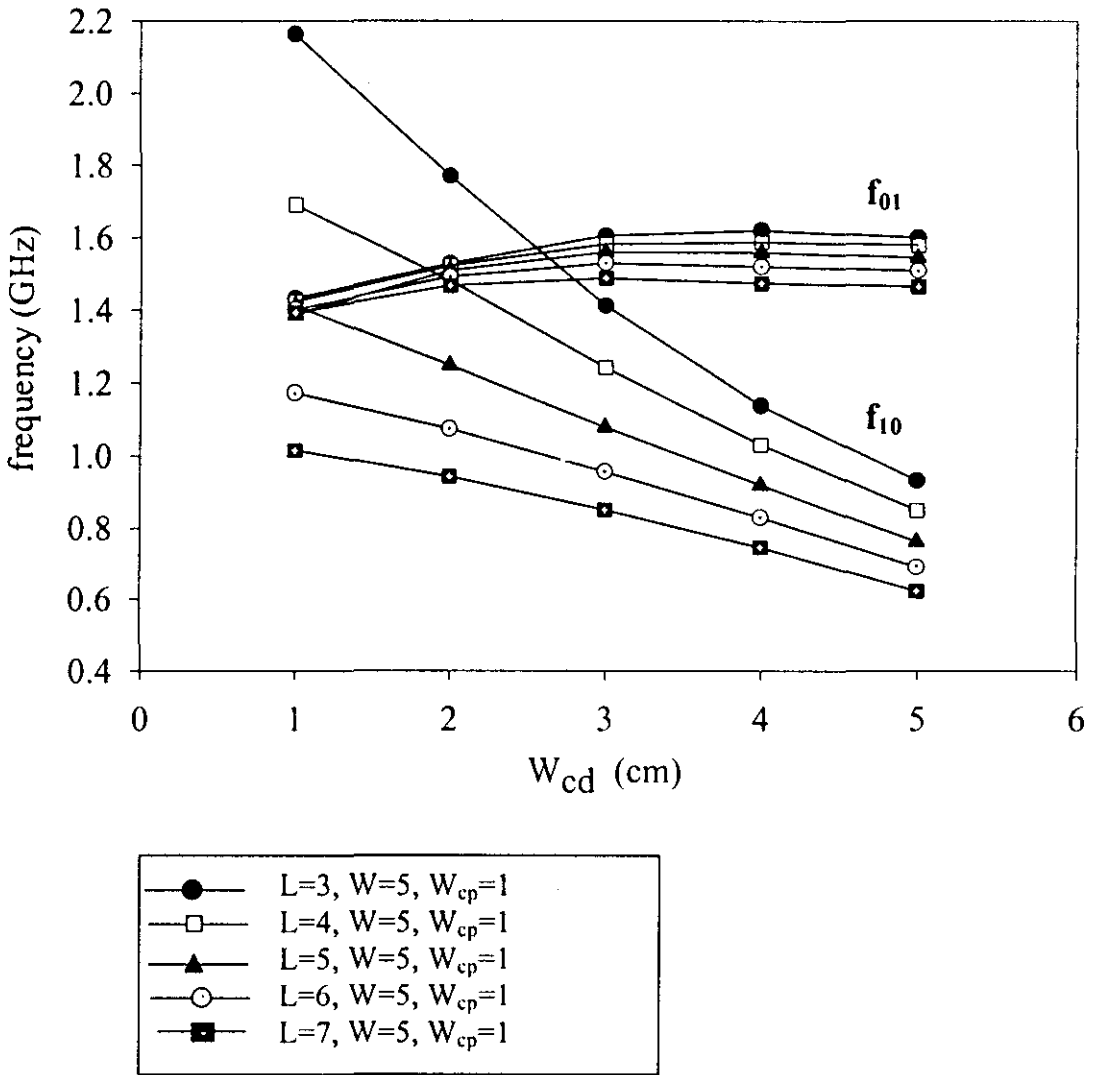


Figure 4.2 Variation of TM_{10} and TM_{01} mode frequencies with intruding triangle height W_{cd} ($\epsilon_r=4.28$, $h=0.16$ cm)

Table 4.2 Variation of TM_{10} and TM_{01} mode frequencies with protruding triangle height ' W_{cp} '

| L (cm) | W (cm) | W_{cp} (cm) | W_{cd} (cm) | h (cm) | ϵ_r | Frequency f_{01} (GHz) | Frequency f_{10} (GHz) |
|--------|--------|---------------|---------------|--------|--------------|--------------------------|--------------------------|
| 3 | 5 | 0.5 | 1 | 0.16 | 4.28 | 1.515 | 2.156 |
| | | 1.0 | | | | 1.432 | 2.164 |
| | | 1.5 | | | | 1.367 | 2.170 |
| | | 2.0 | | | | 1.296 | 2.172 |
| 4 | 5 | 0.5 | 1 | 0.16 | 4.28 | 1.501 | 1.682 |
| | | 1.0 | | | | 1.424 | 1.691 |
| | | 1.5 | | | | 1.352 | 1.697 |
| | | 2.0 | | | | 1.284 | 1.703 |
| 5 | 5 | 0.5 | 1 | 0.16 | 4.28 | 1.486 | 1.374 |
| | | 1.0 | | | | 1.412 | 1.387 |
| | | 1.5 | | | | 1.342 | 1.390 |
| | | 2.0 | | | | 1.275 | 1.394 |
| 6 | 5 | 0.5 | 1 | 0.16 | 4.28 | 1.480 | 1.159 |
| | | 1.0 | | | | 1.401 | 1.171 |
| | | 1.5 | | | | 1.331 | 1.179 |
| | | 2.0 | | | | 1.260 | 1.187 |
| 7 | 5 | 0.5 | 1 | 0.16 | 4.28 | 1.470 | 1.004 |
| | | 1.0 | | | | 1.393 | 1.016 |
| | | 1.5 | | | | 1.320 | 1.024 |
| | | 2.0 | | | | 1.249 | 1.027 |
| 8 | 5 | 0.5 | 1 | 0.16 | 4.28 | 1.458 | 0.883 |
| | | 1.0 | | | | 1.381 | 0.894 |
| | | 1.5 | | | | 1.307 | 0.902 |
| | | 2.0 | | | | 1.239 | 0.908 |

4.1.3.3 Resonant frequency variation with length 'L' of the patch

Arrow shaped antennas were constructed with different lengths 'L' keeping the other parameters constant. The variation in frequencies of the two modes is shown in Figure 4.3. TM_{10} mode frequency decreases rapidly with increase in 'L', TM_{01} mode remains almost constant, with a slight decrease with increase in the length of the antenna.

4.1.3.4 Effect of patch width 'W'

Variation of resonance frequencies of both modes with width 'W' of the patch is shown in Figure 4.4. As expected, there is a wide variation for TM_{01} mode frequency and slight variation for TM_{10} mode. TM_{10} mode frequency increases slightly with increase in the width of the patch.

4.1.3.5 Effect of varying height 'h' and permittivity ' ϵ_r ' of the substrate

Arrow shaped antennas were fabricated on substrates with different height 'h' and permittivity ' ϵ_r '. The resonant frequencies obtained are shown in Table 4.3. It is clear that both the frequencies decrease with the increase in the permittivity and increase in the height of the patch. The behavior is similar to that of a rectangular patch.

From these observations, it is concluded that TM_{10} mode frequency is determined mainly by slanted length. The TM_{01} mode frequency is determined by the effective width i.e., the combined effect of W, W_{cp} , W_{cd} . These conclusions are used for deducing the design equations, which will be explained in Chapter 5.

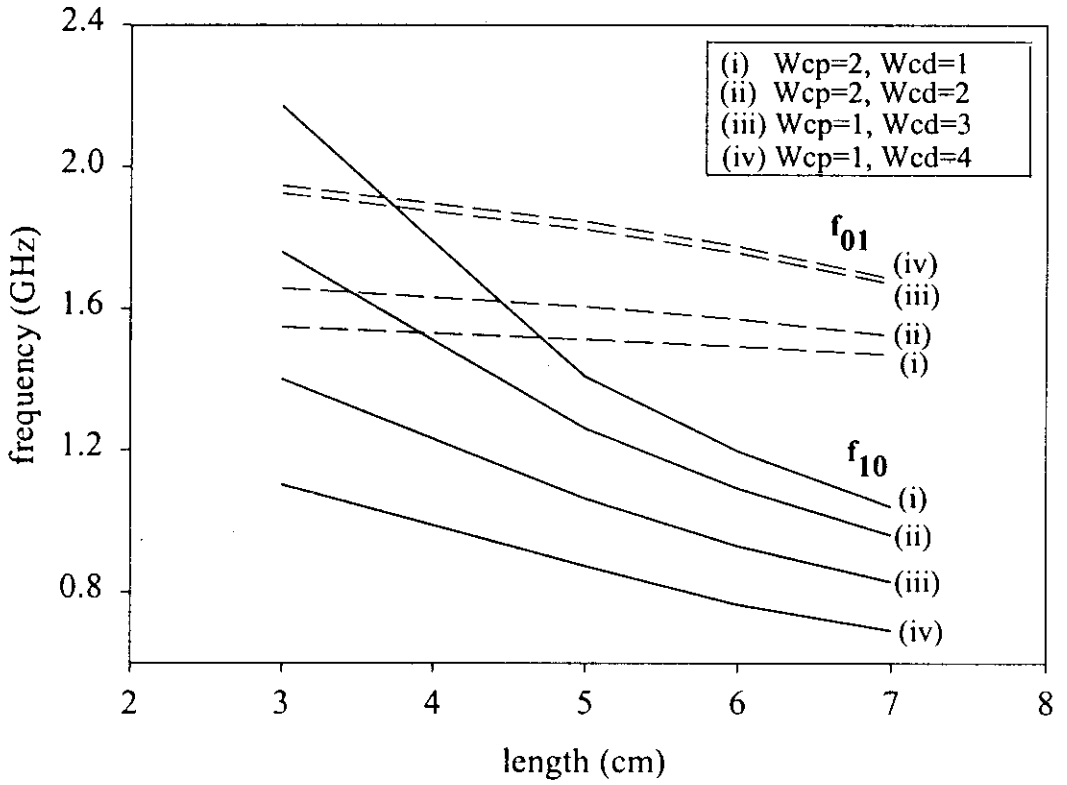


Figure 4.3 Variation of TM_{10} and TM_{01} mode frequencies with length L ($W=4\text{cm}$, $h=0.16\text{cm}$, $\epsilon_r=4.28$).

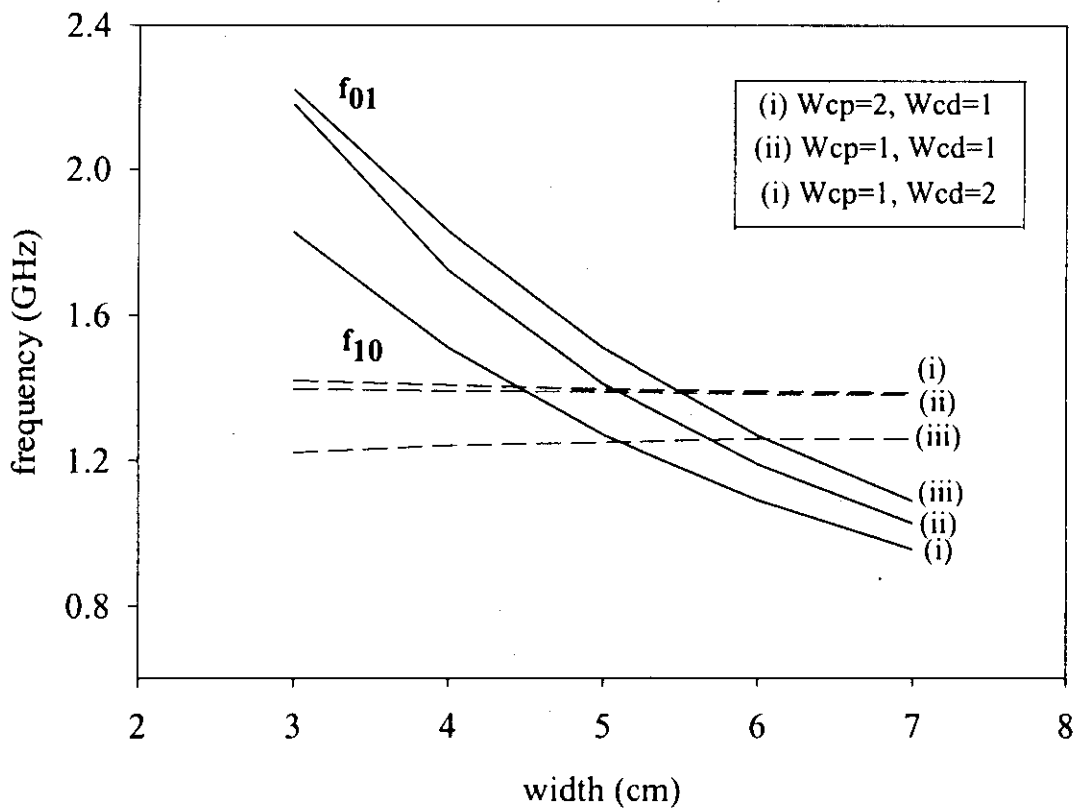


Figure 4.4 Variation of TM_{10} and TM_{01} mode frequencies with width W ($L=5\text{cm}$, $h=0.16\text{cm}$, $\epsilon_r=4.28$).

Table 4.3 Variation of TM_{10} and TM_{01} mode frequencies with height 'h' and permittivity ' ϵ_r '

| L (cm) | W (cm) | W_{cp} (cm) | W_{cd} (cm) | h (cm) | ϵ_r | Frequency f_{01} (GHz) | Frequency f_{10} (GHz) |
|-----------|-----------|------------------|------------------|-----------|--------------|-----------------------------|-----------------------------|
| 3 | 5 | 1 | 1 | 0.066 | 10.2 | 0.938 | 1.425 |
| | | | | 0.160 | 4.28 | 1.432 | 2.164 |
| | | | | 0.318 | 2.20 | 1.962 | 2.871 |
| | | | | 0.080 | 2.20 | 1.987 | 2.982 |
| 4 | 5 | 1 | 1 | 0.066 | 10.2 | 0.931 | 1.112 |
| | | | | 0.160 | 4.28 | 1.424 | 1.691 |
| | | | | 0.318 | 2.20 | 1.928 | 2.252 |
| | | | | 0.080 | 2.20 | 1.975 | 2.346 |
| 5 | 5 | 1 | 1 | 0.066 | 10.2 | 0.926 | 0.906 |
| | | | | 0.160 | 4.28 | 1.412 | 1.387 |
| | | | | 0.318 | 2.20 | 1.903 | 1.903 |
| | | | | 0.080 | 2.20 | 1.963 | 1.919 |
| 6 | 5 | 1 | 1 | 0.066 | 10.2 | 0.929 | 0.763 |
| | | | | 0.160 | 4.28 | 1.401 | 1.171 |
| | | | | 0.318 | 2.20 | 1.883 | 1.580 |
| | | | | 0.080 | 2.20 | 1.954 | 1.620 |
| 7 | 5 | 1 | 1 | 0.066 | 10.2 | 0.915 | 0.659 |
| | | | | 0.160 | 4.28 | 1.393 | 1.016 |
| | | | | 0.318 | 2.20 | 1.862 | 1.374 |
| | | | | 0.080 | 2.20 | 1.941 | 1.401 |
| 8 | 5 | 1 | 1 | 0.066 | 10.2 | 0.900 | 0.579 |
| | | | | 0.160 | 4.28 | 1.381 | 0.894 |
| | | | | 0.318 | 2.20 | 1.847 | 1.217 |
| | | | | 0.080 | 2.20 | 1.925 | 1.234 |

4.1.4 IE3D SIMULATION

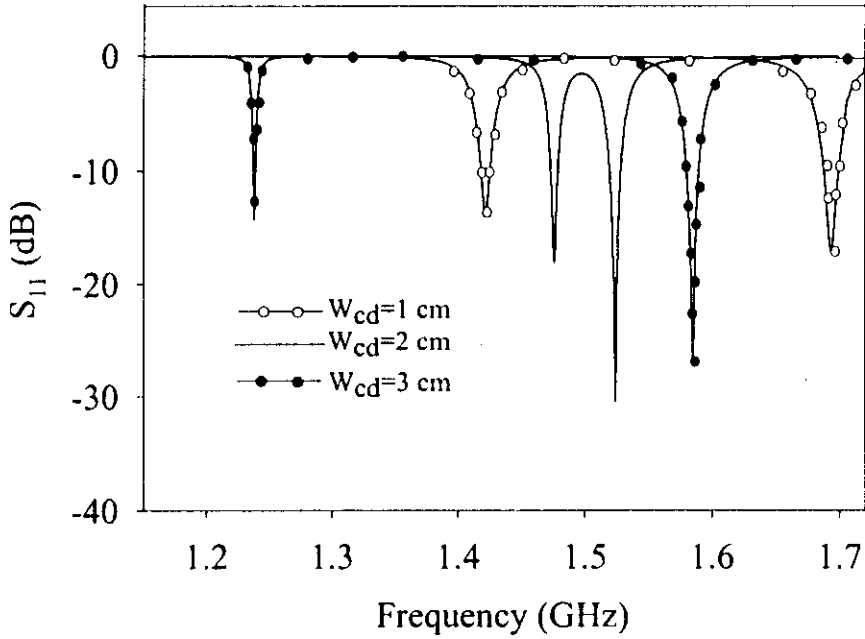
IE3D simulation code can be used to optimize the dimensions of the patches for a particular frequency design. We can also generate the radiation pattern, and various other characteristics using this simulation software as explained in chapter 3. This section gives details of the simulation measurements carried out using IE3D.

Variations of return loss with frequency for different antenna dimensions are shown in Figure 4.5 (a, b).

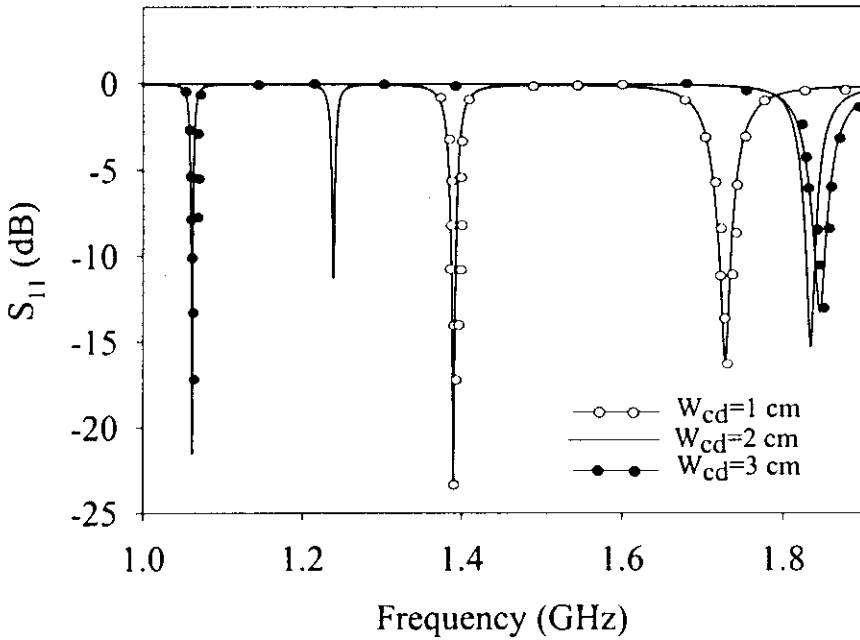
The radiation patterns and other characteristics like 3dB beam width, gain etc. obtained for different dimensions using the simulation results are shown in Figure 4.6 (a, b, c, d, e) and Figure 4.7 (a, b, c, d, e).

From the Figure 4.6 it is clear that for first frequency E-Plane copolar pattern is the plot at E_0 ($\Phi=90^\circ$) and for second frequency E-Plane copolar pattern is the plot at E_0 ($\Phi=0^\circ$). For H-Plane copolar pattern also for the two frequencies there is a phase difference of 90° . Hence the two frequencies excited are of opposite polarization.

From the simulated results, antenna optimum parameters for a particular resonance frequency are selected, which is fabricated for conducting measurements.



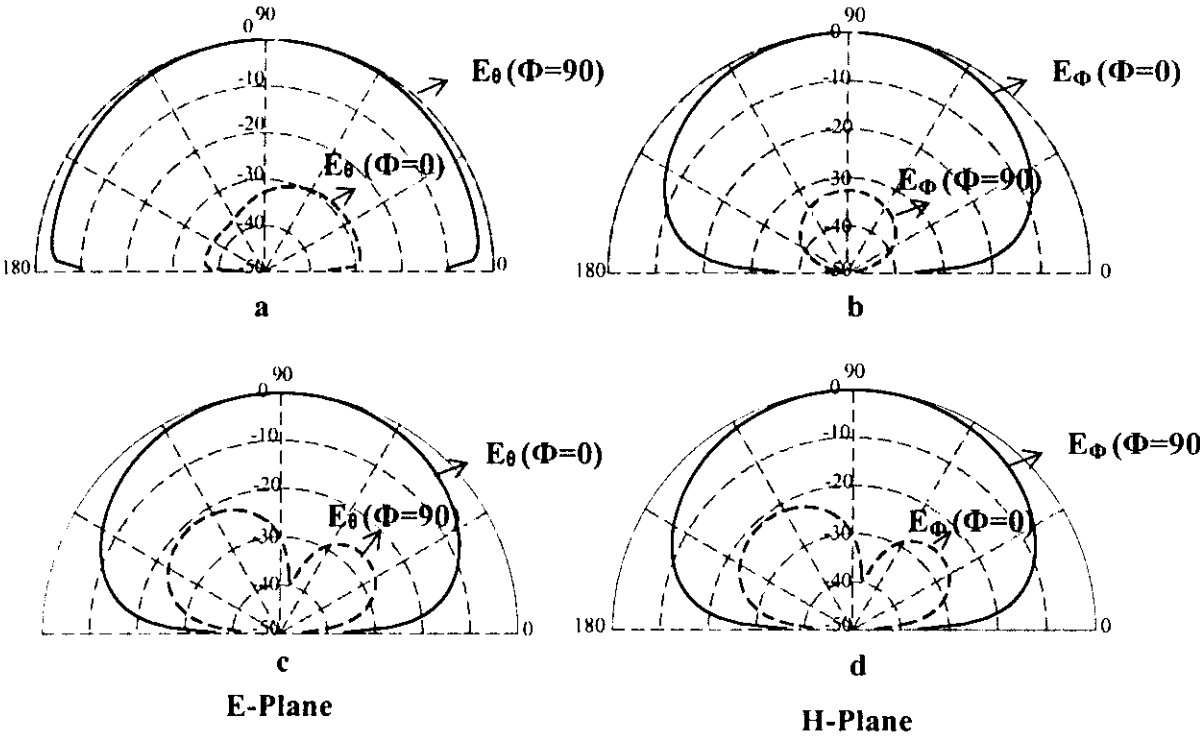
(a)



(b)

Figure 4.5 Variation of return loss with frequency for an arrow shaped antenna with different W_{cd}

(a) $L=4\text{ cm}$, $W=5\text{ cm}$, $W_{cp}=1\text{ cm}$ (b) $L=5\text{ cm}$, $W=4\text{ cm}$, $W_{cp}=1\text{ cm}$.



| Properties | Frequency (f_{01}) | Frequency (f_{10}) |
|------------------------|-------------------------|-------------------------|
| Frequency | 1.42 (GHz) | 1.69 (GHz) |
| Incident Power | 0.01 (W) | 0.01 (W) |
| Input Power | 0.00947559 (W) | 0.00942013 (W) |
| Radiated Power | 0.00736073 (W) | 0.0076949 (W) |
| Average Radiated Power | 0.000585748 (W/s) | 0.000612341 (W/s) |
| Radiation Efficiency | 77.6809% | 81.6858% |
| Antenna Efficiency | 73.6073% | 76.949% |
| Linear Gain | 4.92041dBi | 5.20551 dBi |
| Linear Directivity | 6.25121 dBi | 6.34348 dBi |
| 3dB Beam Width | (86.5187, 160.818) deg. | (83.0185, 160.724) deg. |

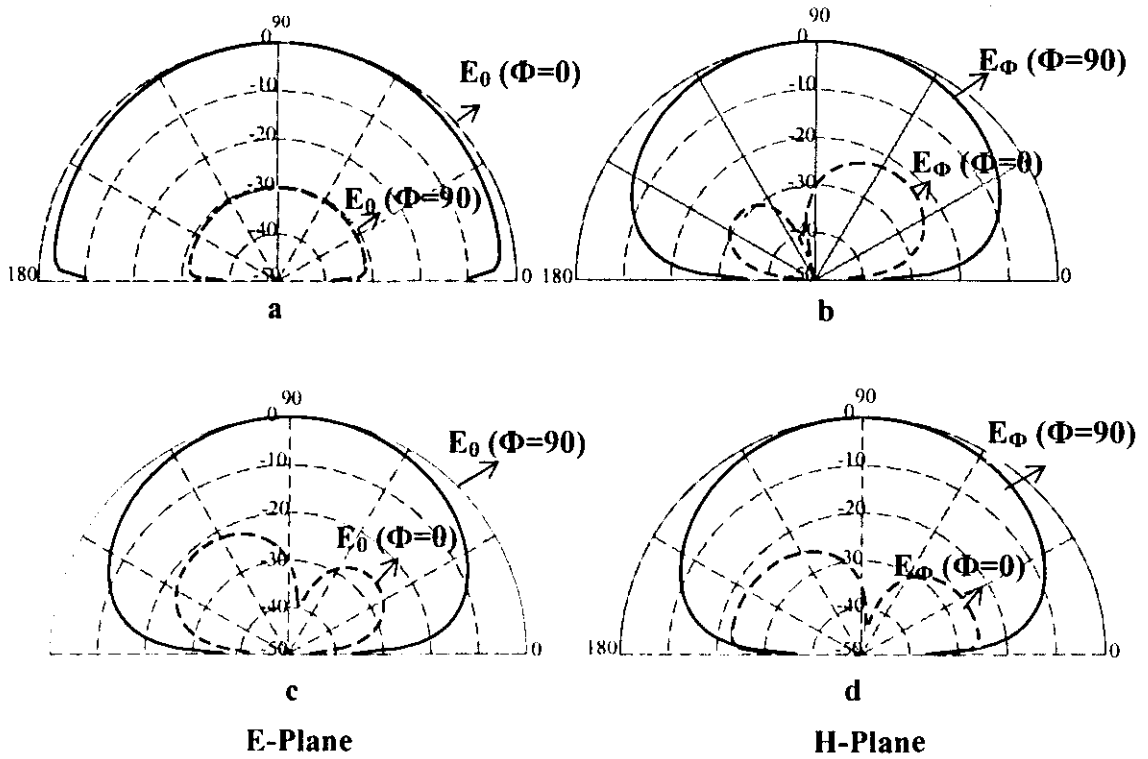
e) Frequency Properties

Figure 4.6 Simulated E-Plane and H-plane patterns of an arrow shaped antenna.

$L=4\text{cm}$, $W=5\text{cm}$, $W_{cp}=1\text{cm}$, $W_{cd}=1\text{cm}$.

(a, b) $f_{01}= 1.424\text{ GHz}$

(c, d) $f_{10}= 1.691\text{ GHz}$



| Properties | Frequency (f_{10}) | Frequency (f_{01}) |
|------------------------|-------------------------|-------------------------|
| Frequency | 1.39 (GHz) | 1.72 (GHz) |
| Incident Power | 0.01 (W) | 0.01 (W) |
| Input Power | 0.00997169 (W) | 0.00899654 (W) |
| Radiated Power | 0.0074693 (W) | 0.00754234 (W) |
| Average Radiated Power | 0.000594388 (W/s) | 0.0006002 (W/s) |
| Radiation Efficiency | 74.9051% | 83.836% |
| Antenna Efficiency | 74.693% | 75.4234% |
| Linear Gain | 4.94928 dBi | 5.1677 dBi |
| Linear Directivity | 6.21648 dBi | 6.39264 dBi |
| 3dB Beam Width | (86.7044, 162.638) deg. | (82.5855, 158.768) deg. |

e) Frequency Properties

Figure 4.7 Simulated E-Plane and H-plane patterns of an arrow shaped antenna

($L=5\text{cm}$, $W=4\text{cm}$, $W_{cp}=1\text{cm}$, $W_{cd}=1\text{cm}$, $h=0.16\text{cm}$, $\epsilon_r=4.28$).

(a, b) $f_{10}=1.39\text{GHz}$

(c, d) $f_{01}=1.727\text{GHz}$

4.1.5 TYPICAL ANTENNA DESIGN AND STUDY OF ITS CHARACTERISTICS

The data shown in Table 4.1, Table 4.2 and Table 4.3 reveals that choice of different parameters results into an optimum design for a desired frequency band. A typical antenna having dimensions $L= 8.6\text{cm}$, $W= 5\text{cm}$, $W_{cp}=0.5\text{cm}$, $W_{cd}=3.2\text{cm}$ is etched on a substrate of thickness $h=0.16\text{cm}$ and permittivity $\epsilon_r=4.28$ and its characteristics are studied. The antenna is excited by feeding at the point $f_p(x_0, y_0)$ where $x_0 = 0.6\text{cm}$ and $y_0 = 0.4\text{cm}$. The two resonance frequencies obtained are $f_{10} = 0.681\text{GHz}$ and $f_{01} = 1.44\text{GHz}$. The return loss characteristic of the antenna is shown in Figure 4.8.

4.1.5.1 Impedance Bandwidth

Since the microstrip antenna is primarily a resonating type of antenna its impedance bandwidth is quite narrow. It is defined as the range of frequencies over which $VSWR < 2$ (return Loss $> 10\text{dB}$). The bandwidth for the TM_{10} mode is 1.28% and for TM_{01} mode is 1.91% which are typical values for standard rectangular and circular patches.

4.1.5.2 Radiation Pattern

E and H plane patterns for the antenna are plotted for both the modes. The measured copolar and crosspolar radiation patterns at the corresponding central frequencies are shown in Figure 4.9 (a, b). The 3-dB beam width for H-Plane pattern of f_{10} and f_{01} are 106° and 89° respectively. For E-plane pattern the values are 104° and 90° . The beam widths of this antenna are comparable to that of a rectangular patch antenna. The cross polar levels are found to be less than -20dB .

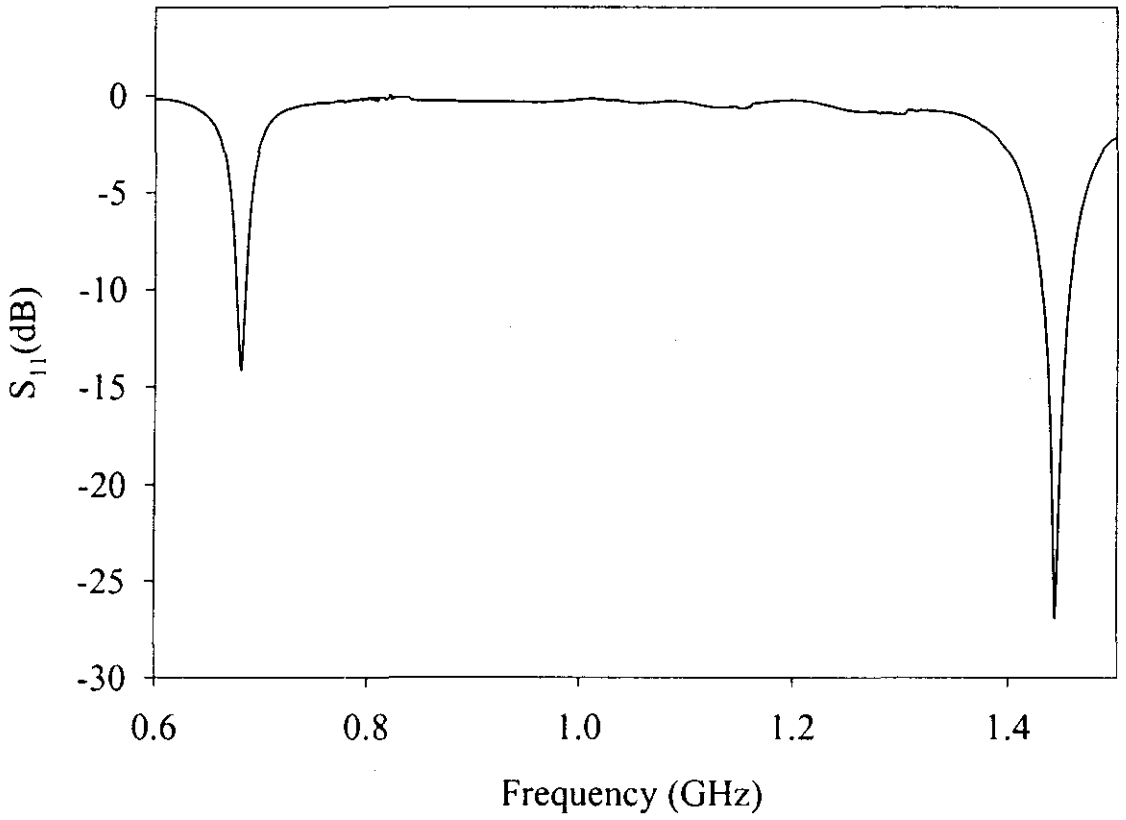


Figure 4.8 Variation of return loss with frequency for a typical antenna
($L=8.6$ cm, $W=5$ cm, $W_{cp}=0.5$ cm, $W_{cd}=3.2$ cm)

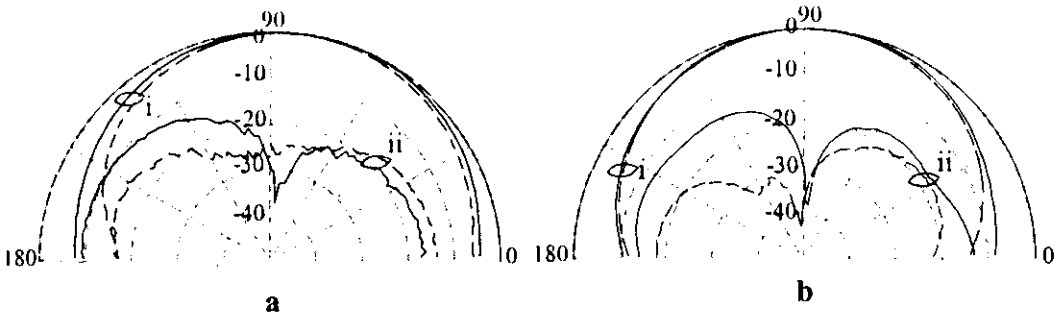


Figure 4.9 E- Plane and H- Plane radiation pattern (a) for $f_{01} = 0.681$ GHz and (b) for $f_{01} = 1.44$ GHz

(i) Copolar

(ii) Crosspolar

—— E-Plane

----- H-Plane

4.1.5.3 Gain

Relative gain of the antenna is measured as explained earlier. Gain is compared to that of a rectangular microstrip antenna resonating at the same frequency fabricated on the same substrate and is found to be reduced by ~2dB as shown in figure 4.10. This small reduction in gain due to reduction in patch area can be compensated by integrating suitable amplifier circuits [83] or loading with suitable superstrates.

4.1.5.4 Compactness

The patch area of the typical antenna constructed is compared with other standard microstrip patches in Table 4.4. The antenna provides an area reduction of ~68% for the TM_{10} mode frequency compared to the rectangular patch designed for the same frequency. From the data it can also be noted that the antennas provide greater area reduction and improved gain [figure 4.10] compared to compact drum shaped patches. This compactness is achieved with out any degradation in radiation pattern and bandwidth.

Table 4.4 Comparison of characteristics of arrow shaped, rectangular and drum shaped antennas

| Antenna Characteristics | Rectangular patch | Arrow shaped antenna | | Drum shaped antenna | |
|--|-------------------|----------------------|----------|---------------------|----------|
| Resonant Frequencies (GHz) | f_{10} | f_{10} | f_{01} | f_{10} | f_{01} |
| | .681 | .681 | 1.44 | .681 | 1.44 |
| Gain Compared to rectangular patch for f_{10} (dB) | 0 | -2 | | -5 | |
| Overall Area (cm ²) for f_{10} | 136 | 45.15 | | 52.8 | |
| % Area reduction for f_{10} compared to standard rectangular patch designed for the same frequency | - | ~67 | | ~61 | |

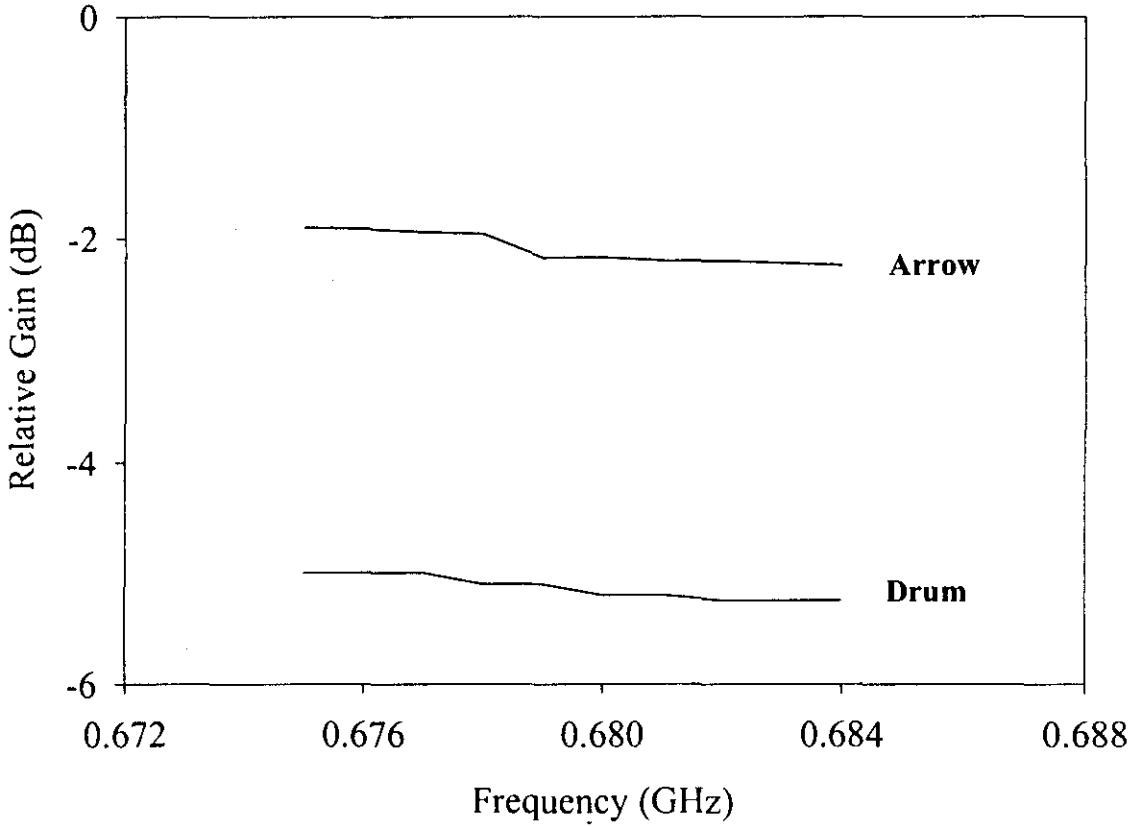


Figure 4.10 Comparison of relative gain of the arrow shaped antenna ($L=8.6\text{cm}$, $W=5\text{cm}$, $W_{cp}=0.5\text{cm}$, $W_{cd}=3.2\text{cm}$) and compact drum shaped antenna over a band with centre frequency at $f_{10}=0.681\text{GHz}$.

4.1.6 FREQUENCY RATIO TUNING

The value of the two orthogonal polarized resonant frequencies f_{10} and f_{01} depend on the different antenna parameters as inferred from Table 4.1, 4.2 and 4.3. So by properly selecting the patch parameters, desired frequency ratio can be achieved. The dual frequency design presented here provides a tunable frequency ratio of 1.36 to 2.47 for the two operating frequencies as shown in Table 4.5.

Table 4.5 Dimensions, TM_{10} mode frequency, TM_{01} mode frequency and frequency ratio of various arrow shaped microstrip antenna showing frequency tuning.

| L, W, Wcp, Wcd (cm) | h (cm) | ϵ_r | TM_{10} mode frequency (f_{10}) (GHz) | TM_{01} mode frequency (f_{01}) (GHz) | Frequency Ratio (f_{01})/ (f_{10}) |
|---------------------------|-----------|--------------|---|---|---|
| 8, 5, 2.0, 1.0 | 0.16 | 4.28 | 0.9086 | 1.239 | 1.36 |
| 8, 5, 1.0, 1.5 | | | 0.9025 | 1.307 | 1.44 |
| 8, 5, 1.0, 1.0 | | | 0.8945 | 1.378 | 1.54 |
| 8, 5, 0.5, 1.0 | | | 0.8833 | 1.458 | 1.65 |
| 8, 5, 1.0, 2.0 | | | 0.8372 | 1.436 | 1.71 |
| 8, 5, 1.0, 3.0 | | | 0.7598 | 1.438 | 1.89 |
| 8, 5, 1.0, 4.0 | | | 0.6737 | 1.418 | 2.10 |
| 8, 5, 1.0, 5.0 | | | 0.5725 | 1.415 | 2.47 |

4.2 ELECTROMAGNETICALLY COUPLED ARROW SHAPED ANTENNA

In the following experiments to change the antenna characteristics like polarization, bandwidth etc. electromagnetic coupling as explained earlier is used to couple EM energy due to the flexibility in determining the matching point. A microstrip feed line having impedance of 50 ohm etched on a separate substrate and placed below the patch, act as the feeding element. Geometry of the arrow shaped microstrip antenna using e. m. coupled microstrip feed is shown in Figure 4.11.

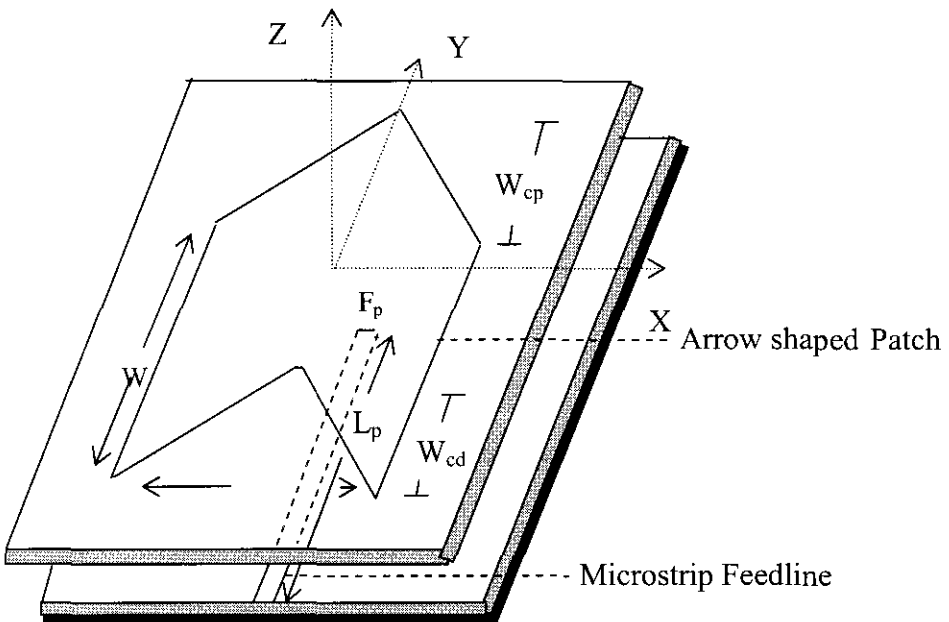


Figure 4.11 Geometry of the arrow shaped microstrip antenna using microstrip feed.

4.2.1 POLARISATION DIVERSITY

The arrow shaped microstrip antenna can be modified so as to excite waves of different polarizations. The polarization diversity is obtained by changing the various parameters and properly choosing at the feed point.

A typical antenna having dimensions $L = 4\text{cm}$, $W = 6\text{cm}$, $W_{cp} = 1\text{ cm}$ is etched on a substrate of thickness ' h ' = 0.16cm and permittivity ' ϵ_r ' = 4.28. The antenna is excited by electromagnetic coupling using a 50 ohm feed line fabricated on the same substrate. W_{cd} is varied and the polarization diversity is studied in detail. The results so obtained given in Table 4.6 and Figure 4.12 shows

- Dual-band dual polarization operation
- Circular Polarization
- Dual band, one with linear and the other with Circular Polarization

Dual polarized microstrip antennas with enhanced bandwidth and well defined radiation characteristics can be used in air-borne and space-borne based SAR systems.

Circularly polarized (CP) radiators are employed in radars to provide response to a linearly polarized wave of arbitrary orientation and for the suppression of precipitation of clutter.

For dual band antennas with dual polarization operation (one circular and one linear); linearly polarized one can be used for terrestrial communication and circularly polarized one can be used for satellite mobile communication.

This section gives a brief description of design techniques of different polarized radiators together with some useful experimental results.

Table 4.6 Table showing the variation of frequencies and polarizations with W_{cd}

| W_{cd} (cm) | f_1 (GHz) | f_2 (GHz) | Polarization | |
|------------------|----------------|----------------|--------------|-----------|
| | | | For f_1 | For f_2 |
| 2.0 | 1.300 | 1.535 | Linear | Linear |
| 3.0 | 1.302 | 1.373 | Linear | Linear |
| 3.5 | 1.340 | - | Circular | - |
| 4.0 | 1.033 | 1.405 | Circular | Linear |
| 5.0 | 0.954 | 1.405 | Linear | Linear |

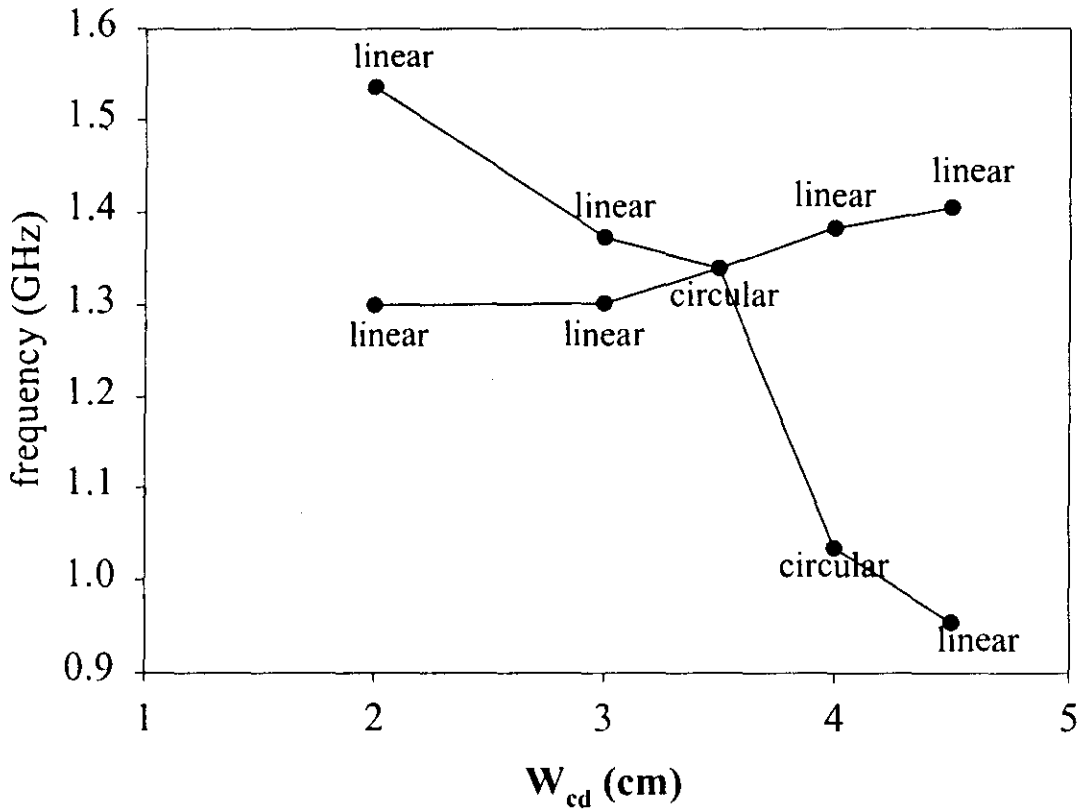


Figure 4.12 Graph showing the variation in polarization obtained by trimming the width W_{cd} ($L = 4\text{cm}$, $W = 6\text{cm}$, $W_{cp} = 1\text{ cm}$, $h=0.16\text{cm}$, $\epsilon_r=4.28$)

4.2.1.1 Circularly Polarized Radiator – Antenna design and experimental results

In this section the design details of an arrow shaped microstrip antenna giving Circular Polarization is discussed. Circularly polarized antennas are widely used as efficient radiators in communication systems, remote sensing, navigation and radar. At present mobile-satellite-communication and direct-broadcasting satellite systems use circular polarization, as they do not need polarization tracking.

The configuration of a single-fed CP antenna is as shown in Figure 4.11. The principle of this antenna is based on the fact that by properly setting the intruding triangle height ' W_{cd} ', two orthogonal mode frequencies f_{10} and f_{01} merge to give CP at a single frequency. This enables the antenna to act as a CP radiator in spite of single feeding.

Antenna is excited by electromagnetic coupling using a microstrip feed line of length L_p at F_p as shown in the figure. The optimum design values obtained by IE3D simulation is implemented and investigated. It has dimensions $L=4$ cm, $W=4$ cm, $W_{cp}=1.9$ cm, $W_{cd}=1.5$ cm and is fabricated on a substrate of $\epsilon_r=4.28$ and $h=0.16$ cm.

Figure 4.13 shows the measured return loss against frequency of the antenna. The merging of two near-degenerate resonant modes is clearly seen in the figure.

The axial ratio of the antenna in the band is measured using a rotating linearly polarized standard horn antenna. The variation of axial ratio with frequency is shown in Figure 4.14. The centre frequency, defined to be the frequency with minimum axial ratio, is 1.653 GHz, with a 3 dB axial ratio bandwidth of 1.2%. Figure 4.15 shows E-Plane and H-plane radiation patterns at centre frequency.

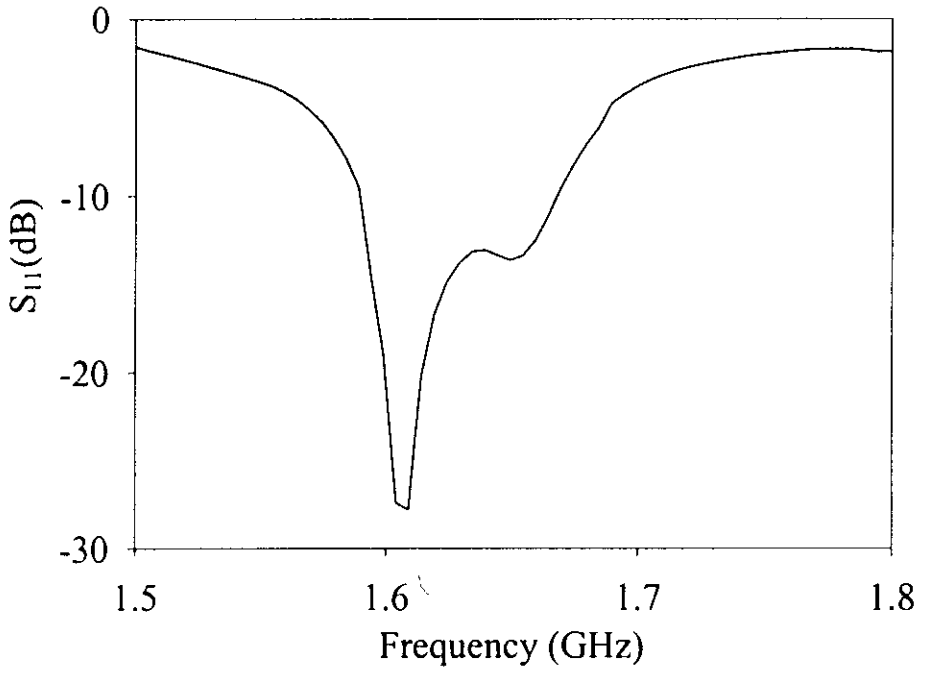


Figure 4.13 Measured return loss against frequency for the CP radiator at centre frequency 1.653 GHz ($L=4$ cm, $W=4$ cm, $W_{cp}=1.9$ cm, $W_{cd}=1.5$ cm, $h=0.16$ cm, $\epsilon_r=4.28$)

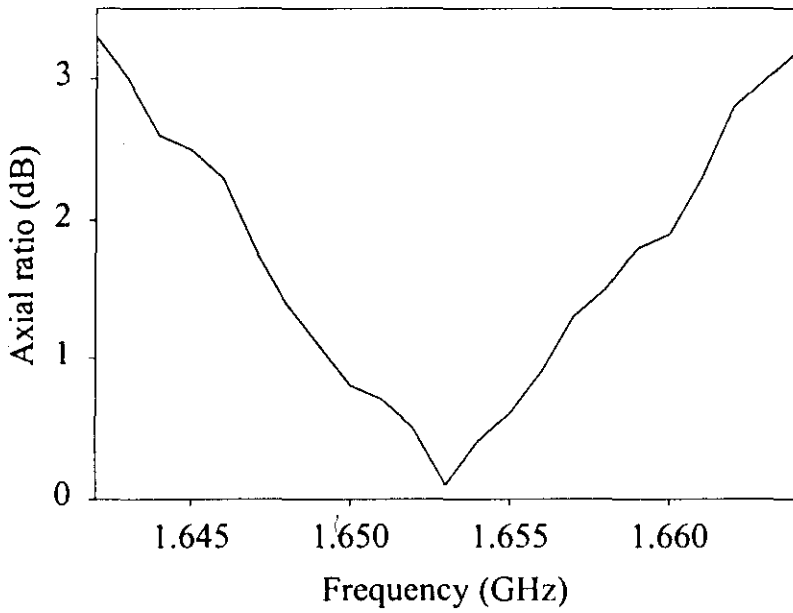


Figure 4.14 Measured axial ratio against frequency ($L=4$ cm, $W=4$ cm, $W_{cp}=1.9$ cm, $W_{cd}=1.5$ cm, $h=0.16$ cm, $\epsilon_r=4.28$)

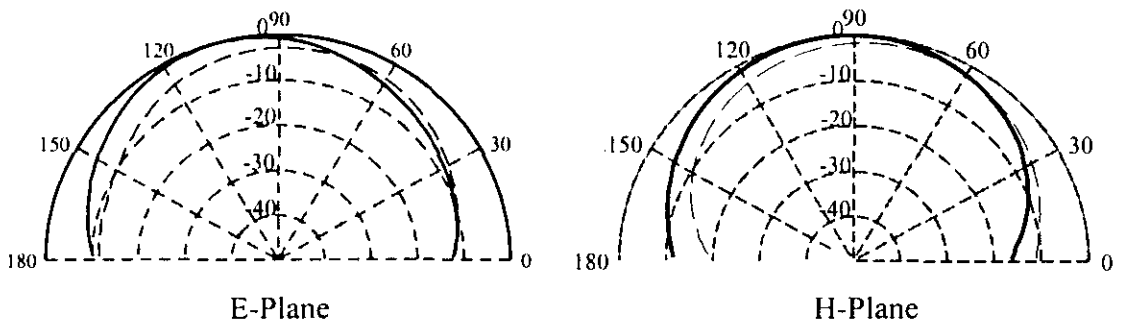


Figure 4.15 E-Plane and H-plane patterns at the centre frequency

($L=4$ cm, $W=4$ cm, $W_{cp}=1.9$ cm, $W_{cd}=1.5$ cm, $h=0.16$ cm, $\epsilon_r=4.28$)

———— Co-Polar
 - - - - - Cross-Polar

4.2.1.2 Dual frequency design : One linear polarization and other circular polarization

Arrow shaped antenna geometry for two bands- one linear and one circular, is proposed and studied. Multiband, multimode handsets or data transmissions capable of communicating with terrestrial and satellite networks find wide application in the fast developing world of mobile communications. A dual band, dual polarized antenna capable of receiving both linearly and circularly polarized waves can be used for this purpose. Relatively very few designs are available in the open literature for achieving the above requirement.

Figure 4.11 shows the geometry of the proposed microstrip antenna. It has dimensions $L=4$ cm, $W =6$ cm, $W_{cp}=1$ cm, $W_{cd}=4$ cm and is fabricated on a substrate of $\epsilon_r = 4.28$ and $h=0.16$ cm. A microstrip feed line of length $L_p = 7$ cm and width $W_p = 0.3$ cm is used to provide electromagnetic coupling.

Figure 4.16 shows the measured return loss against frequency of the antenna. The antenna is resonating at two frequencies 1.0336 GHz and 1.394 GHz. S_{21} measurement with a rotating linearly polarized antenna showed that the radiation at 1.0336 GHz is circularly polarized and that at 1.394 GHz is linearly polarized.

Figure 4.17 (a, b, c, d) show the E-Plane and H-Plane radiation patterns at first and second resonant frequencies. The variation of axial ratio with frequency is shown in figure 4.18. The 3dB axial ratio bandwidth of the circularly polarized band is nearly 1%. 2:1 VSWR bandwidth for the linearly polarized band is 2.41%

From the experimental observations it is found that these properties are achieved with a size reduction of $\sim 70\%$ compared to conventional rectangular patch antenna.

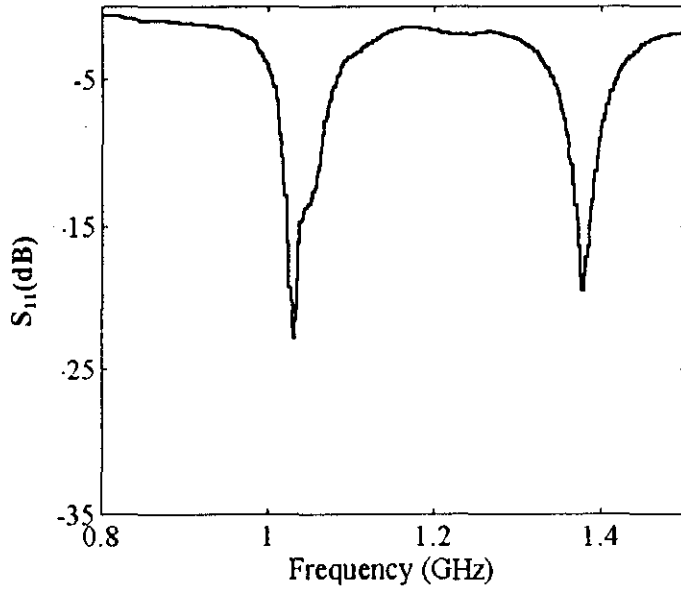


Figure 4.16 Variation of return loss with frequency of an arrow shaped antenna designed for one linear and one circularly polarized band

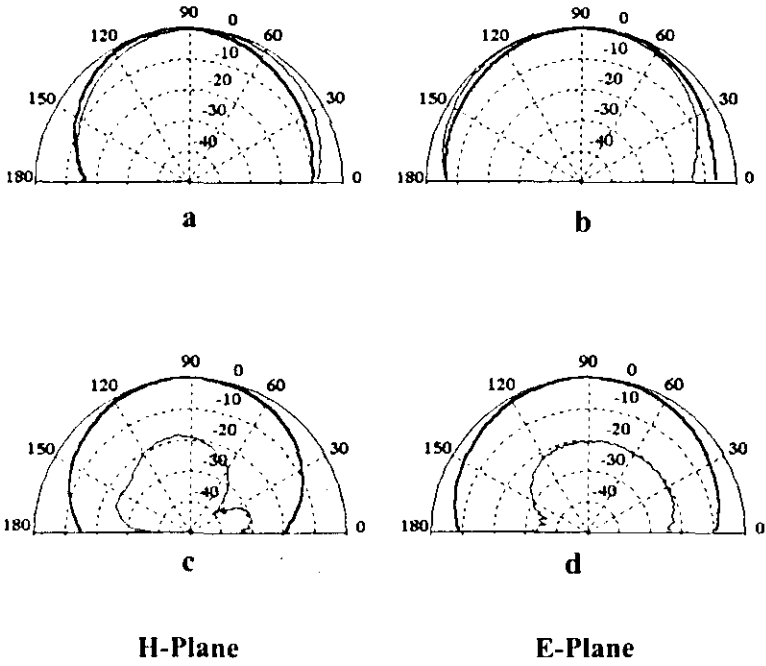


Figure 4.17 H-plane and E-plane patterns (a, b) for circularly polarized band at 1.033 GHz and (c, d) for linearly polarized band at 1.394 GHz.

—— Co-Polar
 - - - - Cross-Polar

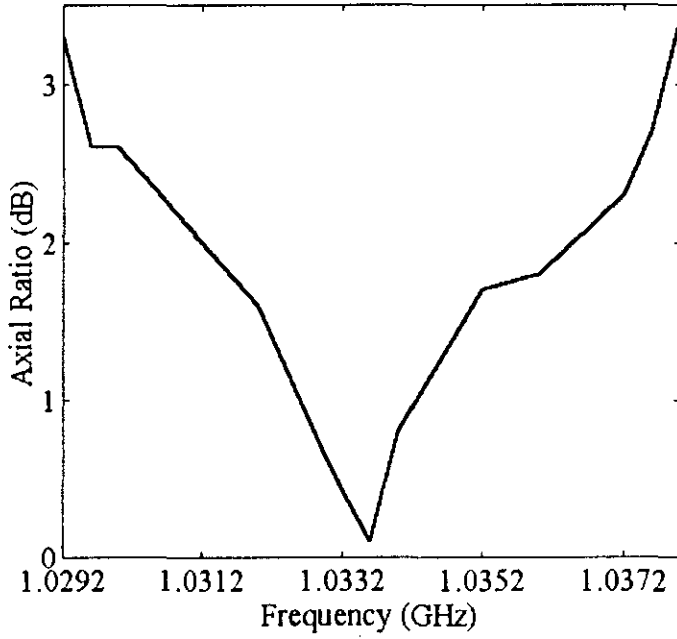


Figure 4.18 Measured axial ratio against frequency for the CP band at 1.033 GHz

4.3 SLOT LOADED ARROW SHAPED MICROSTRIP ANTENNA

Slot loading techniques can be employed in microstrip patches to excite a new resonant frequency other than the fundamental modes. This new excited frequency has same or different polarizations compared to the fundamental frequency of the patch antenna. Also, this frequency can be tuned by changing the dimensions of the slot. By introducing slots of proper size and shape, two adjacent resonant modes with similar polarization and radiation characteristics can be excited, which significantly enhances the bandwidth of the antenna. Due to the presence of slot in the patch, the large inductive reactance component of the input impedance for the feed is found to be reduced, making the impedance matching very easy. Experimental results on arrow shaped patch antenna with different types of slot loading are presented and discussed in the following sections.

4.3.1 ARROW SHAPED ANTENNA WITH A SINGLE RECTANGULAR SLOT

Arrow shaped microstrip antenna with a single rectangular slot is proposed in this section. By embedding a rectangular slot in the patch an additional resonance frequency having opposite polarization compared to the TM_{10} mode is generated. This new frequency is much lower than the TM_{01} mode frequency of the patch without slot and may be considered as $TM_{0\delta}$ ($0 < \delta < 1$) mode [97]. The ratio between the two resonant frequencies can be tuned in a wide range 1 to 1.86 by changing the slot length. For a particular slot length two nearby orthogonal mode frequencies are excited and gives circular polarization.

4.3.1.1 Antenna Geometry

The proposed configuration of a dual frequency arrow shaped patch antenna with rectangular slot is shown in Figure 4.19. A slot having a dimensions of $l_s \times w_s$ is placed at a distance 's' from the edge. The ratio between the two operating frequencies can be tuned by changing the length of the slot. The antenna is excited by electromagnetic coupling using a 50Ω microstrip feed line.

4.3.1.2 Experimental Results

Arrow shaped antenna with an embedded slot is implemented and investigated. It has dimensions $L = 6\text{cm}$, $W = 3\text{cm}$, $W_{cp} = 1\text{cm}$ and $W_{cd} = 2\text{cm}$ and is fabricated on a substrate of thickness $h=0.16\text{cm}$ and dielectric constant $\epsilon_r=4.28$. A rectangular slot having dimensions $l_s = 5\text{cm}$, and $w_s = 2\text{cm}$ is etched at a distance $s = 0.5\text{cm}$ from the edge. A 50 ohm microstrip feed line is etched on a substrate of same thickness and permittivity and kept below the antenna to provide electromagnetic coupling.

Figure 4.20 shows the measured return loss against frequency for different slot lengths. It is found that the frequency ratio is changing with length of the slot. Variation of dual frequencies and the frequency ratio with slot length is presented in Table 4.7.

The two modes have different polarization planes and similar radiation patterns. Figure 4.21 (a, b, c, d) show the radiation patterns of the antenna having slot length $l_s = 5\text{cm}$ for the two resonances at 1.09 GHz and 1.34 GHz respectively. For slot length $l_s = 5.8\text{cm}$ two nearby frequencies of orthogonal polarization are excited and gives circular polarization as shown in Figure 4.20.

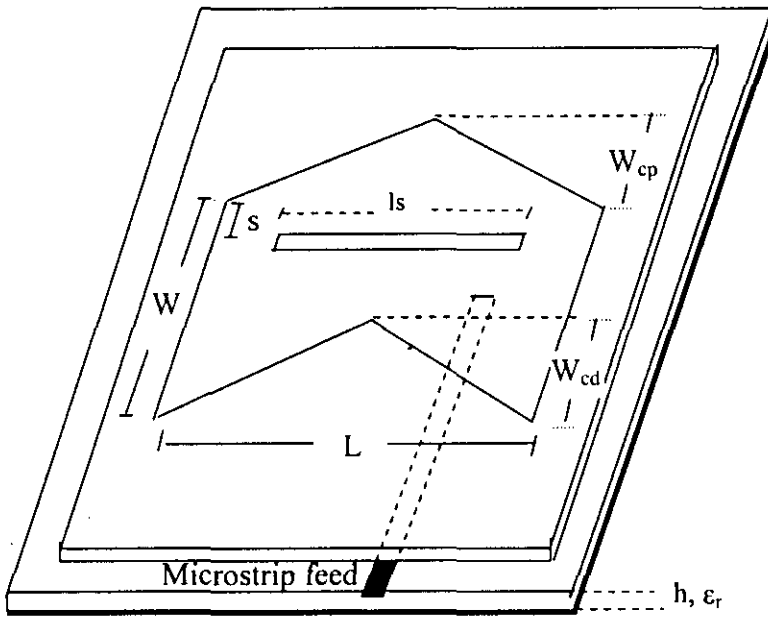


Figure 4.19 Geometry of the arrow shaped microstrip antenna with a rectangular slot.

Table 4.7 Variation of frequencies and the frequency ratio with slot length (l_s) for a typical patch designed

| Slot Length l_s (cm) | Frequency | | Frequency Ratio f_2/f_1 |
|---------------------------|-------------|-------------|------------------------------|
| | f_1 (GHz) | f_2 (GHz) | |
| 2.0 | 1.060 | 1.980 | 1.86 |
| 4.0 | 1.078 | 1.583 | 1.46 |
| 5.0 | 1.090 | 1.340 | 1.22 |
| 5.8 | 1.0875 (CP) | | 1.00 |

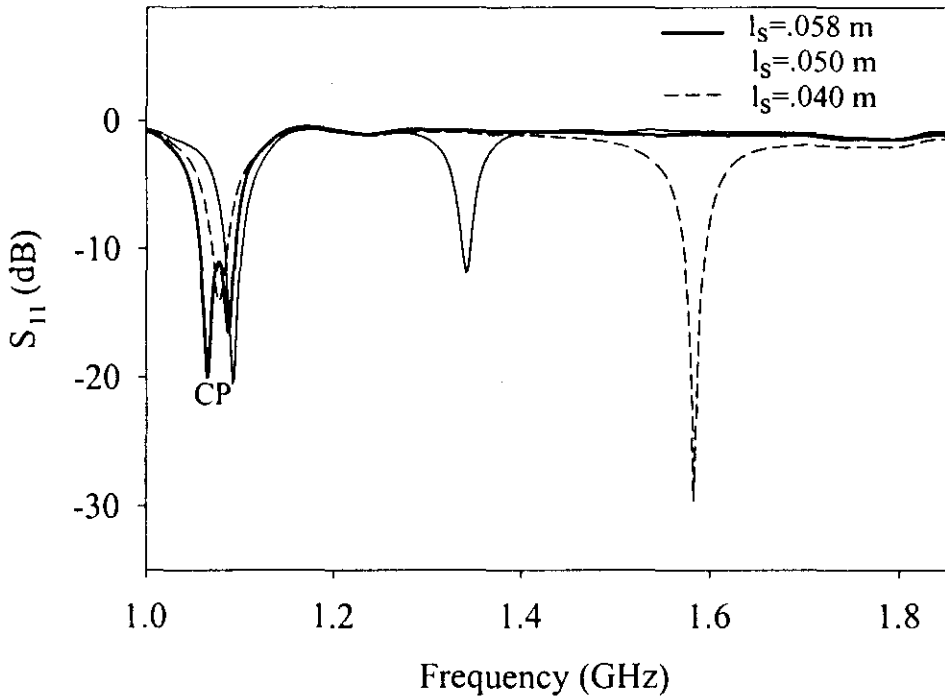


Figure 4.20 Variation of return loss with frequency for different slot length (l_s)

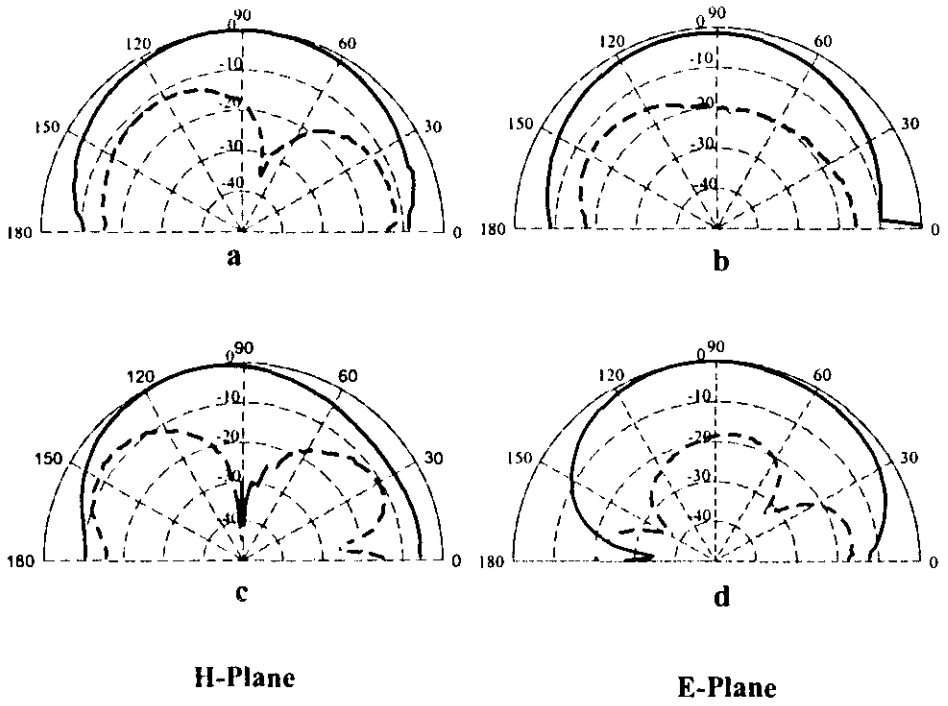


Figure 4.21 Radiation patterns of the antenna at frequencies (a, b) for 1.07 GHz and (c, d) for 1.34GHz

—— Co-Polar
 - - - - Cross-Polar

4.3.1.3 Discussion on the resonant modes and its variation with different antenna parameters

As already explained, by embedding a rectangular slot inside the arrow shaped patch, a new frequency is excited which is having an opposite polarization compared to the fundamental TM_{10} mode. This new mode frequency is always found to be less than TM_{01} mode of the unslotted patch. Hence this mode is regarded as $TM_{0\delta}$ mode, where $(0 < \delta < 1)$ [97].

In this section, the effect of various parameters on the resonant frequencies is explained in detail. In Table 4.8 the variation of TM_{10} and $TM_{0\delta}$ modes of the slotted arrow shaped patch with slot length (l_s) is shown. The TM_{10} and TM_{01} mode frequencies of the unslotted patch are also given for a comparative study. It is found that TM_{10} mode frequency is the same for slotted and unslotted patches. But for the slotted patch a new frequency is generated which is less than TM_{01} mode, and decreases rapidly with increase in the slot length.

The second parameter to be studied is the variation with the position of the slot from the edge ('s') keeping slot length constant. The results are shown in Table 4.9. It can be noted that TM_{10} mode frequency remains the same as that of unslotted patch. The new mode $TM_{0\delta}$ slightly changes with the position of the slot. So it can be concluded that $TM_{0\delta}$ mode is independent of the position of the slot and depends only on the length of the slot.

The next parameter to be studied is the variation of frequencies with width (' w_s ') of the slot. Table 4.10 shows the variation of resonant frequencies with width of the slot (' w_s '). Here also TM_{10} mode remains the same as the unslotted patch and $TM_{0\delta}$ mode changes very slightly.

Table 4.8 Variation of frequencies with slot length (l_s) for the arrow shaped patch with an embedded rectangular slot

| L, W, W_{cp} , W_{cd} (cm) | Distance from edge 's' (cm) | Width of the Slot ' w_s ' (cm) | Length of the Slot ' l_s ' (cm) | Frequencies of the unslotted patch | | Frequencies of the slotted patch | |
|--|---|--|---|--|-------------------|--|-------------------|
| | | | | f_{10} (GHz) | f_{01} (GHz) | f_{10} (GHz) | f_{0s} (GHz) |
| 6, 5, 1, 1 | 2 | 0.2 | 2 | 1.171 | 1.401 | 1.156 | 1.287 |
| | | | 3 | | | 1.159 | 1.169 |
| | | | 4 | | | 1.155 | 1.059 |
| | | | 5 | | | 1.155 | 0.909 |
| 6, 5, 1, 2 | 2 | 0.2 | 2 | 1.075 | 1.492 | 1.112 | 1.334 |
| | | | 3 | | | 1.112 | 1.222 |
| | | | 4 | | | 1.112 | 1.100 |
| | | | 5 | | | 1.112 | 0.943 |
| 6,5,1,3 | 2 | 0.2 | 2 | 0.9566 | 1.529 | 1.065 | 1.378 |
| | | | 3 | | | 1.063 | 1.266 |
| | | | 4 | | | 1.061 | 1.138 |
| | | | 5 | | | 1.060 | 1.056 |

Table 4.9 Variation of frequencies with distance of the slot from the edge of the antenna ('s')

| L, W, W _{cp} , W _{cd} (cm) | Distance from edge 's' (cm) | Width of the Slot 'w _s ' (cm) | Length of the Slot 'l _s ' (cm) | Frequencies of the slotted patch | |
|---|--------------------------------|---|--|----------------------------------|--------------------------|
| | | | | f ₁₀ (GHz) | f ₀₈ (GHz) |
| 6, 5, 1, 1 | 0.5 | 0.2 | 5 | 1.152 | 0.980 |
| | 1.0 | | | 1.152 | 0.938 |
| | 1.5 | | | 1.152 | 0.915 |
| | 2.0 | | | 1.156 | 0.909 |
| | 2.5 | | | 1.156 | 0.903 |
| | 3.0 | | | 1.156 | 0.900 |

Table 4.10 Variation of frequencies with slot width ('w_s')

| L, W, W _{cp} , W _{cd} (cm) | Distance from edge 's' (cm) | Width of the Slot 'w _s ' (cm) | Length of the Slot 'l _s ' (cm) | Frequencies of the slotted patch | |
|---|--------------------------------|---|--|----------------------------------|--------------------------|
| | | | | f ₁₀ (GHz) | f ₀₈ (GHz) |
| 6, 5, 1, 1 | 2.0 | 0.2 | 5 | 1.156 | 0.909 |
| | | 0.4 | | 1.151 | 0.885 |
| | | 0.6 | | 1.148 | 0.861 |
| | | 0.8 | | 1.147 | 0.839 |
| | | 1.0 | | 1.147 | 0.823 |

4.3.2 ARROW SHAPED ANTENNA WITH SLOTS ON ITS RADIATING EDGES

A dual frequency design having same polarization planes is obtained using a pair of narrow slots embedded close to the radiating edges of the patch. This antenna has a greater area reduction and a smaller frequency ratio compared to drum shaped antenna. In slot loaded drum shaped antenna, dual frequency operation is based on the two resonant frequencies of the perturbed TM_{10} and TM_{30} mode with frequency ratio tunable from 2 to 3 [95].

In this present design, a lower frequency ratio range is achieved by the excitation of the two adjacent resonant frequencies of TM_{10} and $TM_{\delta 0}$ modes ($1 < \delta < 2$). This makes the antenna more suitable for dual frequency applications where lower frequency ratio is required. Experimental results of the dual frequency characteristics are presented and analyzed.

4.3.2.1 Antenna Geometry

The proposed configuration of arrow shaped patch antenna with a pair of narrow slots having a dimensions of $l_s \times w_s$ embedded in the patch parallel to the radiating edges at a distance 's' from the edges is shown in Figure 4. 22. By choosing suitable values for W_{cd} and W_{cp} , two frequencies of same polarization can be obtained. Keeping W_{cp} a constant and varying W_{cd} the ratio of the two operating frequencies can be tuned. The antenna is excited by electromagnetic coupling using a 50Ω microstrip feed line.

4.3.2.2 Typical Antenna Design and Experimental Results

Typical design of the proposed antenna is implemented and investigated. It has dimensions $L = 6\text{cm}$, $W = 3\text{cm}$, $W_{cp} = 1\text{cm}$ and $W_{cd} = 2\text{cm}$ and is fabricated on a substrate of thickness $h=0.16\text{cm}$ and dielectric constant $\epsilon_r=4.28$. Slots having dimensions $l_s = 2.6\text{cm}$, and $w_s = 0.2\text{cm}$ are etched at a distance $s = 0.3\text{cm}$ from the radiating edges.

Figure 4.23 shows the measured return loss and transmission characteristics against frequency. Variation of dual frequencies with W_{cd} is presented in Table 4.11.

The two modes have same polarization planes. Figure 4.24 (a, b, c, d) show the radiation patterns of the antenna for the two frequencies at 0.987 GHz and 1.13 GHz. From the patterns it is clear that the cross polar performance of the patch is better than 20 dB.

This design achieves two very close frequencies of same polarization and has an area reduction of 77% for the first frequency and 70% for the second frequency compared to the standard rectangular patch.

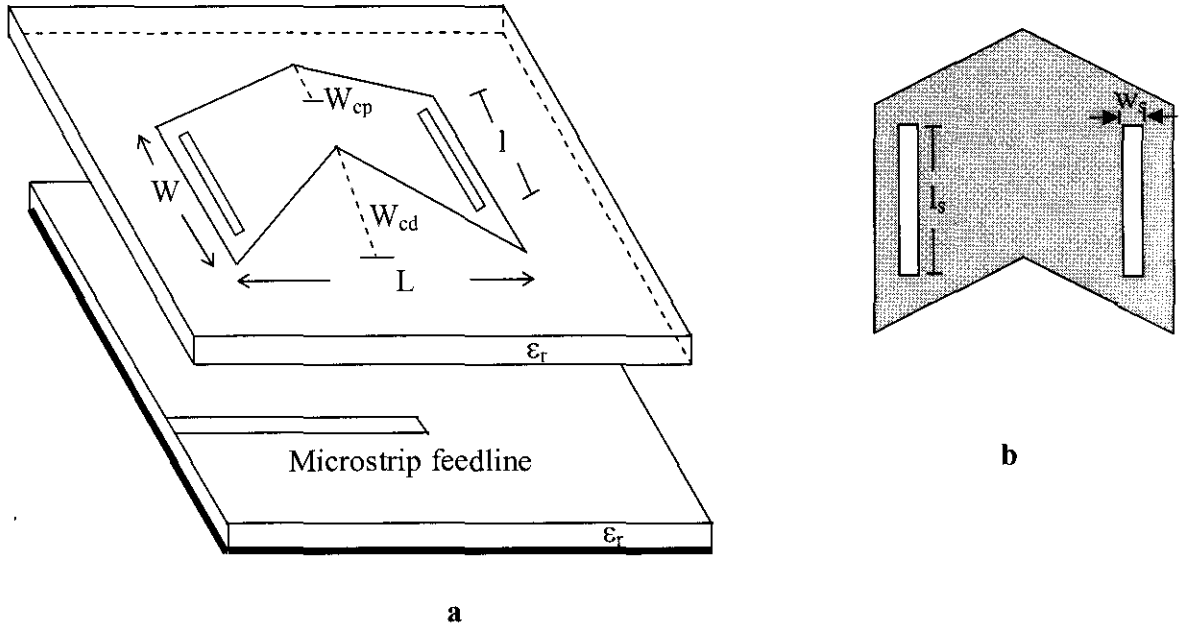


Figure 4.22 (a) Arrow shaped microstrip antenna with slots on its radiating edges
 (b) Patch Geometry

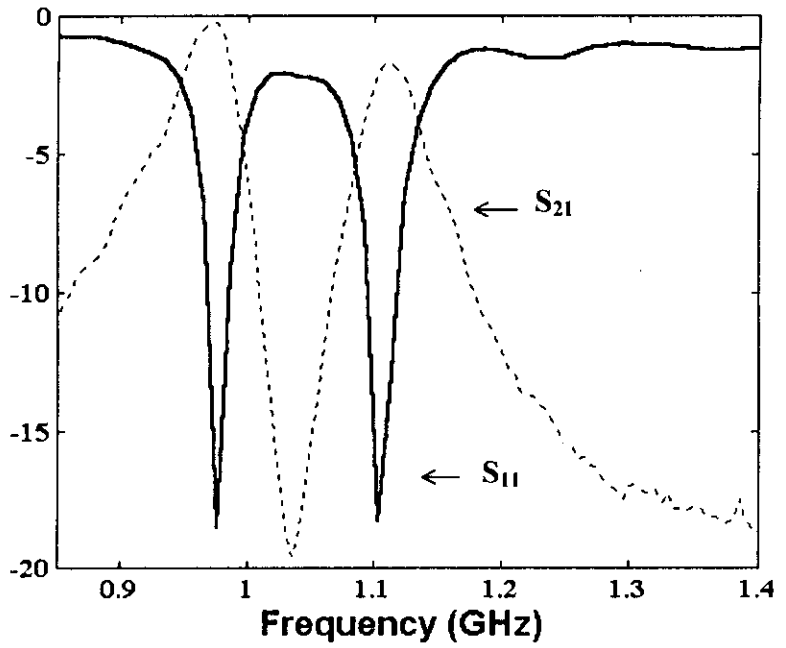


Figure 4.23 Measured scattering parameters of the arrow shaped slotted microstrip antenna.

Table 4.11 Variation of dual frequency with W_{cd} ($W_{cp} = 1$ cm)

| W_{cd} (cm) | Frequency f_1 (GHz) | Frequency f_2 (GHz) |
|------------------|--------------------------|--------------------------|
| 1.0 | 0.969 | 1.197 |
| 1.5 | 0.974 | 1.197 |
| 2.0 | 0.987 | 1.130 |
| 2.5 | 0.932 | 1.093 |

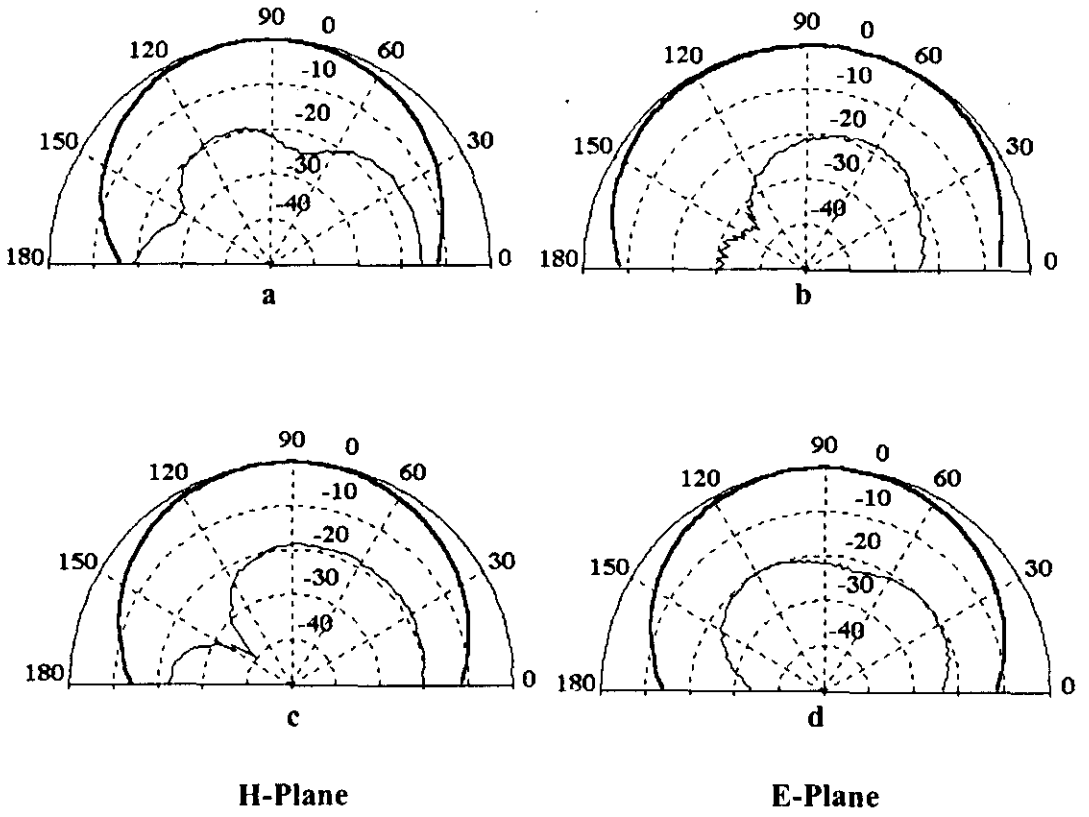


Figure 4.24 Radiation patterns of the antenna at frequencies (a, b) for 0.987 GHz and (c, d) for 1.13GHz

—— Co-Polar
 - - - - Cross-Polar

4.3.3 ARROW SHAPED ANTENNA WITH SLOTS ON ITS NON RADIATING EDGES FOR BANDWIDTH ENHANCEMENT

Microstrip patch antennas are known to have a relatively narrow bandwidth of $\sim 2\%$ ($VSWR \leq 2$). During, the last decade a great deal of research has been devoted to techniques for increasing the bandwidth of microstrip antennas. A popular method is the use of parasitic patches, either in another layer (stacked geometry [126]) or in same layer (coplanar geometry [54]). The former has the disadvantage of increasing the thickness of the antenna while the latter has the disadvantage of increasing the lateral size of the antenna and increases the complexity of the antenna design. The bandwidth can also be improved by the use of thick foam substrate [131].

Rectangular slot antenna with a pair of bent slots close to the non radiating edges has been demonstrated [97], two operating frequencies having same polarization planes and similar broadside radiation patterns are excited. Here a new mode $TM_{\delta 0}$ mode ($1 < \delta < 2$) is found to be excited between TM_{10} and TM_{20} mode. Broadband design in rectangular microstrip patch is achieved by embedding tooth brush shaped slots inside the patch which makes the antenna geometry more complicated.

In this section, an arrow shaped patch antenna designed for broadband operation by cutting slots on its non radiating edges is demonstrated. The broadband operation is achieved by the co-existence of two adjacent resonant frequencies of the TM_{10} and $TM_{\delta 0}$ modes ($1 < \delta < 2$). Experimental and simulated (IE3D) results of this broadband antenna are presented and discussed.

4.3.3.1 Antenna Geometry

The configuration of broadband arrow shaped patch antenna is shown in Figure 4.25. A pair of narrow slots having width w_s are embedded in the patch parallel to the non radiating edges at a distance 's' from the edges. By choosing suitable values for W_{cd} and W_{cp} two different modes can be excited. For a particular design, these two different frequencies merge together, and significantly enhance its bandwidth. The antenna is excited by electromagnetic coupling using a 50 ohm microstrip feed line.

4.3.3.2 Antenna design and experimental results

The proposed antenna configuration is simulated using IE3D software and experimentally investigated. A typical design has dimensions $L = 6\text{cm}$, $W = 3\text{cm}$, $W_{cp} = 1\text{cm}$ and $W_{cd} = 2\text{cm}$ fabricated on a substrate of thickness $h = 0.16\text{cm}$ and dielectric constant $\epsilon_r=4.28$. Slots having width $w_s = 0.2\text{cm}$ are placed at a distance $s = 0.3\text{cm}$ from the non-radiating edges.

By varying the height of the intruding triangle (W_{cd}) of the arrow shaped antenna frequency ratio between two resonant frequencies of same polarization can be varied. The simulated frequency response of the arrow shaped patches with different W_{cd} is shown in Figure 4.26. For an optimum value of W_{cd} these two frequencies merge together to produce large bandwidth. Results show that for $W_{cd} = 2\text{cm}$, the antenna offers a 2:1 VSWR bandwidth of 62 MHz (~ 6%).

The optimum antenna is fabricated and the radiation characteristics in the operating band are studied. Figure 4.27 shows typical radiation patterns at start, stop and centre frequencies of the operating band. The antenna offers similar radiation patterns and identical polarization in the entire band. Also, a good cross polar discrimination better than 20 dB is obtained. For a comparison, a

rectangular patch antenna operating at the same frequency is constructed and investigated. From the observations it is inferred that the arrow shaped slot antenna is giving a bandwidth of 3.5 times that of the rectangular patch with an area reduction of ~75%. The above performance is obtained with a reduction in gain of <2dB.

4.3.3.3 Discussion on the effect of various slot parameters on resonant mode frequencies

As already explained a new mode frequency, $TM_{\delta 0}$ ($1 < \delta < 2$) is generated by the introduction of slots. The variation of the frequencies for TM_{10} and $TM_{\delta 0}$ modes with various parameters of the antenna are investigated in detail and presented here.

Table 4.12 shows the variation of both resonant modes with slot length ' l_s '. The TM_{10} mode frequency is almost the same as that excited by unslotted arrow shaped patch. $TM_{\delta 0}$ mode frequency decreases with increase in the slot length of the patch. The variation of the two mode frequencies of the slotted patch with slot length is clearly pictured in Figure 4.28.

Effect of slot length on return loss characteristics are shown in Figure 4.29. As shown in figure, TM_{10} and $TM_{\delta 0}$ modes come very close and finally combine to give bandwidth enhancement.

Variation of resonant frequencies with width of the slot ' w_s ' is shown in Table 4.13. TM_{10} mode frequency remains almost constant. $TM_{\delta 0}$ mode which is determined by the dimensions of the slot decreases with increase in the width of the patch.

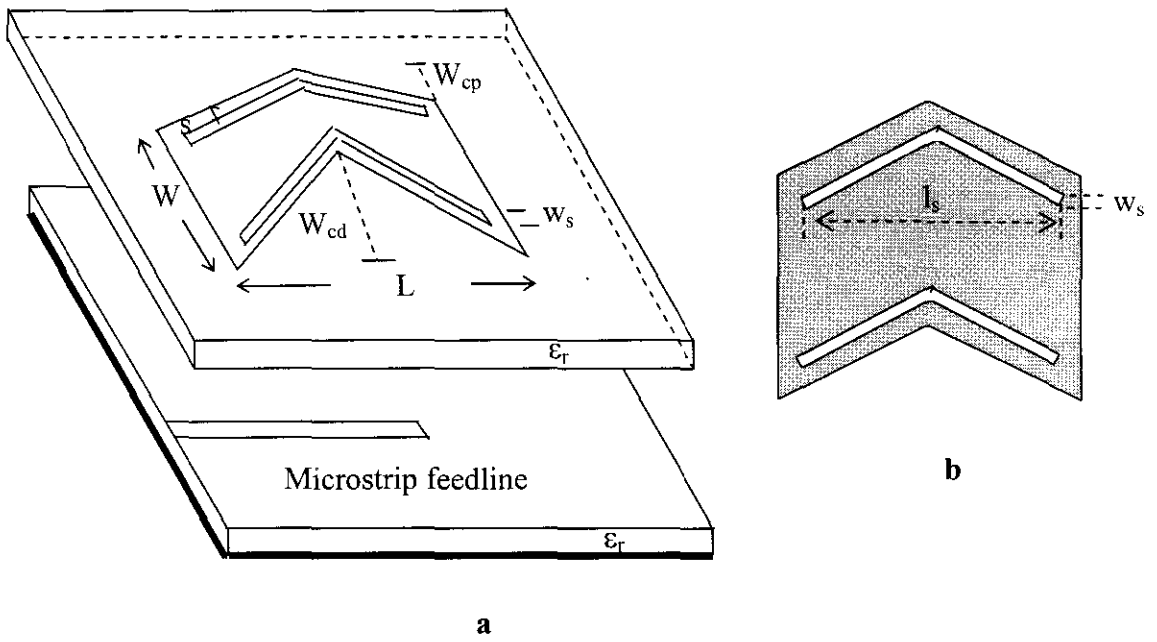


Figure 4.25 (a) Arrow shaped antenna for broadband operation (b) Patch Geometry

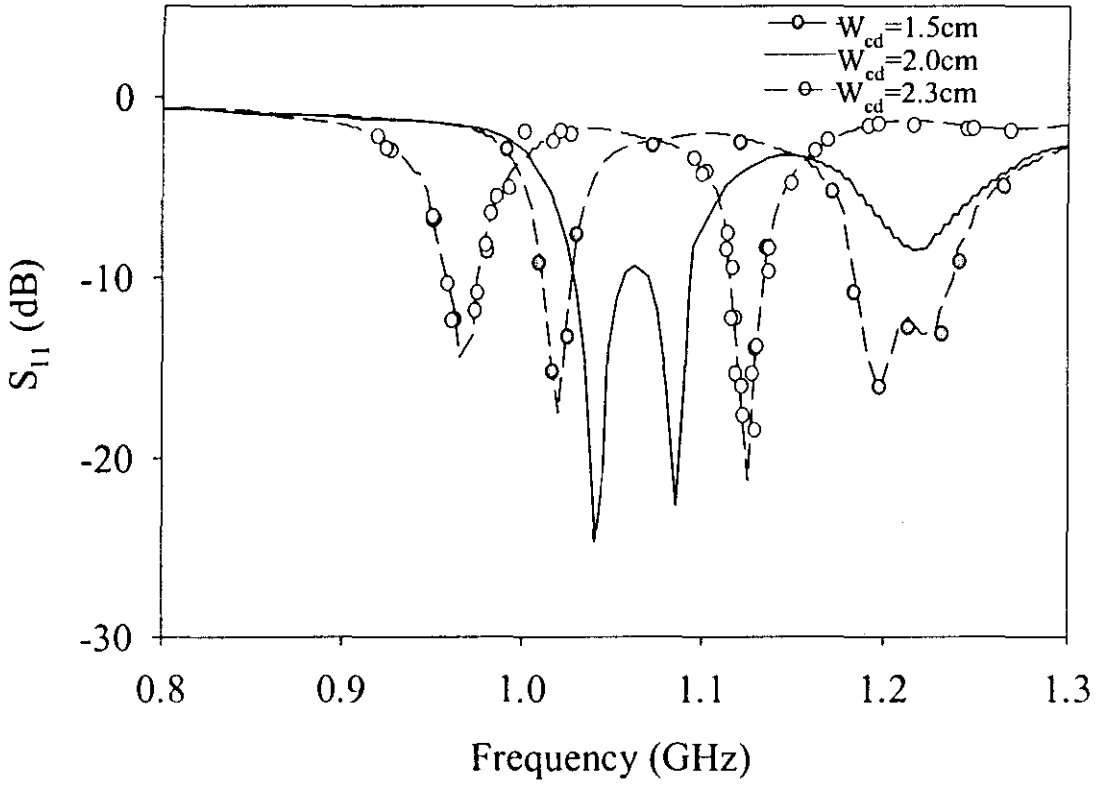


Figure 4.26 Variation of return loss with frequency for different W_{cd} ($L=6\text{cm}$, $W=3\text{cm}$, $W_{cp}=1\text{cm}$)

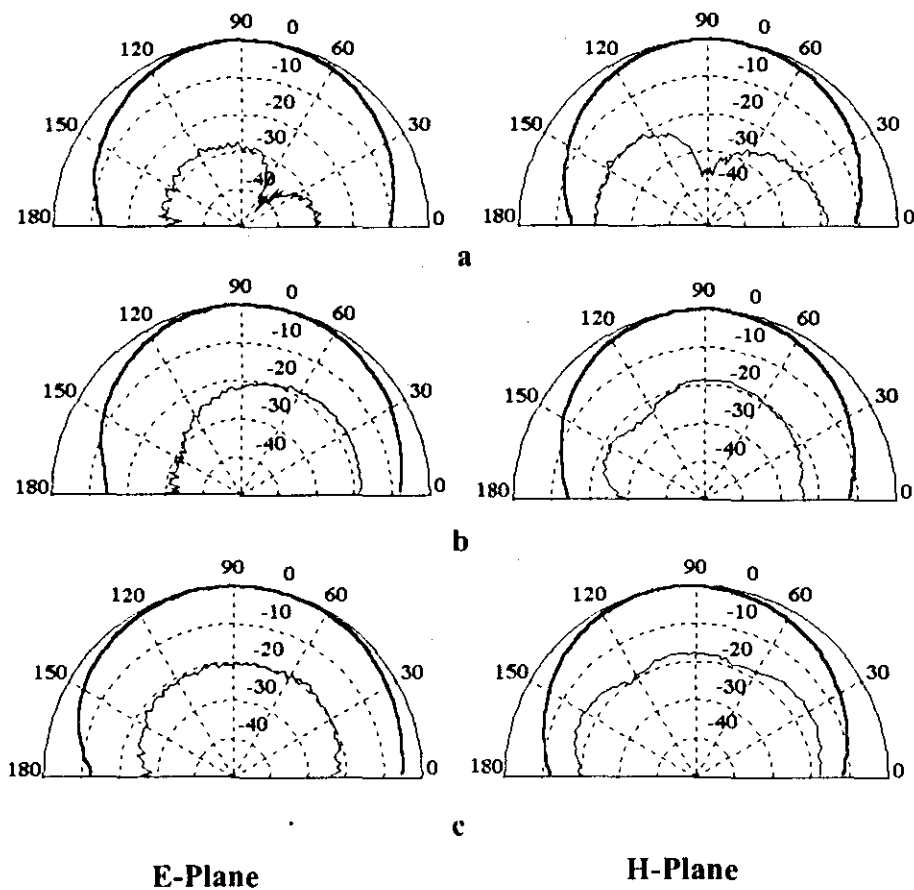


Figure 4.27 Radiation patterns for start, centre and stop frequencies in the operating band.

(a) 1 GHz (b) 1.06 GHz (c) 1.1 GHz

— Co-Polar
 - - - Cross-Polar

Table 4.12 Variation of frequencies with slot length (l_s) for the arrow shaped patch

| L, W, W_{cp} , W_{cd} (cm) | Distance from edge 's' (cm) | Width of the Slot ' w_s ' (cm) | Length of the Slot ' l_s ' (cm) | Frequencies of the unslotted patch | | Frequencies of the slotted patch | |
|--|---|--|---|--|-------------------|-------------------------------------|------------------------|
| | | | | f_{10} (GHz) | f_{01} (GHz) | f_{10} (GHz) | $f_{0\delta}$ (GHz) |
| 6,5,1,1 | 0.2 | 0.2 | 2.0 | 1.171 | 1.401 | 1.152 | 1.366 |
| | | | 3.0 | | | 1.150 | 1.338 |
| | | | 4.0 | | | 1.151 | 1.282 |
| | | | 5.0 | | | 1.160(BW) | 1.160(BW) |
| | | | 5.8 | | | 1.155 | 1.092 |
| 6,5,1,3 | 0.2 | 0.2 | 2.0 | 0.956 | 1.529 | 0.939 | 1.468 |
| | | | 3.0 | | | 0.936 | 1.407 |
| | | | 4.0 | | | 0.935 | 1.259 |
| | | | 5.0 | | | 0.936 | 1.068 |
| | | | 5.8 | | | 0.937(BW) | 0.937(BW) |
| 7,5,1,1 | 0.2 | 0.2 | 2.0 | 1.016 | 1.393 | 0.995 | 1.350 |
| | | | 3.0 | | | 0.994 | 1.330 |
| | | | 4.0 | | | 0.994 | 1.283 |
| | | | 5.0 | | | 0.995 | 1.202 |
| | | | 6.0 | | | 0.997 | 1.068 |
| | | | 6.8 | | | 0.998 | 0.962 |
| 7,5,1,2 | 0.2 | 0.2 | 2.0 | 0.943 | 1.467 | 0.928 | 1.400 |
| | | | 3.0 | | | 0.926 | 1.387 |
| | | | 4.0 | | | 0.926 | 1.316 |
| | | | 5.0 | | | 0.926 | 1.187 |
| | | | 6.0 | | | 0.928 | 1.032 |
| | | | 6.8 | | | 0.929(BW) | 0.929(BW) |

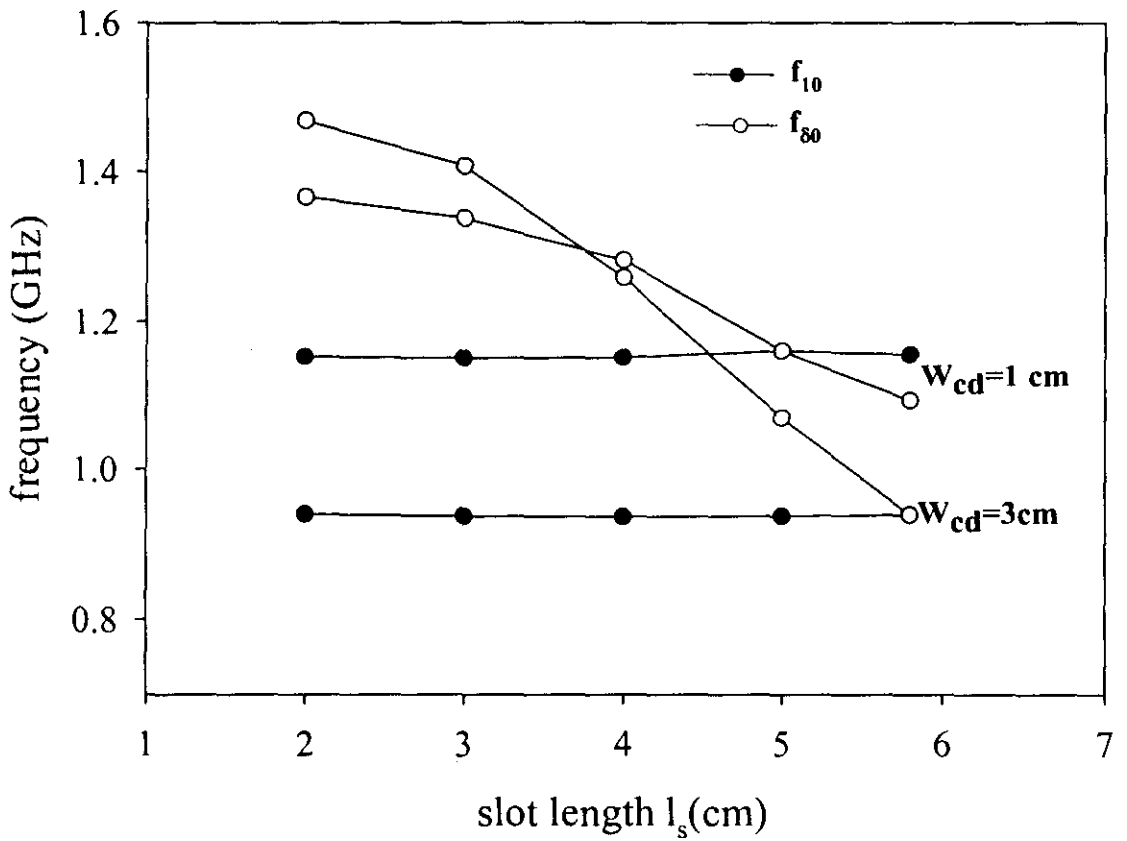


Figure 4.28 Variation of the mode frequencies with slot length for an arrow shaped antenna
 (L=6 cm, W=5 cm, W_{cp} =1cm, w_s =0.2 cm, s =0.2 cm)

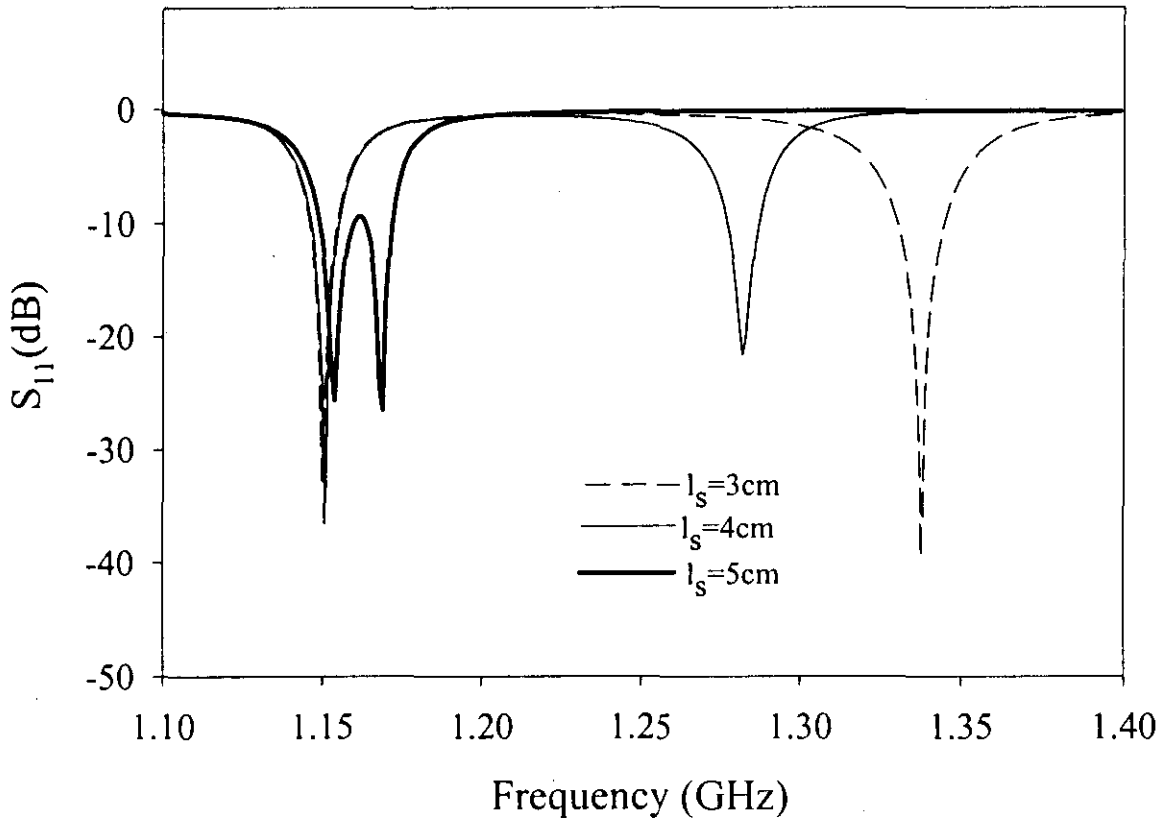


Figure 4.29 Variation of return loss with frequency for different slot length

Table 4.13 Variation of frequencies with slot width (w_s) for the arrow shaped patch

| L, W, W_{cp} , W_{cd} (cm) | Distance from edge 's' (cm) | Width of the Slot ' w_s ' (cm) | Length of the Slot ' l_s ' (cm) | Frequencies of the unslotted patch | | Frequencies of the slotted patch | |
|--|---|--|---|--|-------------------|-------------------------------------|-------------------|
| | | | | f_{10} (GHz) | f_{01} (GHz) | f_{10} (GHz) | f_{08} (GHz) |
| 6, 5, 1, 1 | 2 | 0.2 | 5.8 | 1.171 | 1.401 | 1.152 | 1.366 |
| | | 0.3 | | | | 1.155 | 1.055 |
| | | 0.4 | | | | 1.154 | 1.031 |
| | | 0.5 | | | | 1.154 | 1.011 |
| 6, 5, 1, 2 | 2 | 0.2 | 5.8 | 1.075 | 1.492 | 1.054 | 1.255 |
| | | 0.3 | | | | 1.055 | 0.981 |
| | | 0.4 | | | | 1.053 | 0.957 |
| | | 0.5 | | | | 1.052 | 0.927 |
| 6,5,1,3 | 2 | 0.2 | 5.8 | 0.956 | 1.529 | 0.951 | 0.892 |
| | | 0.3 | | | | 0.951 | 0.871 |
| | | 0.4 | | | | 0.95 | 0.853 |
| | | 0.5 | | | | 0.929 | 0.836 |
| 7,5,1,1 | 2 | 0.2 | 5.8 | 1.016 | 1.393 | 0.998 | 0.962 |
| | | 0.3 | | | | 0.999 | 0.931 |
| | | 0.4 | | | | 0.999 | 0.905 |
| | | 0.5 | | | | 0.999 | 0.884 |

4.4 DUAL PORT ARROW SHAPED ANTENNA

Radar and advanced communication applications require low profile antennas capable of dual frequency dual polarization operation and good isolation between the ports. The severe problem with dual-polarized systems is cross-coupling of co-channels producing interference and cross talk. These effects can be avoided using dual port antennas, which provide excellent isolation between the ports. In this section, an arrow shaped microstrip antenna excited by two feeding ports giving orthogonal polarization is investigated. The two feed lines are electromagnetically coupled to the patch.

4.4.1 Antenna Design and Experimental results

The schematic diagram of the antenna is shown in Figure 4.30. A typical antenna structure of length $L = 4\text{cm}$, width $W = 6\text{cm}$, $W_{cd} = 1\text{cm}$ and $W_{cp} = 1\text{cm}$ is etched on a substrate of thickness $h = 0.16\text{cm}$ and $\epsilon_r = 4.28$. Two 50 ohm microstrip feed lines are fabricated on a similar substrate kept below the patch to provide electromagnetic coupling.

The measured return loss against frequency for the two ports is shown in Figure 4.31. Isolation between the feeding ports in the operating band is measured and plotted in Figure 4.32. Figure 4.33 show their transmission characteristics. From these figures it is clear that the isolation between the ports is better than 25 dB which implies very small cross coupling. The E-Plane and H-Plane patterns for the frequencies 1.2175 GHz and 1.7175 GHz are shown in Figure 4.34. The cross polar performance for both the frequencies is found to be better than 20dB.

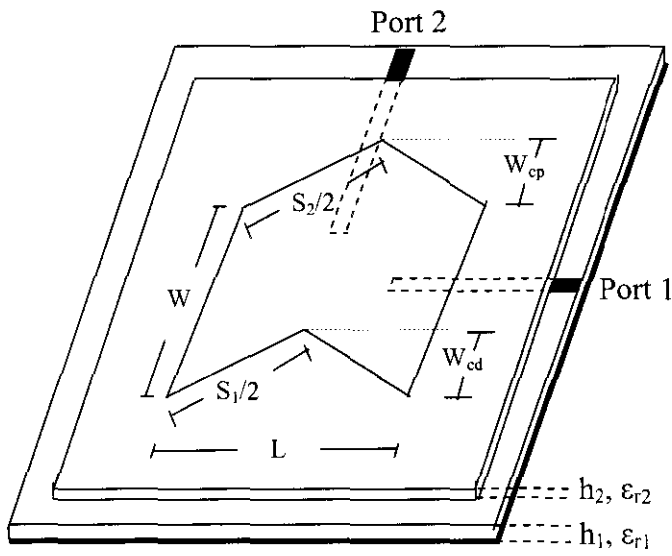


Figure 4.30 Geometry of the dual port microstrip antenna

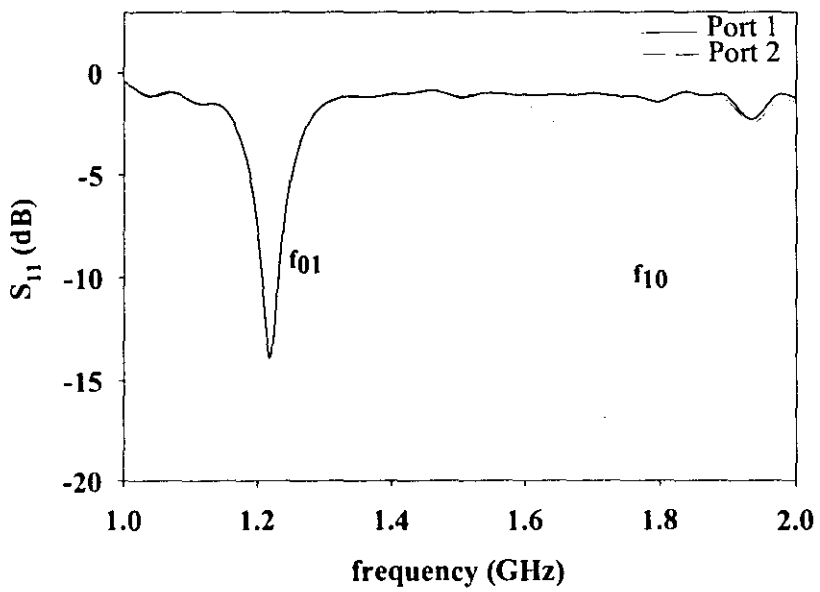


Figure 4.31 Measured return loss against frequency for two ports

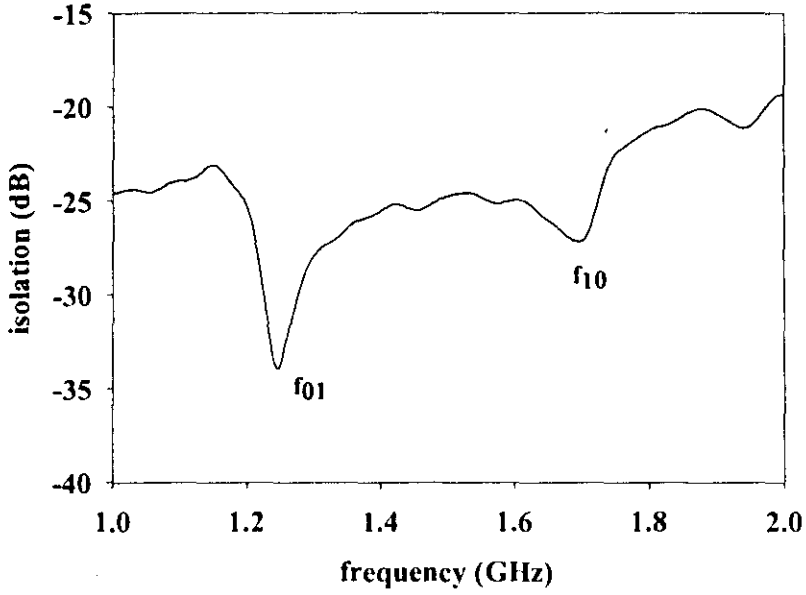


Figure 4.32 Measured isolation between port1 and port2

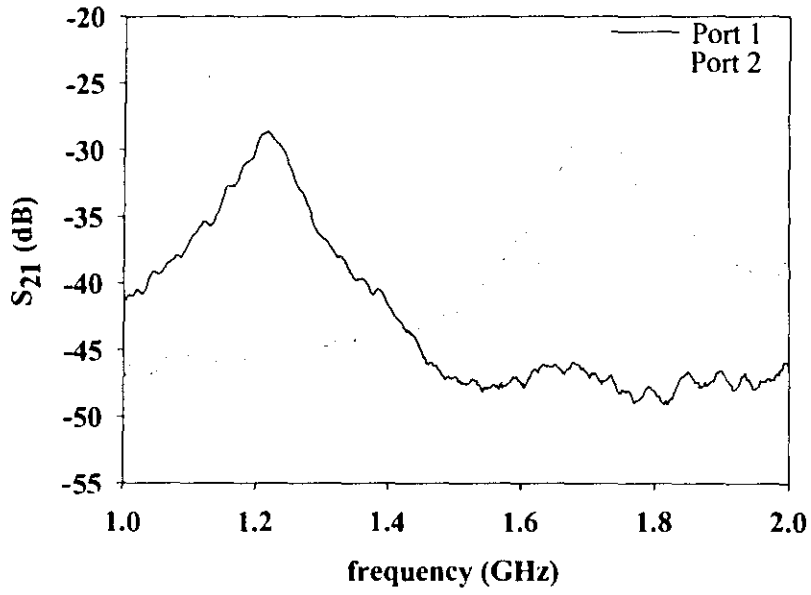


Figure 4.33 Measured transmission characteristics against frequency at two ports

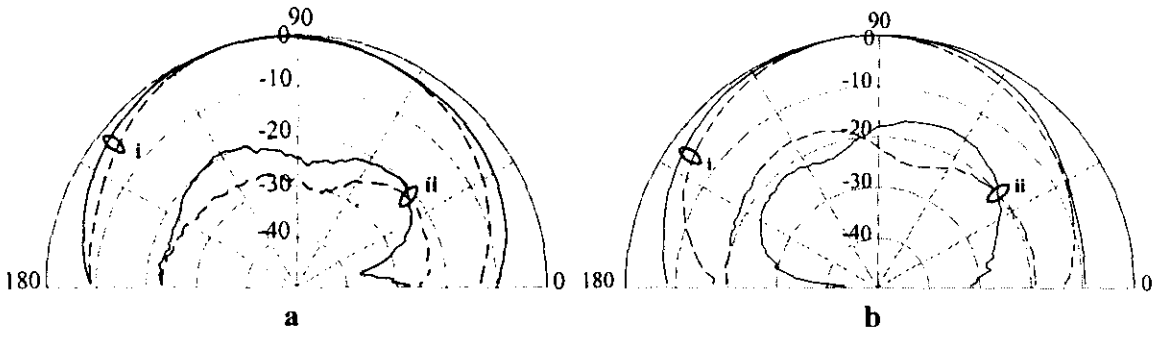


Figure 4.34 E-Plane and H-Plane radiation patterns

a) Port 1 frequency ($f_{01}=1.2175\text{GHz}$)

b) Port 2 frequency ($f_{10}=1.7175\text{GHz}$)

i) Co-polarisation

ii) Cross-polarisation

— E-plane

----- H-plane

CHAPTER 5

THEORETICAL INTERPRETATION AND DESIGN EQUATIONS

Development of closed form expressions for calculating the TM_{10} and TM_{01} mode frequencies of the arrow shaped microstrip antenna is presented in this chapter. The accuracy of the method is validated by experimental results. Characteristics of the new geometry are also analyzed by calculating the current and field distribution over the surface and edges of the patch using IE3D simulation software.

5.1 INTRODUCTION

The design equations of the arrow shaped patch antenna are developed by modifying the standard equations for a rectangular patch. These relations can predict both f_{10} and f_{01} mode frequencies very accurately. This provides a fast and simple way to predict the characteristics of the antenna. The design is also analyzed using experimental measurements and IE3D simulation package. The theoretical predictions are found to be very close to these results and thus establish the validity of design formulae. The design equations of the rectangular patch is discussed followed by the modifications incorporated for the new geometry. Finally the current distributions of the patch at the antenna surface are calculated using IE3D simulation software in order to verify the modes of the resonant frequencies determined from calculations.

5.2 RESONANT FREQUENCIES OF A RECTANGULAR MICROSTRIP PATCH

The design equations for a rectangular patch antenna based on cavity model proposed by Lo et al. [22, 23, 24] is described in this section. In this model microstrip antennas are considered to resemble dielectric loaded cavities and exhibit higher order resonances. The normalized fields within the dielectric substrate can be found more accurately by treating the region as a cavity bounded by electric conductors above and below the patch and by magnetic walls along the perimeter of the patch.

The field configurations can be found using the vector potential approach. Referring to Figure 5.1, the volume beneath the patch can be treated as a rectangular cavity loaded with a dielectric material having dielectric constant ϵ_r . The dielectric material

of the substrate is assumed to be truncated and not extended beyond the edges of the patch. The vector potential A_x must satisfy the homogenous wave equation of

$$\nabla^2 A_x + k^2 A_x = 0 \quad (5.1)$$

whose solution can be written as,

$$A_x = [A_1 \cos(k_x x) + B_1 \sin(k_x x)][A_2 \cos(k_y y) + B_2 \sin(k_y y)][A_3 \cos(k_z z) + B_3 \sin(k_z z)] \quad (5.2)$$

where k_x, k_y, k_z are the wave numbers along x, y, z directions.

The electric and the magnetic fields are related to the vector potential A_x by

$$E_x = \frac{-j}{\omega \mu \epsilon} \left(\frac{\partial^2}{\partial x^2} + k^2 \right) A_x \quad H_x = 0 \quad (5.3)$$

$$E_y = \frac{-j}{\omega \mu \epsilon} \left(\frac{\partial^2 A_x}{\partial x \partial y} \right) \quad H_y = \frac{1}{\mu} \frac{\delta A_x}{\delta z} \quad (5.4)$$

$$E_z = \frac{-j}{\omega \mu \epsilon} \left(\frac{\partial^2 A_x}{\partial x \partial z} \right) \quad H_z = \frac{1}{\mu} \frac{\delta A_x}{\delta y} \quad (5.5)$$

Applying the boundary conditions it can be shown that

$B_1, B_2, B_3 = 0$, and

$$\left. \begin{aligned} k_x &= \frac{m\pi}{h}, & m &= 0, 1, 2, \dots \\ k_y &= \frac{n\pi}{L}, & n &= 0, 1, 2, \dots \\ k_z &= \frac{p\pi}{W}, & p &= 0, 1, 2, \dots \end{aligned} \right\} \quad (5.6)$$

Thus the final form for the vector potential A_x within the cavity is

$$A_x = A_{mnp} \cos(k_x x) \cos(k_y y) \cos(k_z z) \quad (5.7)$$

Since the wave numbers are subject to constraint equation,

$$k_r^2 = k_x^2 + k_y^2 + k_z^2 = \left(\frac{m\pi}{h}\right)^2 + \left(\frac{n\pi}{L}\right)^2 + \left(\frac{p\pi}{W}\right)^2 = \omega_r^2 \mu \epsilon \quad (5.8)$$

the resonant frequencies of the cavity are given by

$$(f_r)_{mnp} = \frac{1}{2\pi\mu\epsilon} \sqrt{\left(\frac{m\pi}{h}\right)^2 + \left(\frac{n\pi}{L}\right)^2 + \left(\frac{p\pi}{W}\right)^2} \quad (5.9)$$

If $L > W > h$, the mode with the lowest frequency is TM_{10} whose resonant frequency is given by

$$(f_r)_{10} = \frac{1}{2L\sqrt{\mu\epsilon}} = \frac{c}{2L\sqrt{\epsilon_r}} \quad (5.10)$$

where c is the speed of light in free space.

The next higher order mode is TM_{01} whose resonant frequency is given by

$$(f_r)_{01} = \frac{1}{2W\sqrt{\mu\epsilon}} = \frac{c}{2W\sqrt{\epsilon_r}} \quad (5.11)$$

If $W > L > h$, then the dominant mode is TM_{01} and the second order mode is TM_{10} .

In all these discussions it was assumed that there are no fringing fields along the edges of the cavity. This is an assumption and is not totally valid.

Since the dimensions of the patch are finite along the length and width, the fields at the edges of the patch undergo fringing. This is illustrated along the length in Figures 5.2 for the two radiating slots of the microstrip antenna. The amount of

fringing is a function of dimensions of the patch and the height of the substrate. Since for microstrip antennas the thickness of the patch is much small compared to patch dimensions, fringing is less; however it must be taken into account because it influences the resonant frequency of the antenna.

Fringing makes the patch look wider electrically compared to its physical dimensions. This is illustrated along the length in Figure 5.2. Since some of the waves travel in the substrate and some in air, an effective dielectric constant ϵ_{reff} is introduced to account for fringing and the wave propagation in the line.

For TM_{10} mode,

$$\epsilon_{\text{reff1}} = \frac{\epsilon_r + 1}{2} + \frac{\epsilon_r - 1}{2} \left(1 + 12 \frac{h}{W} \right)^{-1/2} \quad (5.12)$$

For TM_{01} mode,

$$\epsilon_{\text{reff2}} = \frac{\epsilon_r + 1}{2} + \frac{\epsilon_r - 1}{2} \left(1 + 12 \frac{h}{L} \right)^{-1/2} \quad (5.13)$$

For calculating the TM_{10} mode frequency effective resonating length is considered to take into account the fringing field,

$$L_{\text{eff}} = L + 2\Delta L_1 \quad (5.14)$$

where ΔL_1 is the line extension along the length.

$$\Delta L_1 = 0.412h \frac{(\epsilon_{\text{reff1}} + 0.3) \left(\frac{W}{h} + 0.258 \right)}{(\epsilon_{\text{reff1}} - 0.258) \left(\frac{W}{h} + 0.8 \right)} \quad (5.15)$$

Similarly for TM_{01} mode,

$$W_{\text{eff}} = W + 2\Delta L_2 \quad (5.16)$$

where

$$\Delta L_2 = 0.412h \frac{(\epsilon_{\text{reff}2} + 0.3) \left(\frac{L}{h} + 0.258 \right)}{(\epsilon_{\text{reff}2} - 0.258) \left(\frac{L}{h} + 0.8 \right)} \quad (5.17)$$

Since (5.10) and (5.11) does not account for fringing, must be modified to include the edge effects and can be computed using

$$(f_r)_{01} = \frac{1}{2L_{\text{eff}} \sqrt{\epsilon_{\text{reff}1}} \sqrt{\mu_0 \epsilon_0}} = \frac{c}{2L_{\text{eff}} \sqrt{\epsilon_{\text{reff}1}}} \quad (5.18)$$

$$(f_r)_{01} = \frac{1}{2W_{\text{eff}} \sqrt{\epsilon_{\text{reff}2}} \sqrt{\mu_0 \epsilon_0}} = \frac{c}{2W_{\text{eff}} \sqrt{\epsilon_{\text{reff}2}}} \quad (5.19)$$

These equations are modified to calculate the TM_{10} and TM_{01} mode frequencies of the new arrow shaped geometry which is explained in the next section.

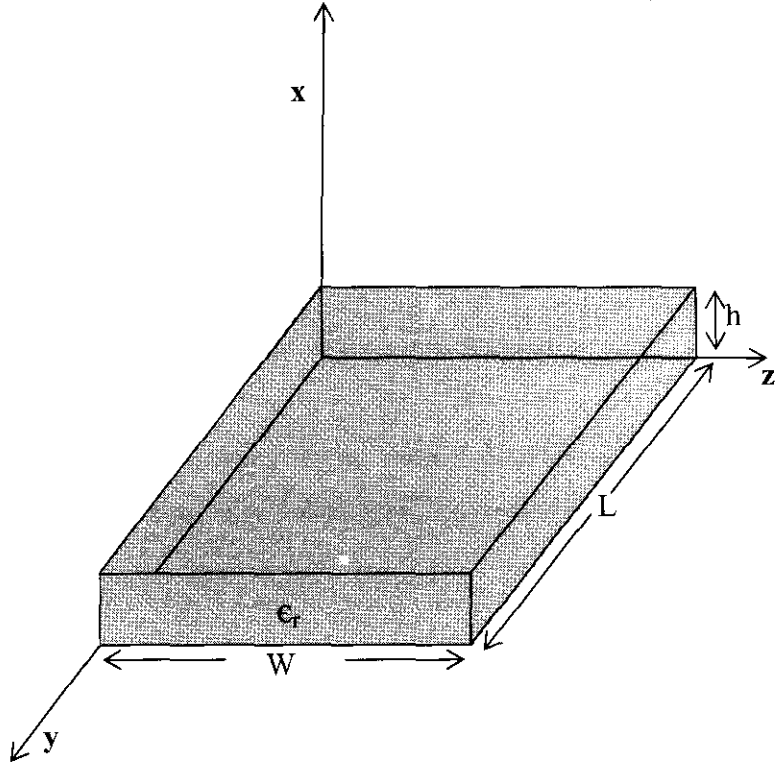


Figure 5.1 Rectangular Microstrip Patch Geometry

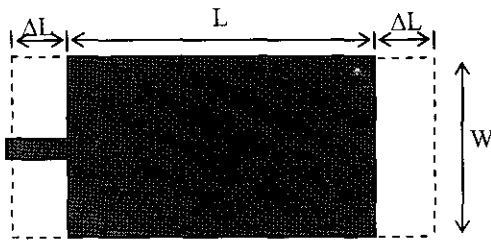


Figure 5.2 Physical and effective lengths of Rectangular Microstrip Patch

5.3 RESONANT FREQUENCIES OF ARROW SHAPED MICROSTRIP PATCH

The resonance frequencies of the arrow shapes microstrip patch antenna are obtained by suitably modifying equations 5.18 and 5.19. Here the effective resonating lengths are calculated by taking into account the height of intruding and protruding triangles.

5.3.1 Coaxially Fed Arrow Shaped Microstrip Antenna

The geometry of the dual frequency arrow shaped microstrip antenna is shown in Figure 4.1. The antenna is coaxially fed at $fp(x_0, y_0)$ to excite TM_{10} and TM_{01} mode frequencies.

The frequencies f_{10} and f_{01} can be calculated as follows

$$f_{10} = \frac{c}{2(S_{\text{eff}} + 2\Delta l_1)\sqrt{\epsilon_1}} \quad (5.20)$$

$$f_{01} = \frac{c}{2(W_{\text{eff}} + 2\Delta l_2)\sqrt{\epsilon_2}} \quad (5.21)$$

In these equations the effective resonating lengths, effective permittivity and line extension factors are modified, which can be calculated using the following empirical relations.

For TM_{10} mode the line extension factor and effective permittivity expressions are obtained from 5.12 and 5.15 of the rectangular patch antenna.

$$\epsilon_1 = \frac{\epsilon_r + 1}{2} + \frac{\epsilon_r - 1}{2} \left(1 + 12 \frac{h}{W} \right)^{-1/2} \quad (5.22)$$

$$\Delta l_1 = 0.412h \frac{(\epsilon_1 + 0.3) \left(\frac{W}{h} + 0.258 \right)}{(\epsilon_1 - 0.258) \left(\frac{W}{h} + 0.8 \right)} \quad (5.23)$$

For TM_{01} mode, these expressions are obtained from equation 5.13 and 5.17, replacing the length 'L' of the rectangular patch by 'S'. 'S' is the mean length calculated from the intruding and protruding triangle lengths S_1 and S_2 as shown in Figure 4.1.

$$\epsilon_2 = \frac{\epsilon_r + 1}{2} + \frac{\epsilon_r - 1}{2} \left(1 + 12 \frac{h}{S} \right)^{-1/2} \quad (5.24)$$

$$\Delta l_2 = 0.412h \frac{(\epsilon_2 + 0.3) \left(\frac{S}{h} + 0.258 \right)}{(\epsilon_2 - 0.258) \left(\frac{S}{h} + 0.8 \right)} \quad (5.25)$$

$$\text{where } S = \frac{S_1 + S_2}{2} \quad (5.26)$$

The calculation of effective length and width are as follows. Two different cases are discussed. The case in which ($L \geq W$), TM_{10} is the dominant mode excited and TM_{01} is the second order mode. The case ($L < W$), the dominant mode cannot be predicted unless the effective resonating lengths are known.

For these two cases effective length and width are calculated by defining a checking factor.

$$\text{Checking Factor (C.F.)} = W_{cd}/W,$$

For C. F. $>1/2$ and C.F. $\leq 1/2$ two sets of equations are defined for both the cases.

CASE (L<W)

$$\left. \begin{aligned} S_{\text{eff}} &= S_i - (.0001/L) + .01W - .68(W_{cd} - .01) - .03(W_{cp} - .01) \\ W_{\text{eff}} &= W + .58W_{cp} - .43W_{cd} \end{aligned} \right\} \text{C.F.} \leq 1/2$$

$$\left. \begin{aligned} S_{\text{eff}} &= 0.5(S_i + L) + .4W_{cd} - .175W - .03(W_{cp} - .01) \\ W_{\text{eff}} &= .78W + .025W_{cd} + .49W_{cp} \end{aligned} \right\} \text{C.F.} > 1/2$$

CASE (L>=W)

No C.F for the calculation of S_{eff} .

$$W_{\text{eff}} = W + .58W_{cp} - .43W_{cd} + .0023(L - W) / W \quad \text{C.F.} \leq 1/2$$

$$W_{\text{eff}} = .78W + .025W_{cd} + .49W_{cp} + .0025W_{cd} / W + .17(L - W - .01) \quad \text{C.F.} > 1/2$$

$$S_{\text{eff}} = S_i + 2.3(L - 2W - 0.0046/L)W_{cd} + 0.00006/L - .1(W_{cp} - .01)$$

5.3.1.1 Comparison between Theoretical and Experimental Results

A comparison between the theoretical and experimental results is made by calculating the percentage errors.

% error in both cases are calculated as

$$\% \text{ error} = \frac{f_{\text{measured}} - f_{\text{calculated}}}{f_{\text{measured}}} * 100\%$$

The theoretical and experimental results for various lengths of arrow shaped antenna for different combinations of W_{cd} and W_{cp} are shown in Figure 5.3. From the graph it can be noted that f_{10} mode frequency varies rapidly and f_{01} frequency remains almost constant for particular W_{cd} and W_{cp} . The theoretical and experimental results are in very good agreement.

Figure 5.4 shows the variation of both calculated and measured frequencies with W . The width variations effect mainly f_{01} mode frequency keeping the other almost constant. Table 5.1 shows the variation of calculated and measured values with intruding triangle height ' W_{cd} ' of the patch and Table 5.2 shows similar variation with ' W_{cp} '. The results of variation of the resonant frequencies with different ' h ' and ' ϵ_r ' combinations are shown in Figure 5.5 and Table 5.3. All the above tables and graphs prove that theoretical results almost follow the experimental values in all cases.

By comparing the experimental and calculated data, it is found that in all cases the percentage error is less than 2. These equations provide a fast and simple method for the design of compact dual frequency microstrip antenna. For calculating the resonant frequencies, the present design equations are less time consuming than general e.m. simulation packages.

Using the above resonant frequency calculation it is possible to design and optimize the various antenna dimensions for desired operating frequency or frequency ratio.

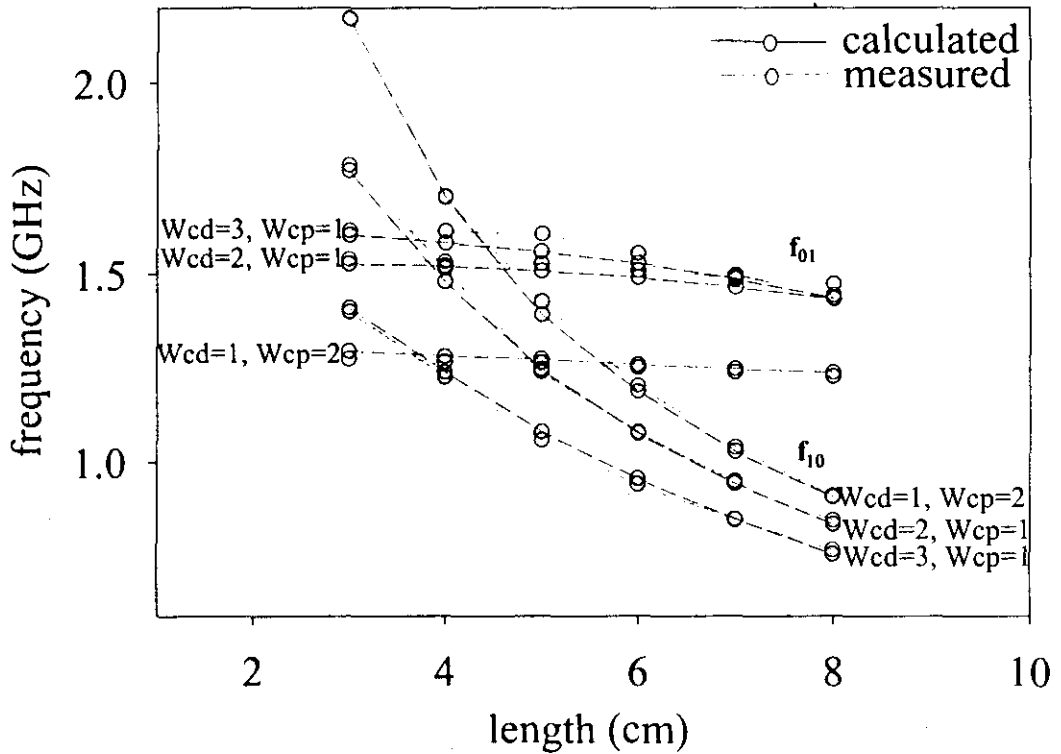


Figure 5.3 Graph showing the variation of calculated and measured TM_{10} and TM_{01} mode frequencies with Length L

($W=5$ cm, $\epsilon_r=4.28$, $h=0.16$ cm)

Table 5.1 Measured and calculated TM_{10} and TM_{01} mode frequencies
(Variation with W_{cd})

| L, W, W _{cp} (cm) | W _{cd} (cm) | h (cm) | ϵ_r | TM ₁₀ mode frequency (f ₁₀) | | | TM ₀₁ mode frequency (f ₀₁) | | |
|----------------------------------|-------------------------|-----------|--------------|--|------------|---------|--|------------|---------|
| | | | | (GHz) | | | (GHz) | | |
| | | | | Measured | Calculated | % error | Measured | Calculated | % error |
| 3.5,1 | 1 | 0.16 | 4.28 | 2.164 | 2.150 | 0.57 | 1.432 | 1.421 | 0.71 |
| | 2 | | | 1.770 | 1.784 | 0.81 | 1.528 | 1.539 | 0.12 |
| | 3 | | | 1.412 | 1.401 | 0.73 | 1.605 | 1.617 | 0.78 |
| | 4 | | | 1.139 | 1.123 | 1.33 | 1.612 | 1.602 | 0.57 |
| | 5 | | | 0.932 | 0.934 | 0.15 | 1.600 | 1.589 | 0.65 |
| 4.5,1 | 1 | 0.16 | 4.28 | 1.691 | 1.689 | 0.10 | 1.424 | 1.413 | 0.74 |
| | 2 | | | 1.481 | 1.516 | 2.00 | 1.522 | 1.533 | 0.75 |
| | 3 | | | 1.242 | 1.228 | 1.09 | 1.582 | 1.612 | 1.98 |
| | 4 | | | 1.032 | 1.016 | 1.48 | 1.587 | 1.599 | 0.79 |
| | 5 | | | 0.850 | 0.862 | 1.46 | 1.579 | 1.587 | 0.51 |
| 6.5,1 | 1 | 0.16 | 4.28 | 1.171 | 1.184 | 1.15 | 1.401 | 1.389 | 0.79 |
| | 2 | | | 1.075 | 1.078 | 0.34 | 1.492 | 1.509 | 1.17 |
| | 3 | | | 0.956 | 0.941 | 1.55 | 1.529 | 1.554 | 1.67 |
| | 4 | | | 0.830 | 0.813 | 1.96 | 1.520 | 1.527 | 0.52 |
| | 5 | | | 0.692 | 0.680 | 2.00 | 1.509 | 1.502 | 0.46 |
| 7.5,1 | 1 | 0.16 | 4.28 | 1.016 | 1.023 | 0.77 | 1.393 | 1.374 | 1.34 |
| | 2 | | | 0.943 | 0.950 | 0.75 | 1.467 | 1.491 | 1.69 |
| | 3 | | | 0.851 | 0.849 | 0.27 | 1.488 | 1.498 | 0.68 |
| | 4 | | | 0.745 | 0.748 | 0.34 | 1.474 | 1.473 | 0.01 |
| | 5 | | | 0.622 | 0.621 | 0.11 | 1.465 | 1.450 | 1.01 |

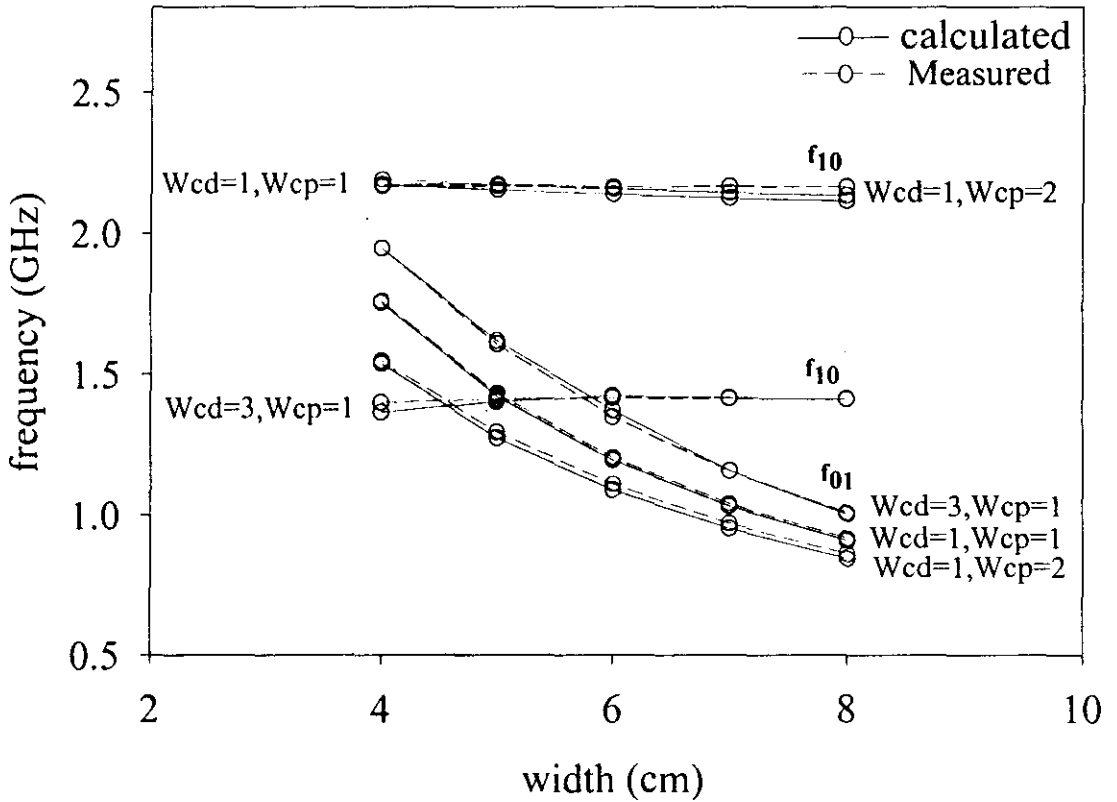


Figure 5.4 Graph showing the variation of calculated and measured TM_{10} and TM_{01} mode frequencies with width 'W'

($L=5$ cm, $c_r=4.28$, $h=0.16$ cm)

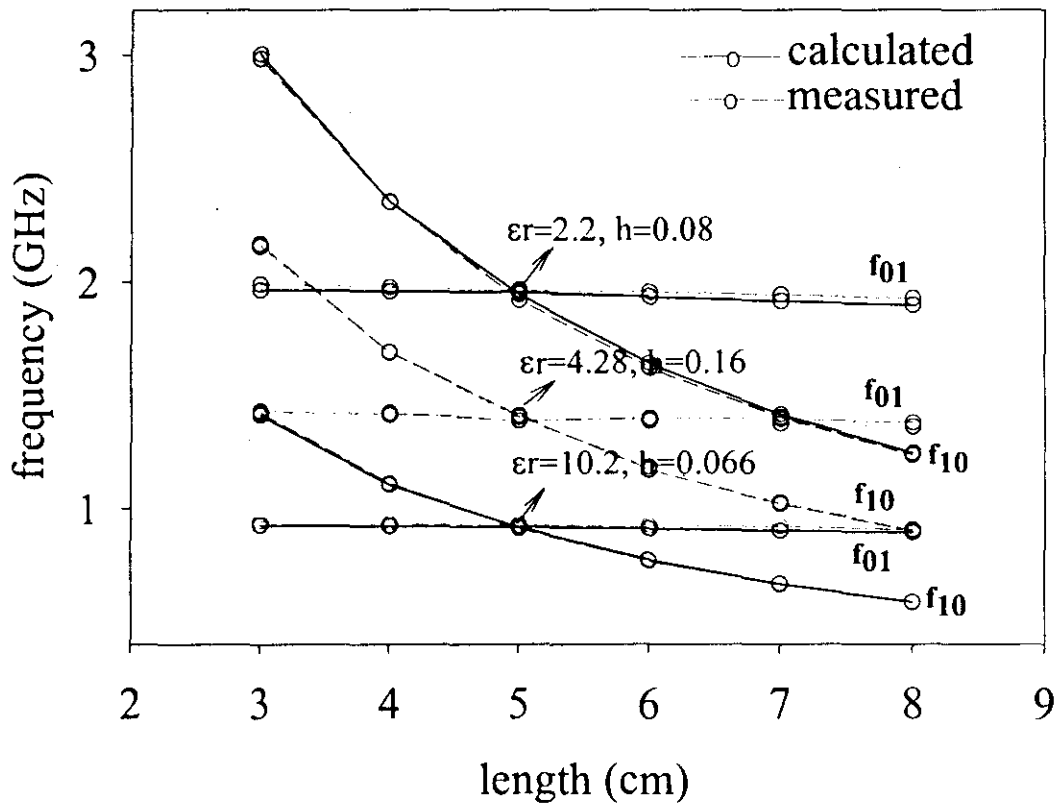


Figure 5.5 Graph showing the variation of calculated and measured TM_{10} and TM_{01} mode frequencies with height 'h' and permittivity ' ϵ_r '.

($W = 5$ cm, $W_{cp} = 1$ cm, $W_{cd} = 1$ cm)

Table 5.2 Measured and calculated TM_{10} and TM_{01} mode frequencies with % error
(Variation with W_{cp})

| W_{cd} (cm) | W_{cp} (cm) | h (cm) | ϵ_r | TM ₁₀ mode frequency (f_{10}) (GHz) | | | TM ₀₁ mode frequency (f_{01}) (GHz) | | |
|------------------|------------------|-----------|--------------|---|------------|---------|---|------------|---------|
| | | | | Measured | Calculated | % error | Measured | Calculated | % error |
| 3,5,1 | 0.5 | 0.16 | 4.28 | 2.156 | 2.142 | 0.60 | 1.515 | 1.507 | 0.52 |
| | 1.0 | | | 2.164 | 2.151 | 0.57 | 1.432 | 1.421 | 0.71 |
| | 1.5 | | | 2.17 | 2.161 | 0.46 | 1.367 | 1.344 | 1.62 |
| | 2.5 | | | 2.172 | 2.170 | 0.07 | 1.296 | 1.275 | 1.60 |
| 4,5,1 | 0.5 | 0.16 | 4.28 | 1.682 | 1.683 | 0.09 | 1.501 | 1.496 | 0.27 |
| | 1.0 | | | 1.691 | 1.689 | 0.10 | 1.424 | 1.413 | 0.74 |
| | 1.5 | | | 1.697 | 1.695 | 0.11 | 1.352 | 1.344 | 1.10 |
| | 2.5 | | | 1.703 | 1.700 | 0.12 | 1.284 | 1.275 | 1.09 |
| 5,5,1 | 0.5 | 0.16 | 4.28 | 1.374 | 1.388 | 1.01 | 1.486 | 1.489 | 0.22 |
| | 1.0 | | | 1.387 | 1.401 | 1.07 | 1.412 | 1.407 | 0.35 |
| | 1.5 | | | 1.390 | 1.415 | 1.80 | 1.342 | 1.332 | 0.69 |
| | 2.5 | | | 1.394 | 1.41 | 1.75 | 1.275 | 1.265 | 0.73 |
| 6,5,1 | 0.5 | 0.16 | 4.28 | 1.159 | 1.175 | 1.39 | 1.480 | 1.470 | 0.65 |
| | 1.0 | | | 1.171 | 1.184 | 1.15 | 1.401 | 1.389 | 0.79 |
| | 1.5 | | | 1.179 | 1.194 | 1.20 | 1.331 | 1.317 | 1.00 |
| | 2.5 | | | 1.187 | 1.203 | 1.34 | 1.260 | 1.252 | 0.87 |
| 7,5,1 | 0.5 | 0.16 | 4.28 | 1.004 | 1.016 | 1.19 | 1.470 | 1.452 | 1.17 |
| | 1.0 | | | 1.016 | 1.023 | 0.77 | 1.393 | 1.374 | 1.34 |
| | 1.5 | | | 1.024 | 1.030 | 0.67 | 1.320 | 1.303 | 1.20 |
| | 2.5 | | | 1.027 | 1.038 | 1.08 | 1.249 | 1.239 | 0.75 |

Table 5.3 Measured and calculated TM_{10} and TM_{01} mode frequencies with % error
(Variation with height and permittivity)

| L, W, W_{cp} , W_{cd} (cm) | h (cm) | ϵ_r | TM ₁₀ mode frequency (f_{10}) (GHz) | | | TM ₀₁ mode frequency (f_{01}) (GHz) | | |
|--------------------------------------|-----------|--------------|---|------------|------------|---|------------|------------|
| | | | Measured | Calculated | % error | Measured | Calculated | % error |
| 3,5,1,1 | 0.066 | 10.2 | 1.425 | 1.412 | 0.87 | 0.938 | 0.921 | 1.85 |
| | 0.080 | 2.20 | 2.982 | 3.003 | 0.70 | 1.987 | 1.962 | 1.25 |
| | 0.318 | 2.20 | 2.871 | 2.865 | 0.19 | 1.962 | 1.926 | 1.7 |
| 4,5,1,1 | 0.066 | 10.2 | 1.112 | 1.102 | 0.08 | 0.931 | 0.918 | 1.44 |
| | 0.080 | 2.20 | 2.346 | 2.348 | 0.08 | 1.975 | 1.956 | 0.92 |
| | 0.318 | 2.20 | 2.252 | 2.274 | 0.99 | 1.928 | 1.915 | 0.64 |
| 5,5,1,1 | 0.066 | 10.2 | 0.906 | 0.911 | 0.59 | 0.926 | 0.915 | 1.16 |
| | 0.080 | 2.20 | 1.919 | 1.943 | 1.29 | 1.963 | 1.953 | 0.50 |
| | 0.318 | 2.20 | 1.903 | 1.900 | 0.14 | 1.903 | 1.906 | 0.18 |
| 6,5,1,1 | 0.066 | 10.2 | 0.763 | 0.768 | 0.65 | 0.920 | 0.905 | 1.61 |
| | 0.080 | 2.20 | 1.620 | 1.639 | 1.19 | 1.954 | 1.933 | 1.06 |
| | 0.318 | 2.20 | 1.580 | 1.613 | 2.09 | 1.883 | 1.883 | 0.03 |
| 7,5,1,1 | 0.066 | 10.2 | 0.659 | 0.662 | 0.46 | 0.915 | 0.896 | 2.00 |
| | 0.080 | 2.20 | 1.401 | 1.415 | 0.991 | 1.941 | 0.914 | 1.30 |
| | 0.318 | 2.20 | 1.374 | 1.400 | 91 | 1.862 | 0.862 | 0.02 |
| 8,5,1,1 | 0.066 | 10.2 | 0.579 | 0.582 | 0.43 | 0.900 | 0.887 | 1.37 |
| | 0.080 | 2.20 | 1.234 | 1.243 | 0.76 | 1.925 | 1.896 | 1.49 |
| | 0.318 | 2.20 | 1.217 | 1.235 | 1.50 | 1.847 | 1.842 | 0.23 |

5.3.2 Electromagnetically Coupled Dual Port Arrow Shaped Microstrip Antenna

The arrow shaped antenna is reconfigured using two perpendicular microstrip feed lines to eliminate cross talk between the two polarizations and to achieve excellent isolation between the ports as explained in Section (4.4). The geometry of the proposed antenna is shown in Figure 4.31. The antenna is etched on a dielectric substrate of thickness h_2 and dielectric constant ϵ_{r2} and fed by proximity coupling using two 50Ω perpendicular microstrip lines etched on a substrate of thickness h_1 and dielectric constant ϵ_{r1} .

The equations given above for the co-axial fed arrow shaped microstrip antenna is modified to obtain the frequencies for the dual ports. Here the thickness of the substrate is modified due to the effect of another substrate with microstrip feedline. Hence 'h' used in the equations 5.22 through 5.25 should be replaced by effective thickness $h_{\text{eff}}=h_1+h_2$. Here only the special case where both the substrates are of the same permittivity are studied and hence the dielectric constant in equations 5.22 and 5.24 are replaced by $\epsilon_r=\epsilon_{r1}=\epsilon_{r2}$.

So, the effective dielectric constant for TM_{10}

$$\epsilon_1 = \frac{\epsilon_r + 1}{2} + \frac{\epsilon_r - 1}{2} \left(1 + 12 \frac{h_{\text{eff}}}{W} \right)^{-1/2} \quad (5.27)$$

$$\Delta l_1 = 0.412 h_{\text{eff}} \frac{(\epsilon_1 + 0.3) \left(\frac{W}{h_{\text{eff}}} + 0.258 \right)}{(\epsilon_1 - 0.258) \left(\frac{W}{h_{\text{eff}}} + 0.8 \right)} \quad (5.28)$$

For TM_{01} ,

$$\epsilon_2 = \frac{\epsilon_r + 1}{2} + \frac{\epsilon_r - 1}{2} \left(1 + 12 \frac{h_{eff}}{S} \right)^{-1/2} \quad (5.29)$$

$$\Delta l_2 = 0.412 h_{eff} \frac{(\epsilon_2 + 0.3) \left(\frac{S}{h_{eff}} + 0.258 \right)}{(\epsilon_2 - 0.258) \left(\frac{S}{h_{eff}} + 0.8 \right)} \quad (5.30)$$

where $h_{eff} = h_1 + h_2$, $\epsilon_r = \epsilon_{r1} = \epsilon_{r2}$ (5.31)

For Port1,

$$f_{01} = \frac{c}{2(W_{eff} + 2\Delta l_2)\sqrt{\epsilon_2}}$$

For Port2,

$$f_{10} = \frac{c}{2(S_{eff} + 2\Delta l_1)\sqrt{\epsilon_1}}$$

S_{eff} and W_{eff} are calculated as explained in the coaxial feeding technique.

The theoretical variation of the two resonant frequencies with L for different values of h_{eff} and ϵ_r are shown in Figure 5.6. The measured curves are given in the same figure to validate the computed results. Here the theoretical results are in good agreement with measured values with maximum percentage error less than 2 as shown in Table 5.4.

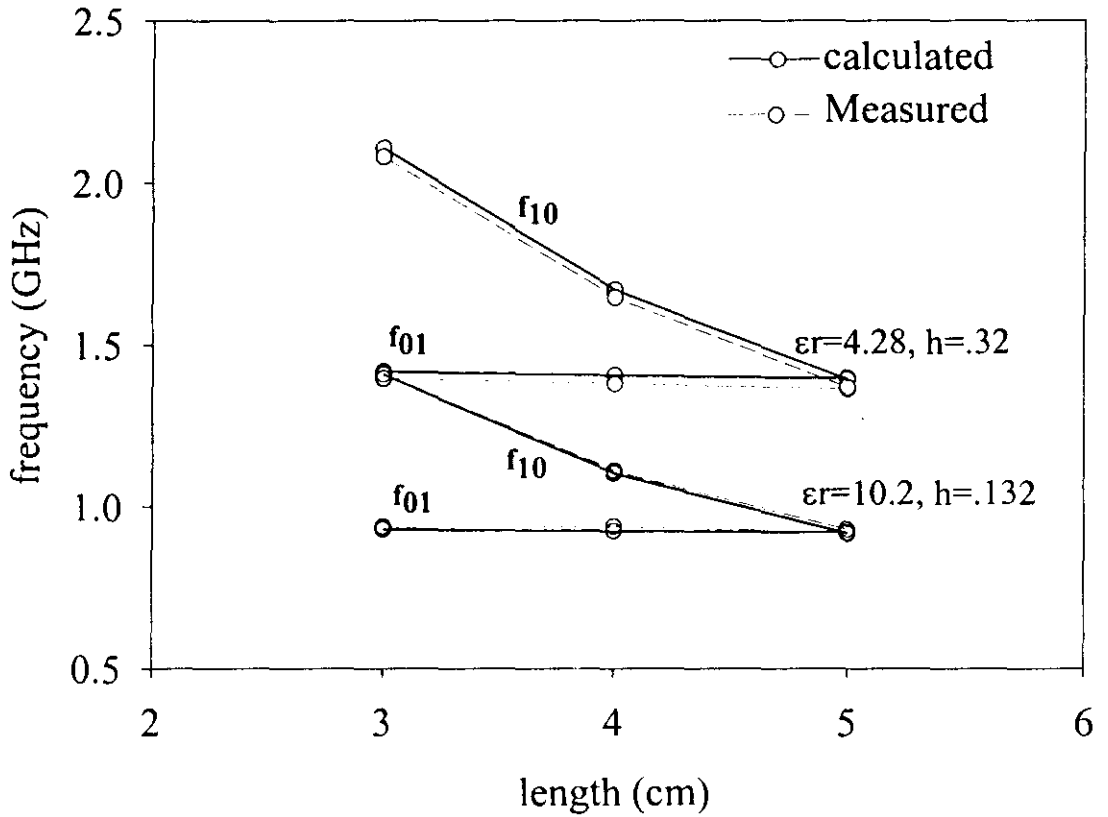


Figure 5.6 Graph showing the variation of calculated and measured TM_{10} and TM_{01} mode frequencies of the dual port antenna with Length L
($W=5\text{cm}$, $W_{cp}=1\text{cm}$, $W_{cd}=1\text{cm}$)

Table 5.4 Measured and calculated TM_{10} and TM_{01} mode frequencies for the dual port antenna

| L,W,Wcp, Wcd (cm) | h (cm) | ϵ_r | TM ₁₀ mode frequency (f ₁₀) (GHZ) | | | TM ₀₁ mode frequency (f ₀₁) (GHZ) | | |
|-------------------------|-----------|--------------|---|------------|---------|---|------------|---------|
| | | | Measured | Calculated | % error | Measured | Calculated | % error |
| | | | 3, 5, 1, 1 | 0.160 | 4.28 | 2.080 | 2.107 | 1.61 |
| 4, 5, 1, 1 | 0.160 | 4.28 | 1.645 | 1.669 | 1.94 | 1.379 | 1.405 | 1.46 |
| 5, 5, 1, 1 | 0.160 | 4.28 | 1.368 | 1.392 | 1.98 | 1.363 | 1.396 | 1.61 |
| 4, 7, 1, 1 | 0.160 | 4.28 | 1.633 | 1.643 | 1.48 | 1.013 | 1.028 | 0.63 |
| 5, 7, 1, 1 | 0.160 | 4.28 | 1.343 | 1.358 | 1.29 | 1.008 | 1.021 | 1.13 |
| 6, 7, 1, 1 | 0.160 | 4.28 | 1.148 | 1.155 | 1.20 | 1.003 | 1.057 | 0.67 |
| 3, 5, 1, 1 | 0.066 | 10.2 | 1.409 | 1.408 | 0.91 | 0.936 | 0.927 | 0.04 |
| 4, 5, 1, 1 | 0.066 | 10.2 | 1.112 | 1.103 | 0.80 | 0.936 | 0.922 | 0.81 |
| 5, 5, 1, 1 | 0.066 | 10.2 | 0.926 | 0.914 | 0.04 | 0.917 | 0.917 | 1.29 |

as there is one half wave variation of current along the width. (Figure 5.8(a)). The second frequency $f_2 = 1.695$ GHz is of TM_{10} mode as there is one half wave of current variation along the length (Figure 5.8 (b)). Comparing it with modes shown in Table 5.1 it is clear that the modes predicted using theoretical calculations are in good agreement. Now, W_{cp} is varied and the same procedure is repeated. For $W_{cp} = 2$ cm, we can notice that there is a change in dominant mode. Here the dominant mode is f_{10} as clear from the Figure 5.8 (a, d). Checking Table 5.1 the same change can be noticed for theoretical calculations.

From the above results we can conclude that modes predicted through theoretical calculations are established from the current calculations using IE3D.

5.4 Verification of the resonating modes using IE3D

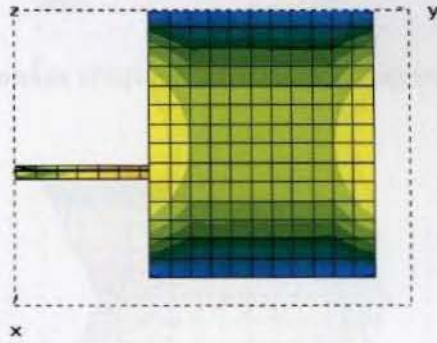
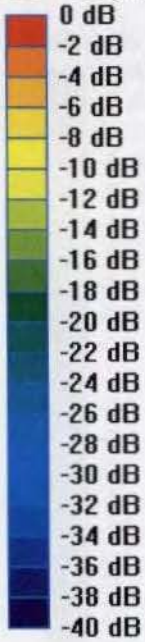
Mode verification can be done by calculating the 3D average current density on the patch surfaces. Mode identification is possible by seeing the current distribution along the edges of the patch.

For verification, a rectangular patch having dimension $L=6\text{cm}$, $W=5\text{cm}$ is simulated and the current distributions on the surface of the patch is calculated. The fundamental modes are given in Figure 5.7(a, b). From the figure it is clear that the first frequency (Figure 5.7(a)) is having a mode TM_{10} as there is one half wave of the field variation along length, second frequency (Figure 5.7(b)) is TM_{01} as there is one half wave variation along width.

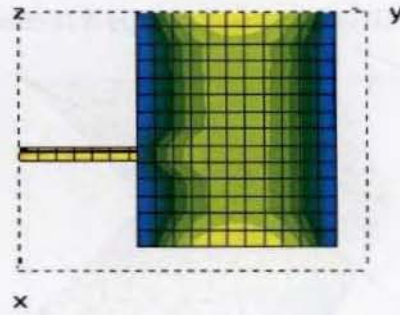
In arrow shaped antenna modes determined by this technique found to agree with the mode predicted using theoretical calculations. For verification, current distributions are calculated for the patches by trimming W_{cd} and compared it with experimental results as shown in Table 5.1. Patch having dimensions $L=4\text{ cm}$, $W=5\text{cm}$, $W_{cd}=1\text{ cm}$, $W_{cp}=1\text{cm}$ is simulated using IE3D and axial currents are determined as shown in Figure 5.8 (a, b). Here the dominant mode frequency $f_1=1.423\text{ GHz}$ is of TM_{01} mode as there is one half wave variation of current along the width (Figure 5.8(a)). The second frequency $f_2 = 1.695\text{ GHz}$ is of TM_{10} mode as there is one half wave of current variation along the length (Figure 5.8 (b)). Comparing it with modes shown in Table 5.1 it is clear that the modes predicted using theoretical calculations are in good agreement. Now W_{cd} is varied and the same procedure is repeated. For $W_{cd}=2\text{ cm}$, we can notice that there is a change in dominant mode. Here the dominant mode is f_{10} as clear from the Figure 5.8 (c, d). Checking Table 5.1 the same change can be noticed for theoretical calculations.

From the above results we can conclude that modes predicted through theoretical calculations are established from the current calculations using IE3D.

0 dB = 20 (A/m)



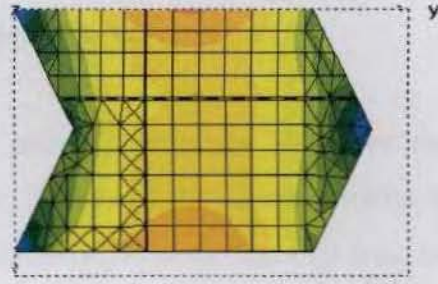
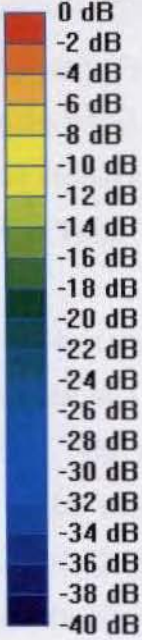
a) First frequency $f_1 = 1.189$ GHz



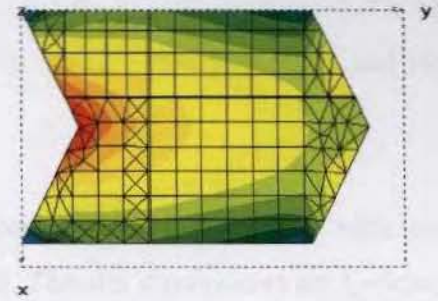
b) Second frequency $f_2 = 1.418$ GHz

Figure 5.7 3D average current density on the surface of the rectangular patch
(L=6 cm, W=5cm)

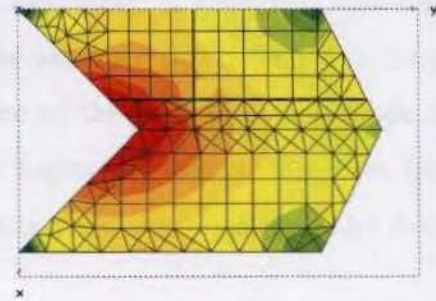
0 dB = 25 (A/m)



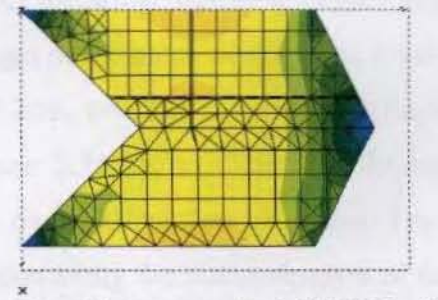
a) First resonant frequency $f_1=1.424$ GHz ($W_{cd}=1$ cm)



b) Second resonant frequency $f_2=1.691$ GHz ($W_{cd}=1$ cm)



c) First resonant frequency $f_1=1.481$ GHz ($W_{cd}=2$ cm)



d) Second resonant frequency $f_2=1.522$ GHz ($W_{cd}=2$ cm)

Figure 5.8 3D average current density on the surface of the patch

($L=4$ cm, $W=5$ cm, $W_{cp}=1$ cm)

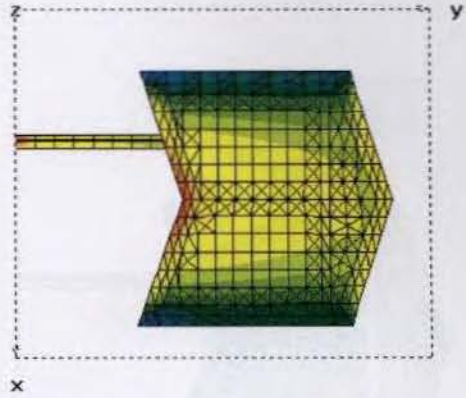
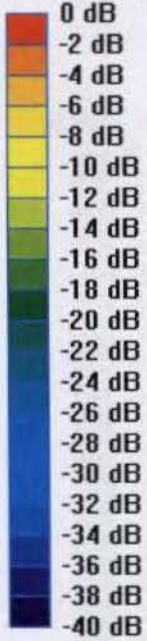
5.5 Mode verification for slotted geometries

Mode verifications can be done for slotted geometries also. For the unslotted geometry ($L=6\text{cm}$, $W=5\text{cm}$, $W_{cd}=1\text{cm}$, $W_{cp}=1\text{cm}$) the current distributions for the first three modes are shown in the Figure 5.9 (a, b, c, d). The first frequency is TM_{10} as there is one variation of current along length (Figure 5.9 (a)), and second TM_{01} as there is variation along width (Figure 5.9 (b)), and the third TM_{11} as there is one variation along both length and width (Figure 5.9 (c)). In Figure 5.9 (d) there is a double variation with almost null current at the centre and edges and identified this mode as TM_{20} .

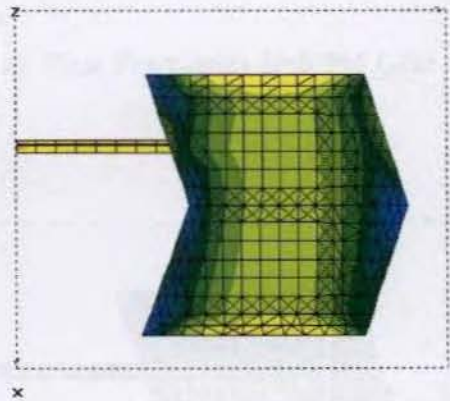
Current is calculated for the above arrow shaped geometry with an embedded rectangular slot as shown in Figure 4.19. The slot dimensions are $l_s=5\text{cm}$, $w_s=0.2\text{cm}$, $s=0.5\text{cm}$. The current distributions for the fundamental modes are shown in Figure 5.10 (a, b). From the graph it is clear a new mode is generated which is less than TM_{10} and TM_{01} mode frequencies of the unslotted patch. The new frequency has current distributions at the circumference of the slot. This new mode have same polarization as TM_{01} as presented in Chapter 4. Hence this new frequency is regarded as the $TM_{0\delta}$ mode ($0<\delta<1$) as it is a new mode generated by the embedded slot.

Current distribution is also calculated for the arrow shaped geometry with two slots embedded close to the non radiating edges of the patch as shown in Figure 4.22. The slot is having dimension $l_s=5\text{cm}$, $w_s=0.2\text{cm}$, $s=0.2\text{cm}$. Current distributions for the fundamental mode are shown in Figure 5.11 (a, b). The first frequency is the fundamental mode generated as in the case of unslotted geometry. For the second frequency we can see the current variation along the circumference of the slot. This frequency has the same polarization as the fundamental mode. This new frequency generated can be said to have a mode $TM_{\delta 0}$ ($1<\delta<2$). It is clearly cited in the figure.

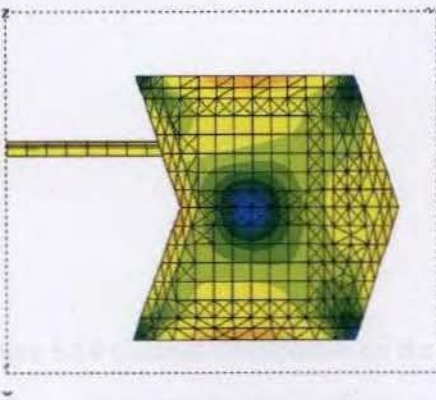
0 dB = 20 (A/m)



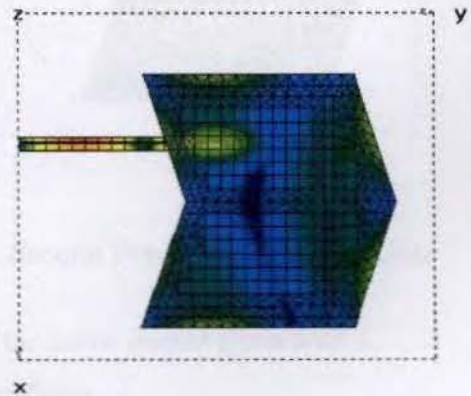
a) First frequency $f_1 = 1.153$ GHz



b) Second frequency $f_2 = 1.37$ GHz



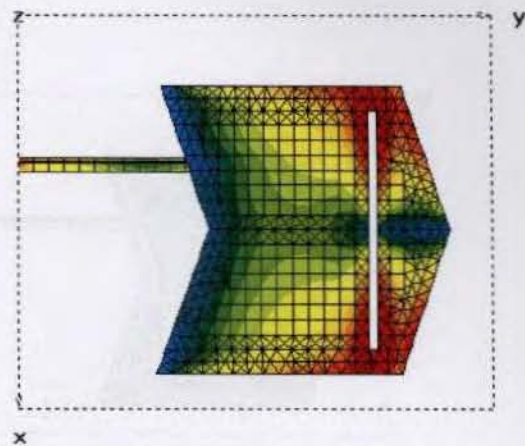
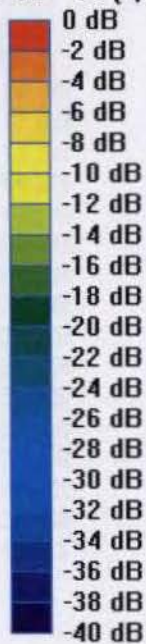
c) Third Frequency $f_3 = 1.871$ GHz



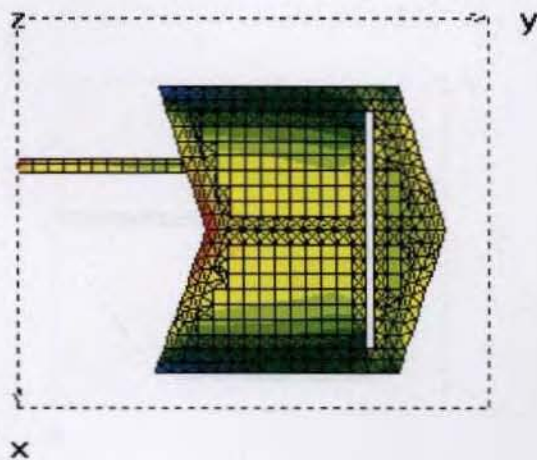
d) Fourth Frequency $f_4 = 2.301$ GHz

Figure 5.9 Current distribution on the surface of the unslotted patch ($L=6$ cm, $W=5$ cm, $W_{cp}=1$ cm, $W_{cd}=1$ cm)

0 dB = 20 (A/m)



a) First Frequency $f_1=0.996$ GHz



b) Second Frequency $f_2=1.147$ GHz

Figure 5.10 Current distribution on the surface of the arrow shaped patch with a rectangular slot ($l_s=5\text{cm}$, $w_s=0.2\text{cm}$, $s=0.5\text{cm}$)

CHAPTER 6

CONCLUSIONS

This chapter presents the conclusions drawn from the experimental and theoretical investigations carried out on arrow shaped compact microstrip antenna. Suggestions for further research work in the field are also given.

6.1 INFERENCES FROM EXPERIMENTAL AND THEORETICAL INVESTIGATIONS

The main aim of the work presented in the thesis was to develop a dual frequency microstrip antenna. Emphasis was also given in reducing the patch area compared to conventional microstrip patch antennas. The investigations started with a study of the characteristics of drum shaped microstrip antennas which is known to be a compact antenna compared to a rectangular patch. The drum shaped patch is modified in the present study by removing triangles from the smaller dimension of a rectangular patch as explained in Appendix C. Thus two closely spaced resonances of opposite polarization are achieved.

The drum has been modified to an 'arrow' shape as discussed in Section 4.1. with a view to improve the cross polarization performance. This structure is obtained by removing a triangle (intruding) from an edge and adding a triangle (protruding) to the other edge of a rectangular patch. This structure was simulated for various values of W_{cp} and W_{cd} . From the experimental or simulated measurements the antenna is found to be resonating at dual frequencies and the ratio between them can be tuned by trimming intruding triangle height W_{cd} or protruding triangle height W_{cp} . The two resonant modes excited are TM_{10} and TM_{01} . By varying W_{cd} , TM_{10} mode frequency varies rapidly and TM_{01} mode frequency remains almost constant as shown in Figure 4.2. The effect of W_{cp} on both the mode frequencies is negligible as shown in Table 4.2. The variation of radiation characteristics with other parameters like length 'L' and width 'W' are also investigated. TM_{10} mode frequency changes rapidly with Length 'L' and TM_{01} mode remains almost constant as shown in Figure 4.3. The variation of width 'W' changes TM_{01} mode frequency and slightly changes TM_{10} mode. Both the frequencies decrease with increase in the permittivity and height of the patch as in the standard rectangular microstrip antennas. So it is concluded that the

variation in TM_{10} mode frequency is due to the slanted lengths and TM_{01} mode frequencies is determined by the effective width.

Characteristics of this new geometry are compared with other standard geometries like rectangular and drum shaped antennas in Table 4.4. The antenna provides an area reduction of ~68% for the TM_{10} mode frequency compared to the rectangular patch designed for the same frequency with slight reduction in gain. The antennas also provides greater area reduction and improved gain [figure 4.10] compared to compact drum shaped patches. The 2:1 VSWR bandwidth, 3dB beam width etc. are comparable to that of the standard rectangular patch as inferred from Section 4.1.5.

Polarization diversity can be obtained by changing the intruding triangle height (W_{cd}) as shown in Section 4.2.1. Dual band operation with one linearly polarized band and one circularly polarized band, find applications in multiband, multimode handsets or data communicators, where communication with terrestrial and satellite networks are needed. Circularly polarized band can be used for satellite communications as they do not need polarization tracking. Different polarized bands obtained by adjusting the single parameter W_{cd} makes the design more attractive.

Different slotted geometries are investigated in Section 4.3. Depending on the type of slots inside the patch, a new frequency having same or opposite polarization compared to the fundamental mode is excited. When a single rectangular slot is etched inside the patch a new band having opposite polarization is excited. This newly generated frequency decreases rapidly with the slot length keeping the other modes almost the same as that of unslotted geometries. This new mode is slightly affected by the variation of the slot width and the position of the slot inside the patch.

By embedding a pair of slots on the radiating edges of the arrow shaped antenna a new frequency which has same polarization. TM_{10} mode frequency remains the same as the unslotted patch. This new mode is regarded as $TM_{\delta 0}$ as explained in mode verifications using IE3D simulation software.

A pair of slots is embedded close to the non radiating edges of the patch. Here also a new mode $TM_{\delta 0}$ having the same polarization as TM_{10} is generated. For a particular slot length, fundamental mode and the new mode combine to give bandwidth enhancement. This new frequency is found to be affected by the width of the slot also. It decreases with increase in the width of the slot.

Dual port geometry is proposed for the dual polarized antenna to avoid cross talk between the frequencies. Here the isolation between the ports is better than 25 dB which implies very small cross coupling between the frequencies.

Closed form expressions for calculating the TM_{10} and TM_{01} mode frequencies of the arrow shaped microstrip antenna presented in Chapter 5 provides a fast and simple way to predict the characteristics of the antenna. The accuracy of these simple formulae is validated by experimental results. Current distributions on the surface of the patch are studied to confirm the modes predicted from the design equations. The current variations for the slotted and unslotted geometries show the new mode ($TM_{0\delta}$ or $TM_{\delta 0}$) generation in the slotted one.

6.2 SOME POSSIBLE APPLICATIONS OF THE PROPOSED ANTENNA

Compact dual frequency microstrip antennas are attracting more attention due to the fast developments in communications. This antenna can effectively replace conventional rectangular and circular patches in applications like phased arrays as there is little deterioration in gain compared to an equivalent rectangular patch

antenna. Being a compact dual frequency antenna, it can be integrated with active devices in Monolithic Microwave Integrated Circuits (MMICs).

A dual band, dual polarised antenna capable of receiving both linearly and circularly polarised waves can be used for multiband, multimode handsets: mono polar mode for terrestrial cellular communication and circularly polarised for satellite mobile.

Circularly polarized antennas are widely used as efficient radiators in communication systems, remote sensing, navigation and radar. Mobile-satellite-communication use circular polarization, as they do not need polarization tracking.

Arrow shaped antenna with a pair of slots at the nonradiating edges improves the bandwidth of the antenna. Here the antenna can also be used as a dual frequency antenna with two frequencies having same polarization. On the other hand, the dual frequency dual polarized antenna when excited by two independent ports provides excellent isolation between the ports also. Radar and advanced communication applications, such as synthetic aperture radar (SAR), the global positioning system (GPS) and vehicular communication require low profile antennas capable of dual frequency dual polarization operation with large bandwidth and good isolation.

6.3 SCOPE FOR FURTHER WORK IN THE FIELD

By reconfiguring the antenna geometry it will be possible to excite dual band giving CP operations of different helicity. These elements can be applied to satellite systems where two channels are needed to receive/transmit the telecommand and telemetry signals (GPS receivers) or in hand-held message communication terminal.

The concept of using the same frequency band to transmit separate carriers is referred as frequency reuse. This increases the information capacity of the link without increasing link bandwidth. The present CP antenna can be modified for frequency reuse using a dual port, one port giving right hand circularly polarized band (RHCP) and the other port giving left hand circularly polarized band (LHCP). Since bandwidth preservation is vital in satellite links, this will find wide applications.

Stacked geometries using the compact dual band arrow shaped antennas improves the bandwidth, with the advantage of being physically smaller than similar stacked designs.

Simple formulae can be obtained for slotted arrow shaped designs, which help in the fast and easy prediction of the characteristics of these slotted patches.

Study of the temperature and humidity effects on the characteristics of the antenna is important when the antenna is used on high speed vehicles or in space applications.

Further geometrical modifications by altering the irregular side periphery using logarithmic and parabolic curves can be studied in detail for enhancing various characteristics of the antenna. Modifications in proximity coupled feeds like L-shaped or T-shaped probes can further improve the bandwidths of the antenna. By changing the type and nature of slots we can further check the improvement in characteristics.

Since the overall aperture size of the antenna is very small, the possibility of micro machined antenna using this geometry can be tried for GSM applications.

Appendix A

Dual Frequency Dual Port Microstrip Antenna

Experimental and simulated results are presented for a dual port dual polarized microstrip antenna. The antenna excites two resonant frequencies of TM_{11} and TM_{21} modes providing an isolation of ~ 30 dB between the ports. Its geometry consists of two circular arcs of different radii with their centers displaced by a distance. The antenna offers an area reduction of 70% compared to standard rectangular microstrip antenna with a reduction in gain of 1.7dB. The cross polarization radiation levels are better than 20 dB for both the modes.

A.1 INTRODUCTION

In radar and satellite communication applications simultaneous transmit and receive operations can be performed using dual frequency dual polarized microstrip antennas. A dual polarized satellite link must have a good level of isolation between the two ports, as there will always be some interference and thereby the cross-talk between the two polarizations.

In this appendix a crescent shaped microstrip antenna that provides two ports with orthogonal polarization and a very good isolation between the ports is presented. This antenna excites two frequencies of TM_{11} and TM_{21} modes. Energy is coupled electromagnetically to its ports using two perpendicular microstrip feed lines. Green's function based simulation software (IE3D) is used to optimize the antenna parameters in the design of the geometry having different frequency ratios.

A.2 ANTENNA DESIGN

The antenna structure consists of two circular arcs of different radii r_1 and r_2 with their centers C_1 and C_2 displaced by a distance 'd' and fed by electromagnetic coupling using two 50 ohm perpendicular microstrip lines as shown in Figure A.1.

This antenna is fabricated on a substrate with dielectric constant $\epsilon_r=4.28$ and thickness $h=0.16\text{cm}$. The intersection of two circular arcs of radii $r_1=4\text{cm}$ and $r_2=7\text{cm}$ with their centers displaced by a distance $d=6\text{cm}$, is etched on the above substrate. Antenna is excited by electromagnetic coupling using two 50 ohm microstrip feedlines etched on the substrate of same thickness and dielectric constant.

A.3 RESULTS

The antenna resonates at two frequencies 0.9825 GHz and 1.7 GHz for ports 1 and 2 respectively. Variation of return loss with frequency is shown in Figure A.2. The same structure is simulated using IE3D software and the results are also given. Measured isolation between the two ports given in Figure A.3 clearly shows that the antenna offers isolation ~ 30 dB between the ports in the operating frequency range.

The simulated results varying the different parameters r_1 , r_2 , d are presented in Table A.1. From the data given in the table it is clear that antennas having different frequency ratios with good isolation between the ports can be constructed. E-Plane and H-Plane patterns for the ports 1 and 2 are shown in the Figure A.4. The radiation patterns are broad as in the case of ordinary microstrip antennas and offers excellent cross polar performance.

From the experimental results, it is concluded that this simple structure resonates at two modes with very good isolation between two ports. The antenna excites frequencies lower than those of other circular sided patches with good isolation and accounts for its better size reduction. The proposed antenna offers an area reduction of 70% compared to standard rectangular microstrip antenna designed for the same frequency with a small reduction in gain (~ 1.7 dB).

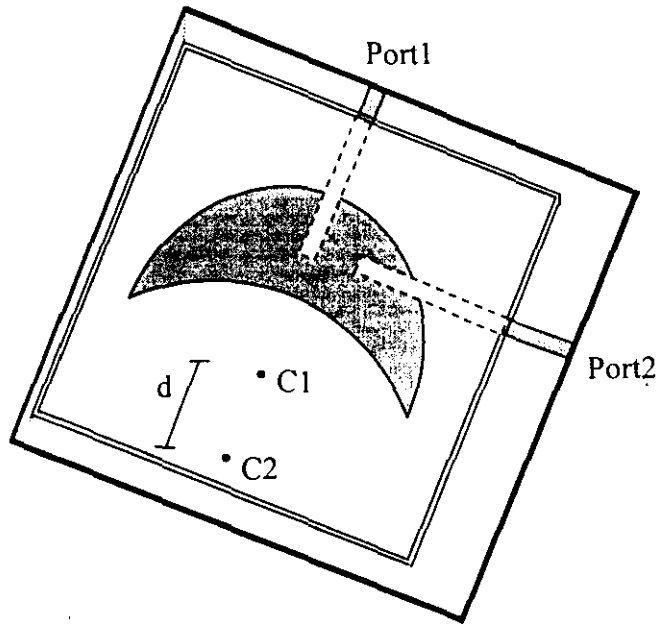


Figure A.1 Geometry of the dual port crescent shaped microstrip antenna

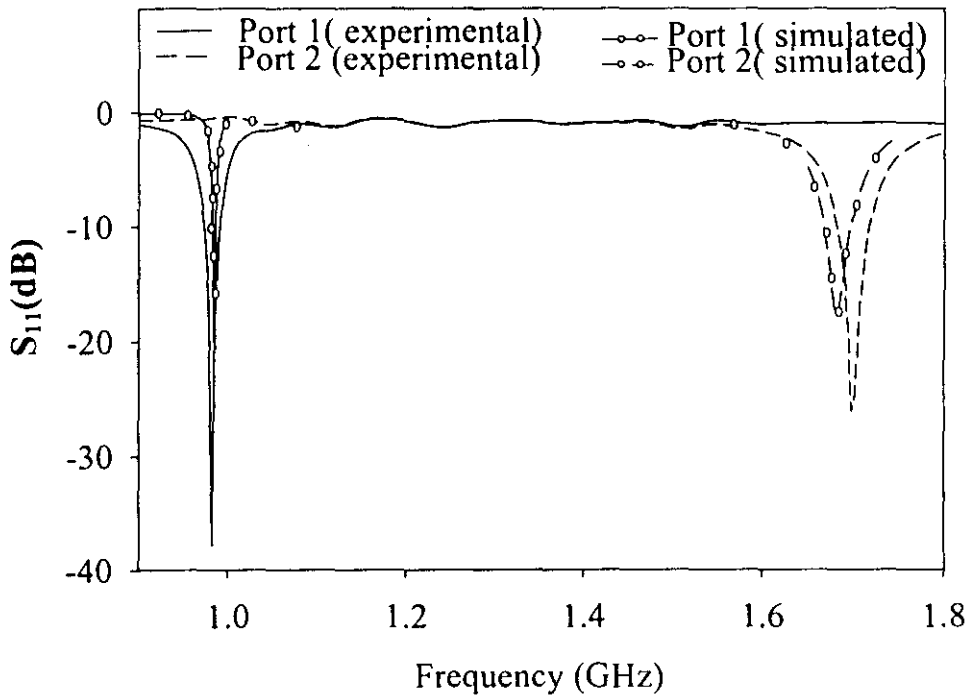


Figure A.2 Variation of return loss against frequency

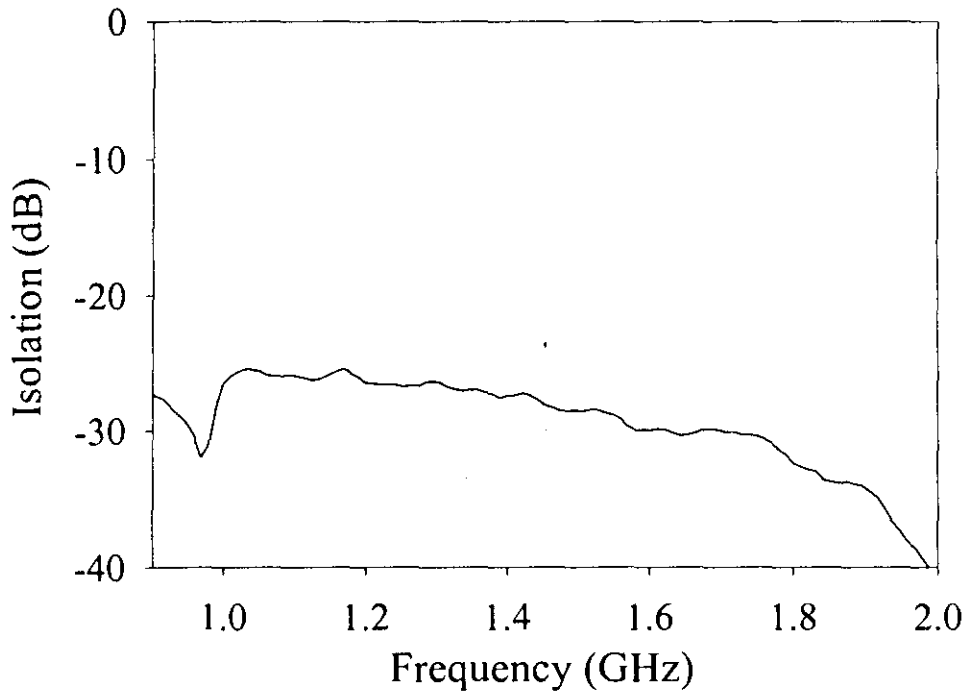


Figure A.3 Measured isolation between port1 and port2

TABLE A.1 IE3D results for the dual port antenna

| r1 (m) | r2 (m) | d (m) | Frequency (GHz) | |
|-----------|-----------|----------|--------------------|-------|
| | | | Port1 | Port2 |
| 0.03 | 0.06 | 0.05 | 1.374 | 2.369 |
| 0.04 | 0.06 | 0.04 | 1.050 | 1.788 |
| 0.05 | 0.07 | 0.05 | 1.352 | 1.906 |
| 0.06 | 0.07 | 0.04 | 1.080 | 1.521 |

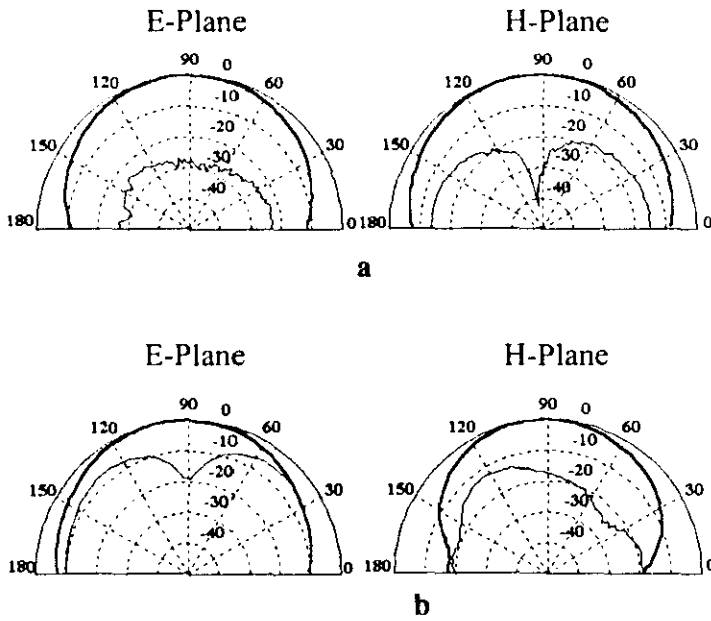


Figure A.4 E- and H- plane radiation patterns at the centre frequencies of the two ports

a Port1 (for frequency 0.9825 GHz)

b Port2 (for frequency 1.7 GHz)

- Copolar
- - - Crosspolar

Appendix B

Compact Circular Sided Microstrip Antenna

A microstrip patch with considerable reduction in antenna size is presented. The proposed design uses curved edges so as to increase the effective resonating length. An area reduction of ~80% compared to a standard rectangular patch is obtained without much reduction in gain. Simple formulae are suggested for calculating the resonant frequency of the new geometry.

B.1 INTRODUCTION

Owing to recent requirements in the miniaturization of personal communication systems, the design of small or reduced size antennas are more relevant now. Many techniques such as introducing shorting pins, cutting slots in the rectangular or circular geometries or by using modified geometries with reduced overall patch area are available in the literature. In this appendix, a more compact microstrip patch, which has a curved resonating edge, is discussed. Simple design formulae, which can predict the resonant frequency of the proposed structure is also presented and its validity has been established by experimental results.

B.2 ANTENNA DESIGN

Geometry of the antenna is as shown in Figure B.1. The antenna structure incorporates two circular arcs of radii r_1 and r_2 with their centers separated by a distance 'd'. The structure is etched on a substrate having thickness 'h' and relative permittivity ' ϵ_r '. The antenna is excited by electromagnetic coupling using a 50Ω microstrip feed line.

B.3 EXPERIMENTAL AND THEORETICAL RESULTS

The standard equations for computing the resonant frequency of a rectangular patch antenna are modified to take into account the effects of the radii of first and second circular arcs and separation between the two centers. The empirical relations are as follows

$$f_r = \frac{c}{2(l_{eff} + 2\Delta l)\sqrt{\epsilon_e}} \quad (1)$$

$$\epsilon_c = \frac{(\epsilon_r + 1)}{2} + \frac{(\epsilon_r - 1)}{2} \left(1 + \frac{12h}{W} \right)^{1/2} \quad (2)$$

$$\Delta l = \frac{0.412h(\epsilon_c + 0.3) \left(\frac{W}{h} + 0.264 \right)}{(\epsilon_c - 0.258) \left(\frac{W}{h} + 0.8 \right)} \quad (3)$$

Effective length l_{eff} is calculated as follows.

Case1 ($r_1=r_2$)

$$l_{\text{eff}} = l_1 - 0.35(l_1 - L) - 0.04(L - r_1)$$

Case2 ($r_1 > r_2$)

$$l_{\text{eff}} = l_1 + 0.05(l_1 - L) + 0.1(r_1 - r_2)$$

Case3 ($r_1 < r_2$)

$$l_{\text{eff}} = l_1 \cdot 0.7(l_1 - L) + 0.05(d - 0.03) \quad r_2 - r_1 \leq 0.02$$

$$l_{\text{eff}} = l_1 \cdot 1.06(l_1 - L) + 0.15(d - 0.04) \quad r_2 - r_1 > 0.02$$

In Case3 a checking factor ($r_2 - r_1$) is required. Here the length of the arc $l_1 = 2r_1\theta_1$ and $\theta_1 = \sin^{-1}(L/2r_1)$ as shown in Figure B.1 (b).

The theoretical variations of the resonant frequency with L for different values of r_1 , r_2 , and d are shown in Figure B.2. The variation of resonant frequency for different ϵ_r and h are shown in Figure B.3. In all these cases the theoretical results are found to be in good agreement with experimental results.

Variation of return loss against frequency for a typical antenna structure with $L=0.06\text{m}$, $r_1=0.04\text{m}$, $r_2=0.04\text{m}$ and $d=0.02\text{m}$ is shown in Figure B.4. The

antenna is fabricated on a substrate of thickness $h=0.0016\text{m}$, and dielectric constant $\epsilon_r=4.28$. A 50Ω microstrip feed line of length $L_p=0.07\text{m}$ and width $W_p=0.003\text{m}$ is etched on a substrate of same thickness and permittivity and kept below the patch to provide electromagnetic coupling. E and H Plane radiation patterns of the antenna at the resonance frequency are shown in Figure B.5. The cross polarization levels are better than 25 dB.

B.4 CONCLUSIONS

A circular-sided compact microstrip antenna having comparable characteristics with a standard rectangular patch has been developed. This design provides an overall area reduction of $\sim 80\%$ compared to standard rectangular patch designed for the same frequency, without much reduction in gain. Simple and accurate expressions have also been developed for predicting the resonant frequency of the proposed geometry.

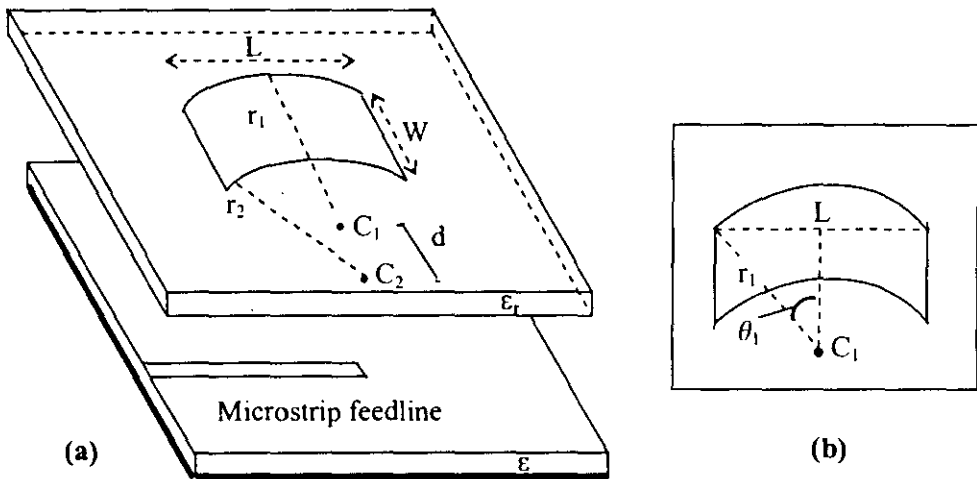


Figure B.1 (a) Geometry of the circular sided microstrip antenna (b) Top view

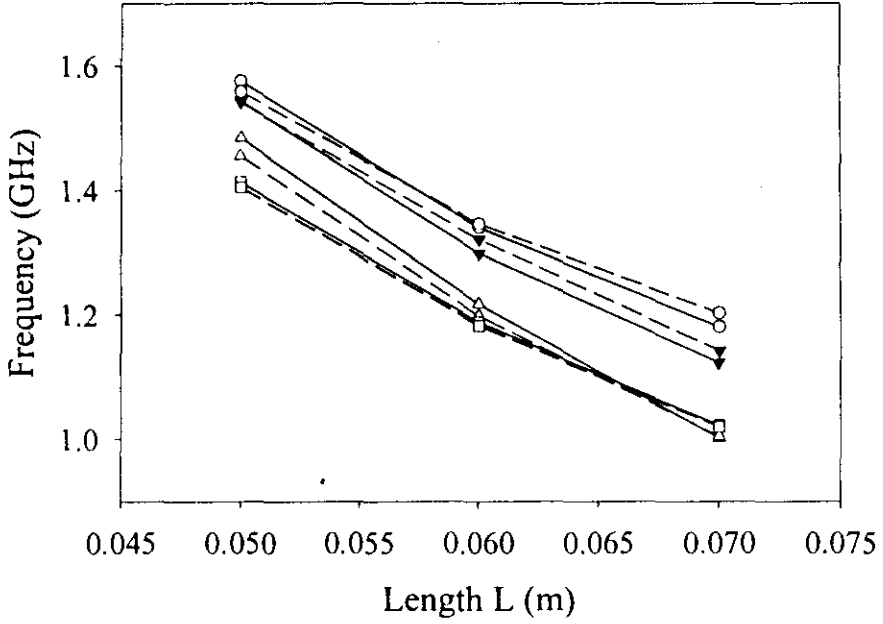


Figure B.2 Variation of resonance frequency with length L for different r_1, r_2 and d ($\epsilon_r=4.28, h=0.0016m$)

----- experimental ——— theoretical

Δ : $r_1, r_2, d = 0.04, 0.04, 0.01m$ \circ : $r_1, r_2, d = 0.05, 0.08, 0.04m$

\square : $r_1, r_2, d = 0.06, 0.07, 0.05m$ \blacktriangledown : $r_1, r_2, d = 0.05, 0.07, 0.03m$

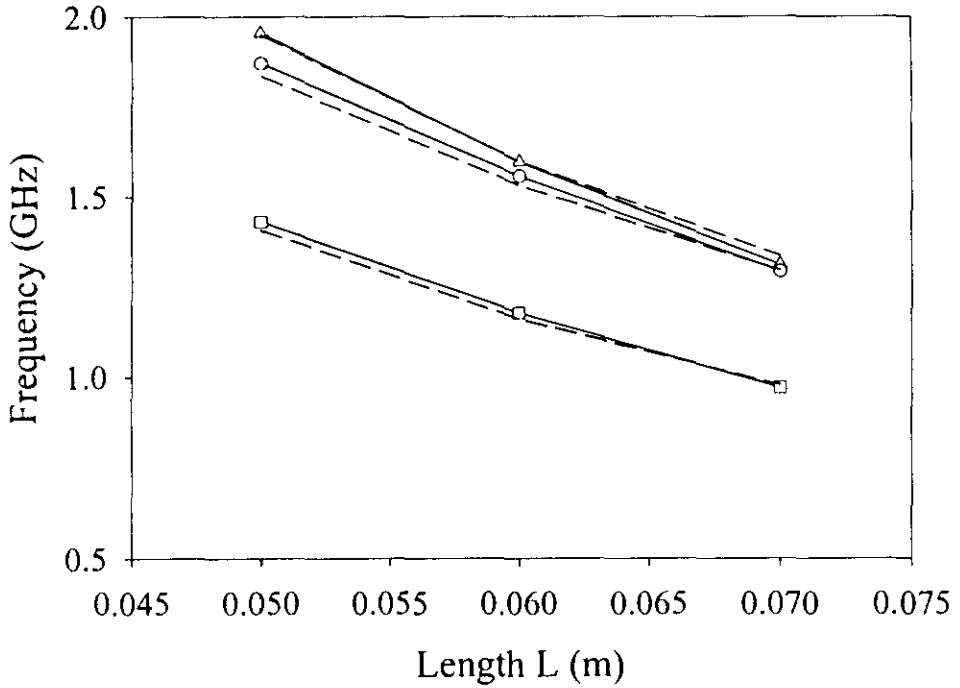


Figure B.3 Variation of resonance frequency with length L for different ϵ_r and h
 ($r_1=r_2=0.04m$, $d=0.02m$)

----- experimental ——— theoretical
 Δ : $\epsilon_r=2.2$, $h=0.08cm$ \circ : $\epsilon_r=2.2$, $h=0.318cm$ \square : $\epsilon_r=4.28$, $h=0.16cm$

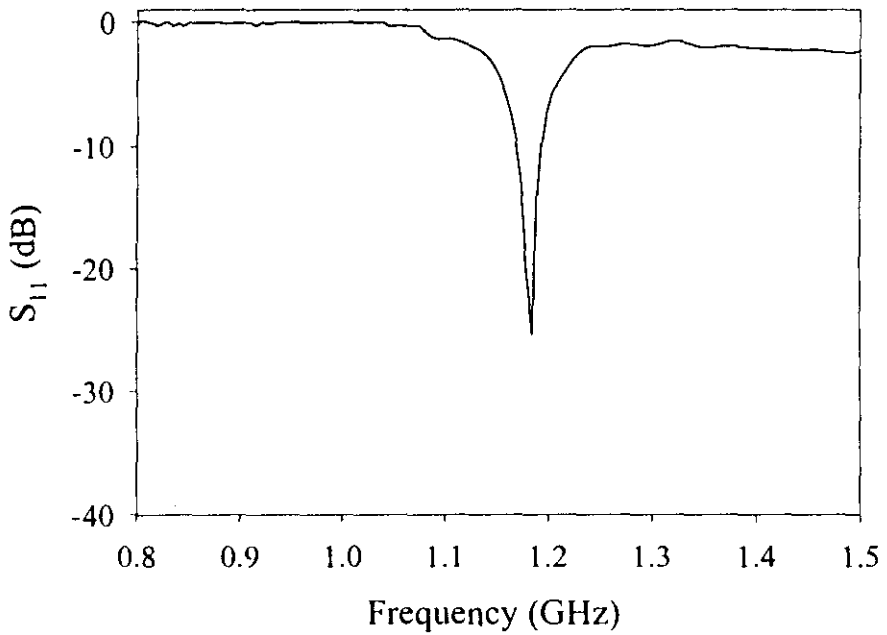


Figure B.4 Variation of return loss with frequency

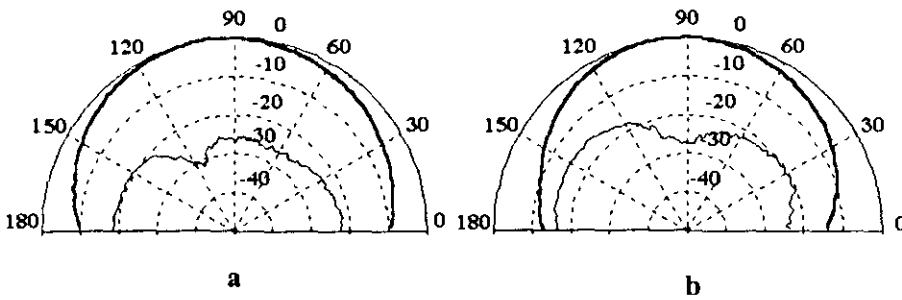


Figure B.5 E- Plane Patterns (a) and H- Plane Patterns (b), for frequency 1.185GHz

- Copolar
- - - Crosspolar

Appendix C

Drum shaped Antenna for dual frequency dual polarized operation and Circular Polarization

Experimental results on a compact dual frequency microstrip antenna are presented. The antenna structure can be modified to achieve desired frequency ratio between the two resonant frequencies and to achieve circular polarization. These antenna configurations provide an area reduction ~40% compared to a standard rectangular antenna operating at the same frequency.

C.1 INTRODUCTION

With the increase of applications in communications, multi frequency planar antennas have become highly desirable. In this appendix drum shaped antenna design for dual frequency and circular polarization operation are presented. By varying the central width of the antenna the ratio between the two resonant frequencies changes and at a particular width combines together to give Circular polarization. Here the compactness is achieved using a drum shaped structure. As the dual frequency and CP design requires only the adjustment of a single parameter the construction is simpler compared to similar designs.

C.2 DUAL FREQUENCY OPERATION

Figure C.1 shows the proposed compact drum shaped antenna with coaxial feed for dual frequency operation. The structure consists of a drum shaped patch etched on a substrate of thickness 'h' and dielectric constant ϵ_r . 'L' denotes length, 'W' is the width and 'W_c' is the central width of the antenna. The antenna is found to resonate with orthogonal polarization when excited using a coaxial feed. The ratio of these lower mode frequencies can be trimmed by the W_c/W ratio.

In a typical design, a drum shaped antenna with length L=3.4cm, width W=5.5cm, and central width W_c= 3.5cm is fabricated on a substrate of $\epsilon_r=4.28$ and h=0.16cm. By properly adjusting the feed point position F_p(X₀=1.2cm, Y₀=0.9cm), both the resonant frequencies can be excited with good matching. This particular antenna is found to resonate with frequencies 1.593GHz and 1.797 GHz.

Figure C.2 shows the variation of return loss with frequency. The frequency ratio is found to be 1.1278. The 2:1 VSWR impedance bandwidths of the antenna are found to be 1.88% for the 1.593GHz band and 1.78% for the 1.797 GHz band. E-

plane and H-plane copolar and crosspolar patterns at the central frequencies of the two bands are shown in Figure C.3. Figure C.4 shows the variation of two resonant frequencies with W_c/W ratio. When the ratio is 0.5 the frequency ratio is minimum.

C.3 CIRCULAR POLARISATION OPERATION

Figure C.5 shows the proposed compact drum shaped antenna using microstrip feed for CP radiation. By choosing the suitable dimension for the central width W_c , two orthogonal resonant modes for the CP can be excited. The antenna is excited by an electromagnetic coupling using a 50 ohm microstrip feed line of length L_p as shown in the figure.

A drum shaped antenna of length $L=4.8\text{cm}$, width $W=5.4\text{cm}$, is fabricated on a substrate of $\epsilon_r=4.28$ and $h=0.16\text{cm}$. A microstrip line of length $L_p=5.8\text{cm}$ and $W_p=0.3\text{cm}$ on a substrate of same thickness and permittivity is kept below the antenna to provide the coupling. It is found that for central width $W_c=2.4\text{cm}$, two orthogonal resonant modes merge to produce circular polarization. Figure C.6 shows the measured return loss against frequency. By considering the centre frequency at 1.68 GHz, where a minimum axial ratio is observed, the proposed design has a CP bandwidth of 1.013%. The measured axial ratio versus frequency is presented in Figure C.7. The E-Plane and H-Plane patterns at the centre frequency are shown in Figure C.8.

C.4 CONCLUSIONS

The proposed antenna uses the variation of the central width of the drum shaped antenna for the excitation of two orthogonal modes. The use of single parameter makes the proposed designs easily implemented with a greater reduction in area.

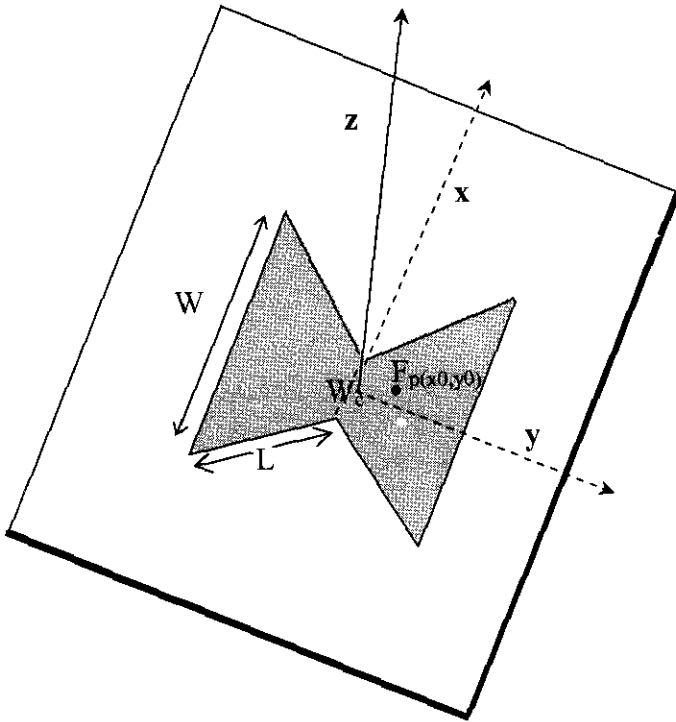


Figure C.1 Geometry of the dual frequency drum shaped antenna with coaxial feed

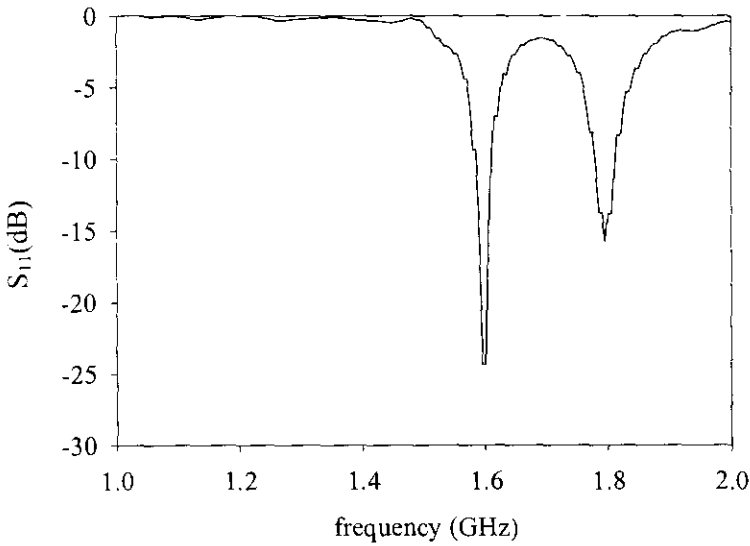


Figure C.2 Variation of return loss with frequency

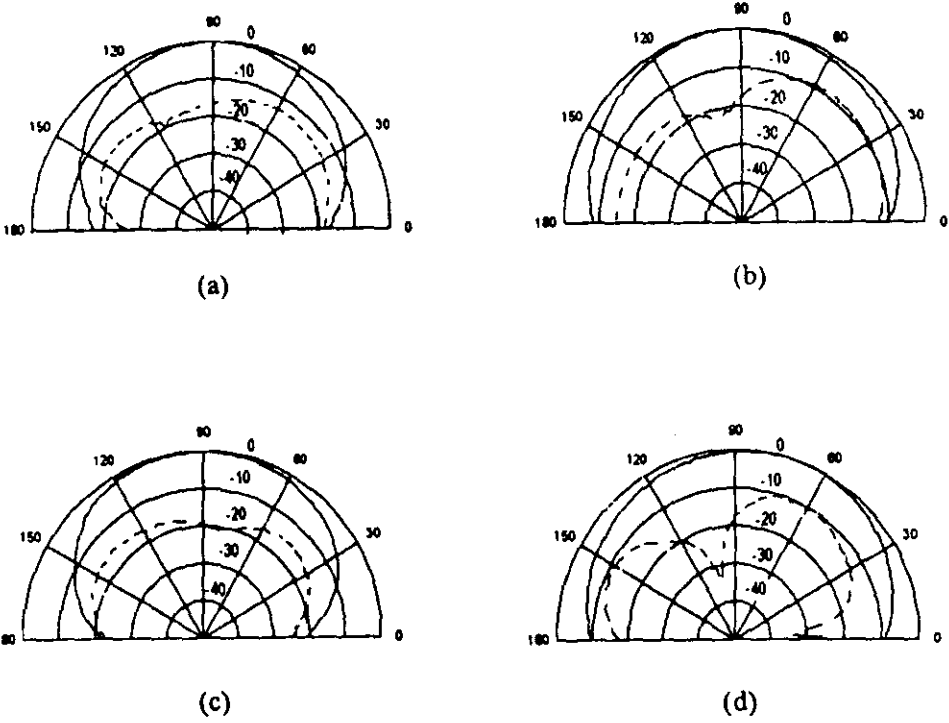


Figure C.3 Radiation pattern of the antenna for the two resonant frequencies

(a) H-Plane (b) E-Plane patterns for 1.593 GHz

(c) H-Plane (d) E-Plane patterns for 1.797 GHz

———— Copolar - - - - - Crosspolar

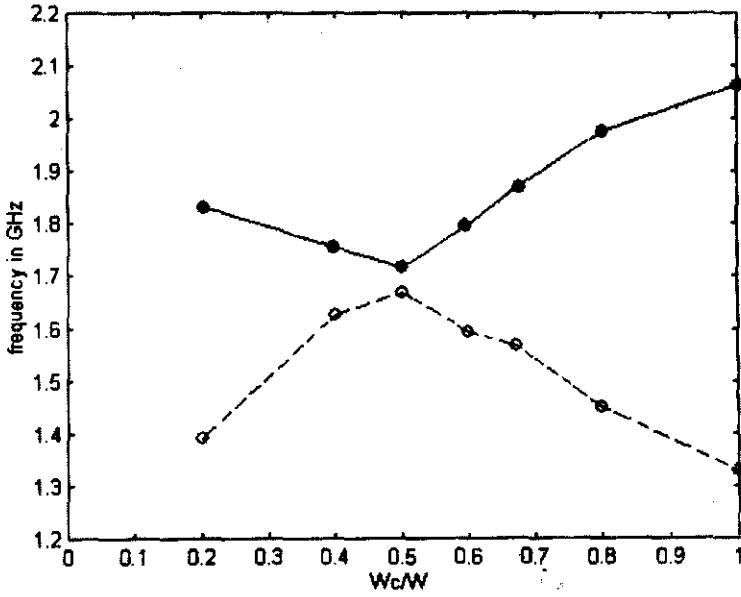


Figure C.4 Variation of first and second resonant frequencies with central width

---○--- First frequency —○— Second frequency

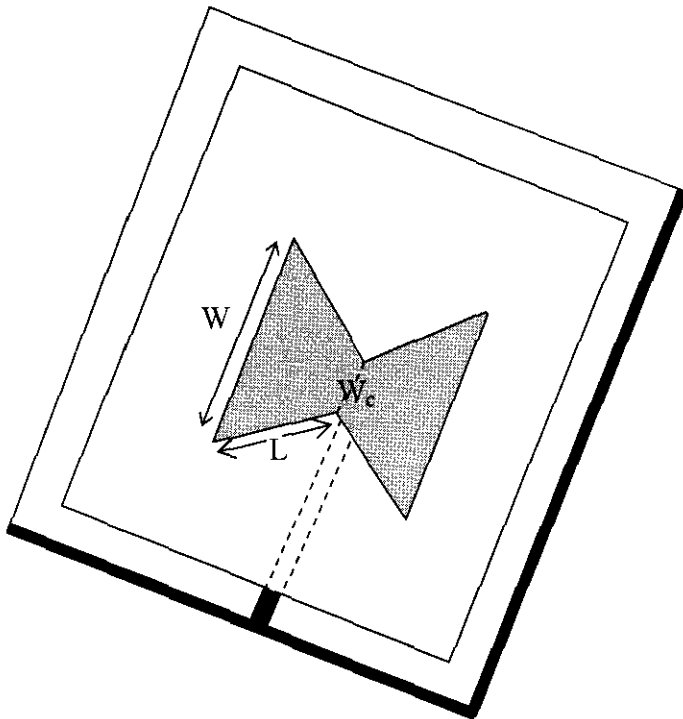


Figure C.5 Geometry of the drum shaped antenna using microstrip feed for CP

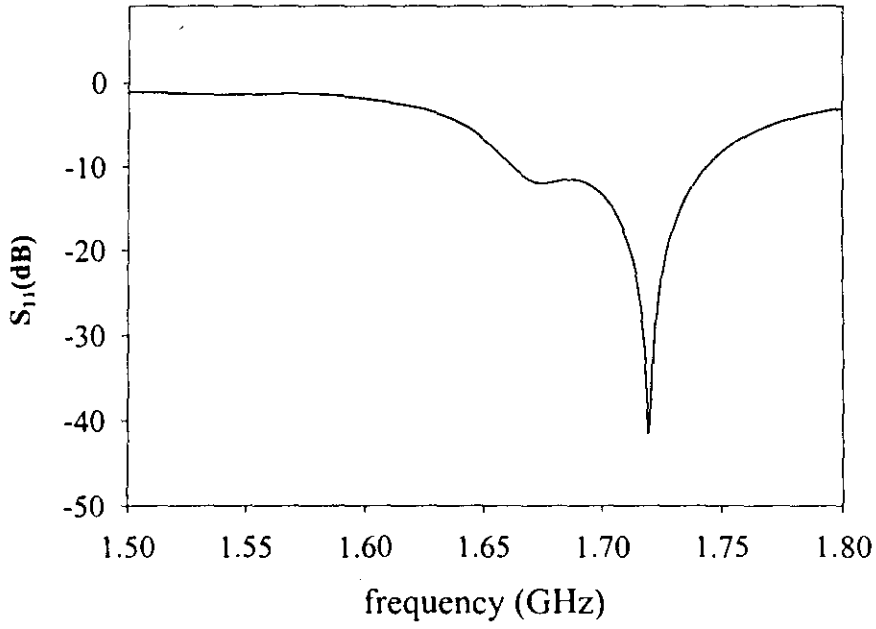


Figure C.6 Variation of return loss with frequency for CP design

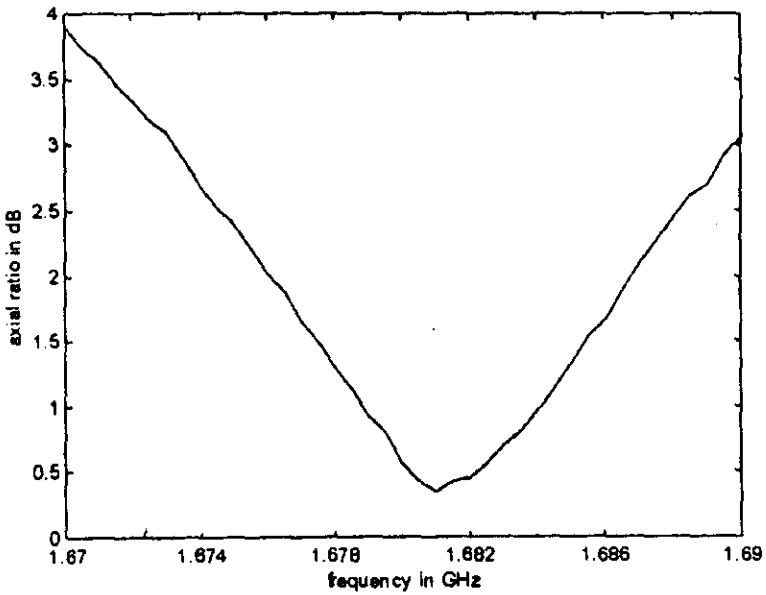


Figure C.7 Measured axial ratio against frequency

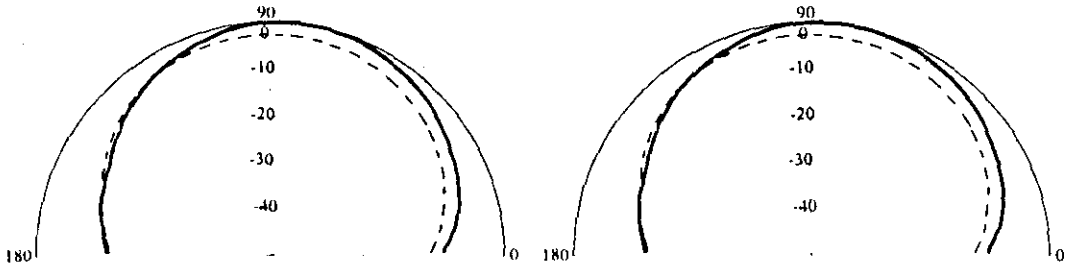


Figure C.8 Radiation pattern at the centre frequency of the CP band

(a) E-Plane (b) H-Plane

———— Copolar - - - - - Crosspolar

REFERENCES

BOOKS

1. I. J. Bahl and P. Bhartia, "Microstrip Antennas", Artech House, Dedham, MA, 1980.
2. K. C. Gupta, R. Garg and R. Chadha, "Computer-aided design of microwave circuits", Artech House, Norwood, MA, 1981.
3. J. R. James, P.S. Hall and C. Wood, "Microstrip antenna – theory and design", London, UK, Peter Peregrinus Ltd., IEE, 1981.
4. C. A. Balanis, "Antenna theory: Analysis and design", Harper and Row, Publishers, New York, 1982.
5. J. D. Kraus, "Antennas", McGraw-Hill, New York, 1988.
6. K. C. Gupta and Abdelaziz Benalla, "Microstrip antenna design", Artech House, Norwood, MA, 1988.
7. J. R. James and P. S. Hall, "Handbook of microstrip antennas", Peter Peregrinus Ltd., IEE Engineers 1V series, 1989.
8. F. Gardiol, "Microstrip Circuits", John Wiley & Sons, Inc., New York, 1994.
9. IE3D User's manual, Release 7, Zealand Software, Inc. December 1999
10. Fidelity User's Manual, Release 3, Zealand Software, April 2000

JOURNALS/ SYMPOSIUM PAPERS

11. G. A. Deshamps, "Microstrip Microwave Antennas", presented at 3rd USAF Symposium on Antennas, 1953.
12. H. Gulton and G. Bassinot, "Flat aerial for ultra high frequencies", French Patent No. 703113, 1955
13. L. Lewin, "Radiation from Discontinuities in Striplines", Proc.IEE, vol. 107, pp 163-170, 1960.
14. E. V. Byron, "A New Flush Mounted Antenna Element for Phased Array application", Proc. Phased Array Antenna Symp., pp. 187-192, 1970.
15. R. E. Munson, "Conformal Microstrip Antennas and Microstrip Phased Arrays" IEEE Trans. Antennas Propagation, vol. AP-22, pp. 74-77, 1974.
16. J. Q. Howell, "Microstrip Antennas", IEEE Trans. Antennas Propagation, vol. AP-23, pp. 90-93, 1975.
17. G. G. Sanford, "Conformal Microstrip Phased Array for Aircraft Tests with ATS-6", Proc. Nat. Electronic Conf., vol. 29, pp. 252-257, 1974.
18. H. D. Weinschel, "Cylindrical array of circularly polarized microstrip antennas", IEEE Antennas Propagat. Soc. Int. Symp., pp. 177-180, 1975.
19. A. G. Derneryd, "Linearly Polarized Microstrip Antennas", IEEE Trans. Antennas Propagation, vol. AP-24, pp. 846-851, 1976.
20. A. G. Derneryd, " Linear Microstrip Array Antenna", Chalmer Univ. Technol., Goteborge, Sweden, Tech. Report, TR 7505, 1975.

21. J. R. James and C. J. Wilson, "Microstrip antennas and arrays Part-I: Fundamental action and limitations", IEE Proc. Microwaves Opt. and Antennas, vol.1, pp. 165-174, 1977.
22. Y. T. Lo, D. Solomon and W. F. Richards, "Theory and Experiments on Microstrip Antennas", IEEE AP-S Symposium (Japan), pp. 53-55, 1978.
23. W. F. Richards, Y. T. Lo and D. D. Harrison, "Improved Theory for Microstrip Antennas", IEE Electron. Lett., vol. 15, pp. 42-44, 1979.
24. Y. T. Lo, D. Solomon and W. F. Richards, "Theory and Experiments on Microstrip Antennas", IEEE Trans. Antennas Propagat., vol. AP-27, pp.137-145, 1979.
25. P. K. Agarwal and M. C. Bailey, "An Analysis Technique for Microstrip Antennas", IEEE Trans. Antennas Propogat., vol. AP-25, pp. 756-759, 1977.
26. K. R. Carver, "A Modal Expansion Theory for the Microstrip antenna", Dig. Int. Symp. Antennas Propogat., Seattle, WA, pp. 101-104, 1979.
27. K. R. Carver and E. L. Coffey, "Theoretical Investigation of the Microstrip Antenna", Tech. Rept. PT 00929, Physical Science Lab., New Mexico State Univ., Las Cruces, 1979.
28. E. L. Coffey and T. H. Lehman, "A New Analysis Technique for Calculating and Self and Mutual Impedance of Microstrip Antennas", Proc. Workshop on Printed Circuit Antennas, New Mexico State Univ., pp.31/1-21, 1979.

29. E. O. Hammerstad, "Equations for Microstrip Circuit Design", Proc. 5th European Microwave Conf., Hamburg, pp. 268-272, 1975.
30. N. G. Alexopoulos and I. E. Rana, " Mutual Impedance Computation Between Printed Dipoles", IEEE Trans. Antennas Propog., vol. AP-29, pp. 106-111, 1981.
31. E. L. Newman, "Strip antennas in a dielectric slab", IEEE Trans. Antennas Propog., vol. AP-26, pp. 647-653, 1978.
32. E. L. Newman and D. M. Pozar, "Electromagnetic modeling of composite wire and surface geometries", IEEE Trans. Antennas Propog., vol. AP-26, pp. 784-787, 1978.
33. P. Hammer, D. Van Bouchante, D. Verschraevan and A. Van de Capelle, "A model for calculating the radiation field of microstrip antennas", IEEE Trans. Antennas Propog., vol. AP-27, pp. 267-270, 1979.
34. J. W. Mink, "Circular ring microstrip antenna elements", IEEE Antennas Propog. Soc. Int. Symp., Quebec City, Canada, June 1980.
35. R. Chadha and K. C. Gupta, "Green's functions for circular sectors, annular rings, and annular sectors in planar microwave circuits", IEEE Trans. Microwave Theory Tech., vol. MTT-29, pp. 68-71, Jan 1981.
36. J. R. Mosig and F. E. Gardiol, "The Near Field of an Open Microstrip structure", IEEE AP-S, Int. Symp. Digest., pp. 379-381, 1979.
37. E. F. Kuester, R.T. Johak, and D.C. Chang, "The Thin Substrate Approximation for Reflection from the End of the Slab Loaded Parallel

- Plate Wave Guide with Application to Microstrip patch”, IEEE Trans. Antennas Propagat., vol. AP-30, pp. 910-917, 1982.
38. I. J. Bahl, P. Bhartia, and S.S. Stuchly, “Design of a Microstrip Antenna Covered with a Dielectric Layer”, IEEE Trans. Antennas Propogat., vol. AP-30, pp. 314-318, 1982.
 39. N. G. Alexopoulos, N. K. Uzunoglu and I. E. Rana, “Radiation by Microstrip Patches”, Dig. Int. Symp. Antennas Propogat., pp. 722-727, 1979.
 40. Y. T. Lo and W. F. Richards, “Perturbation Approach to the Design of Circularly Polarized Microstrip Antennas” Electron. Lett., vol. 17, pp. 383-385, 1981.
 41. A. Henderson and J. R. James, “Design of Microstrip Antenna feeds – Part 1, Estimation of Radiation Loss and Implications”, IEE Proc., vol. 128, Pt.H, pp.19-25, 1981.
 42. P. S. Hall and J. R. James, “Design of Microstrip Antenna Feeds Part 2, Design and Performance Limitations of Triplate corporate feeds”, IEE Proc., vol. 128, Pt.H, pp 26-33, 1981
 43. D. H. Schaubert, F.G. Farrar, A. R. Sindors and S.T. Hayes, “Microstrip Antenna with Frequency Agility and Polarisation Diversity”, *ibid.*, pp. 118-123, 1981.
 44. K. Araki and T. Itoh, “Hankel Transform Domain Analysis of Open Circular Microstrip Radiating Structures”, *ibid.*, pp. 84-89, 1981.

45. T. Itoh and W. Mentzel, "A Full Wave Analysis method for Open Microstrip structures", *ibid.*, pp. 63-67, 1981.
46. J. H. Dahelle and A. L. Cullen, "Electric Probe Measurements on Microstrip", *IEE Trans. On Microwave Theory and Techniques*, vol. MTT-28, No. 7, pp. 752-755, July 1980
47. S. A. Long, L. C. Shen, M. D. Walton, and M. R. Allerding, "Impedance of a Circular Disc Printed Circuit Antenna", *Electron Lett.*, vol. 14, pp. 684-686, 1978.
48. L. C. Shen, S. A. Long, M. R. Allerding, and M. D. Walton, "Resonant Frequency of a Circular Disc Printed Circuit Antenna", *IEEE Trans. Antenna Propagat.*, vol. AP-25, pp 595-596, 1977.
49. L. C. Shen, "The Elliptical Microstrip Antenna with Circular Polarisation", *IEEE Trans. Antenna Propagat.*, vol. AP-29, pp 95-99, 1981.
50. A. G. Derneryd, "Analysis of the Microstrip Disc Antenna Element", *IEEE Trans. Antennas Propogat.*, vol. AP-27, pp. 660-664, 1979.
51. S. N. Das and S. K. Choudhary, "Rectangular Microstrip Antenna on a Ferrite Substrate", *IEEE Trans. Antennas Propogat.*, vol. AP-30, pp. 499-502, 1982.
52. J. L. Kerr, "Microstrip Polarization Techniques", in *Proc. Antenna Application Symposium, Allerton Park, IL, September 1978.*
53. W. C. Wilkinson, "A Class of Printed Circuit Antennas", in *Digest. Int. Symp. Antennas Propogat. Soc., Atlanta, GA, pp. 270-273, June 1974.*

54. Mohammed A Sultan and Vijay K Tripathi, "The mode features of an annular sector microstrip antenna", IEEE Transactions on Antennas and Propagation, vol. 38, No.2, pp. 265-269, February 1990.
55. J. L. Volakis and J. M. Jin, "A scheme to lower the resonant frequency of the microstrip patch antenna", IEEE Microwave and Guided Wave Lett., vol.2, pp.292-293, July 1992.
56. E. K. N. Yung, W. W. S. Lee and K. M. Luk, "A Dielectric Resonator on a microstrip antenna", IEEE Antennas Propogat. Int. Symp. Michigan, pp. 1504-1507, June 1993.
57. V. Palanisamy and R. Garg, "Rectangular ring and H-shaped microstrip antennas- alternatives to rectangular patch antenna", IEE Electron. Lett., vol. 21, No. 19, pp. 874-876, 1985.
58. G. Kossiavas, A. Papiernik, J. P. Boisset, and M. Sauvan, "The C-Patch: A Small Microstrip Element", IEE Electron. Lett., vol. 25, No. 4, pp. 253-254, 1989.
59. Supriyo Dey, C. K. Aanandan, P. Mohanan, and K. G. Nair, "A New Compact Circular Patch antenna", IEEE Antennas Propogat. Soc. Int. Symp., Washington, pp. 822-825, June 1994.
60. Y. Hwang, Y. P. Zhang, G. X. Zheneg and T. K. C. Lo, " Planar Inverted F Antenna loaded with high permittivity material", IEE Electron. Lett., vol. 31, pp. 1710-1712, 1995.
61. S. Dey, S. Chebolu, R. Mittra, I. Park, T. Kobayashi and M. Itoh, "A Compact Microstrip Antenna for CP", IEEE Antennas Propogat. Soc. Int. Symp., California, pp. 982-985, June 1995.

62. M. G. Douglas and R. H. Johnston, "A Compact two way Diversity Microstrip U-Patch Antenna", IEEE Antennas Propogate. Soc. Int. Symp., California, pp. 978-981, June 1995.
63. Mohamed Sanad, "Double C-patch Antennas having different Aperture shapes", IEEE Antennas Propogate. Soc. Int. Symp., California, pp. 2116-2119, June 1995.
64. Jacob George, P. Mohanan and K. G. Nair, "A Broadband Low Profile Microstrip Circular patch Antenna", IEEE Antennas Propogate. Soc. Int. Symp., California, pp. 700-703, June 1995.
65. R. Waterhouse, "Small Microstrip Patch antenna", IEE Electron. Lett., vol. 31, No. 8, pp.604-605, 1995.
66. M. Sanad, "A Compact Dual-Broadband Microstrip Antenna having both Stacked and planar Parasitic Elements", IEEE Antennas Propogate. Soc. Int. Symp., Maryland, pp.6-9, July 1996.
67. K. L. Wong and S. C. Pan, "Compact Triangular Microstrip Antenna", IEE Electron. Lett., vol.33, No.6, pp. 433-434, 1997.
68. K. L. Wong and W. S. Chen, "Compact Microstrip Antenna with dual frequency operation", IEE Electron. Lett., vol.33, No.8, pp. 646-647, 1997.
69. K. L. Wong and Y. F. Lin, "Small Broadband Rectangular Microstrip Antenna with Chip-Resistor Loading", Electron. Lett., vol.33, No. 9, pp. 1593-1594, 1997.

70. C. L. Tang, H. T. Chen and K. L. Wong, "Small Circular Microstrip Antenna with Dual Frequency Operation", *Electron. Lett.*, vol.33, No. 13, pp. 1112-1113, 1997.
71. R. B. Waterhouse, "Printed Antenna suitable for Mobile Communication Handsets", *Electron. Lett.*, vol.33, No. 22, pp. 1831-1832,1997.
72. K. L. Wong and J. Y. Wu, "Single feed small circularly polarized square microstrip antenna", *Electron. Lett.*, vol. 33, No. 22, pp. 1833-1834, 1997.
73. K. L. Wong and K. P. Yang, "Small dual frequency microstrip antenna with cross slot" *Electron. Lett.*, vol.33, No.23, pp 1916-1917, 1997.
74. J. H. Lu, C. L. Tang and K. L. Wong, "Slot-Coupled Small Triangular Microstrip antenna", *Microwave Optical Technol. Lett.*, vol.16, No.6, pp.371-374, Dec. 1997.
75. S. K. Satpathy, K. P. Ray, and G. Kumar, "Compact shorted variations of circular microstrip antennas", *IEE Electron. Lett.*, vol. 34, No.2, pp.137-138, January 1998.
76. C.Y. Huang, J. Y. Wu, C. F. Yang and K. L. Wong, "Gain-enhanced Compact Broadband Microstrip Antenna", *IEE Electron. Lett*, vol. 34, No.2, pp.138-139, January 1998.
77. A. S. Vaello and D. S. Hernandez, "Printed Antennas for dual-band GSM/DCS 1800 Mobile Handsets", *IEE Electron. Lett.*, vol. 34, No. 2, pp. 140-141, January 1998.

78. C. Salvador, L. Borselli, A. Falciani and S. Maci, "Dual frequency planar antenna at S and X bands", IEE Electron. Lett., vol.31, pp. 1706-1707,1995.
79. H. Iwasaki and Y. Suzuki, "Electromagnetically Coupled Circular Patch Antenna Consisting of Multilayered configuration", IEEE Trans. Antennas Propog., vol. AP-44, No.6, pp.777-780, June 1996.
80. H. Nakano and K.Vichien, "Dual frequency square Patch antenna with Rectangular Notch", IEE Electron. Lett., vol.25, No. 16, pp.1067-1068, August 1989.
81. Kin-Lu Wong and Kai-Ping Yang, "Modified Planar Inverted F Antenna", IEE Electron. Lett., vol. 34, No. 1, pp.7-8, January 1998.
82. J. George, M. Deepukumar, C. K. Aanandan, P. Mohanan and K. G. Nair, "New Compact Microstrip Antenna", IEE Electron. Lett., vol.32, No. 6, pp.508-509, March 1996.
83. D. Singh, P. Gardiner and P. S. Hall, "Miniaturized antenna for MMIC Applications", IEE Electronic Letters, vol.33, No.22, pp. 1830-1831, 1830.
84. T. Hyunh, K. F. Lee and R. Q. Lee, "Cross Polarization Characteristics of Rectangular Patch Antennas", IEE Electron. Lett., vol. 24, No. 8, pp. 463-464, April 1988.
85. K. F. Lee, K. M. Luk and P. Y. Tam, "Cross Polarisation Characteristics of Circular Patch Antennas", IEE Electron. Lett., vol.28, No. 6, pp. 587-589, March 1992.

86. F. Carrez and J. Vindevoghel, "Compact Two-Port Microstrip Antenna", IEE Electron. Lett., vol.32, No. 15, pp.1337-1338, July 1996.
87. R. Chair, K. M. Luk and K.F. Lee, "Small Dual Patch Antenna", IEE Electron. Lett., vol.35, No. 10, pp.762-764, May 1999.
88. Z. D. Liu and P. S. Hall, "Dual-band Antenna for Hand Held Portable Telephones", IEE Electron. Lett., vol.35, No. 10, pp.762-764, May 1999.
89. L. Zaid, G. Kossiavas, J. Y. Dauvignac and A. Papiernik, "Very Compact Double C-Patch Antenna", IEE Electron. Lett., vol.34, No. 10, pp.933-934, May 1998.
90. E. Lee, P. S. Hall and P. Gardiner, "Compact Dual-Band Dual-Polarisation Microstrip Patch Antenna", IEE Electron. Lett., vol.35, No. 13, pp.1034-1036, June 1999.
91. J. George, K. Vasudevan, P. Mohanan and K. G. Nair, "Dual Frequency Miniature Microstrip Antenna", IEE Electron. Lett., vol.34, No. 12, pp.1168-1170, June 1998.
92. G. P. Srivastava, S. Bhattacharya and S. K. Padhi, "Dual Band Tunable Microstrip Patch Antenna", IEE Electron. Lett., vol.35, No. 17, pp.1397-1399, August 1999.
93. Kin-Lu Wong and Ming-Huang Chen, "Small Slot-Coupled Circularly-Polarized Microstrip Antenna with modified Cross-Slot and Bent Tuning-Stub", IEE Electron. Lett., vol.34, No. 16, pp.1542-1543, August 1998.
94. Jui-Han Lu, Hung-Chin Yu and Kin-Lu Wong, "Compact Circular Polarization design for Equilateral-Triangular Microstrip Antenna with

- Spur Lines”, IEE Electron. Lett., vol.34, No. 21, pp.1989-1990, October 1998.
95. Kin-Lu Wong and Wen-Shan Chen, “Slot-Loaded Bow-Tie Microstrip Antenna for Dual-Frequency Operation”, IEE Electron. Lett., vol.34, No. 18, pp.1713-1714, September 1998.
 96. Kin-Lu Wong and Jian-Yi Wu, “Bandwidth Enhancement of Circularly Polarized Microstrip Antenna using Chip- Resistor Loading”, IEE Electron. Lett., vol.33, No. 21, pp.1749-1750, October 1997.
 97. Kin-Lu Wong and Jia-Yi Sze, “Dual-Frequency Slotted Rectangular Microstrip Antenna”, IEE Electron. Lett., vol.34, No. 14, pp.1368-1370, July 1998.
 98. Jui-Han Lu, “Single-Feed Dual-Frequency Rectangular Microstrip Antenna with pair of Step-Slots”, IEE Electron. Lett., vol.35, No. 5, pp.354-355, March 1999.
 99. D. Sanchez-Hernandez, G. Passiopoulos, M. Ferrando, E.de los Reyes and I. D. Robertson, “Dual-Band Circularly Polarized Antenna with a Single Feed”, IEE Electron. Lett., vol.32, No. 25, pp.2296-2298, December 1996.
 100. N. Chiba, T. Amano and H. Iwasaki, “Dual-Frequency Planar Antenna for Handsets”, IEE Electron. Lett., vol.34, No. 25, pp. 2362-2363, December 1998.
 101. K. M. Luk, R. Chair and K. F. Lee, “Small Rectangular Patch Antenna”, IEE Electron. Lett., vol.34, No. 25, pp. 2366-2367, December 1998.

102. Kin-Lu Wong and Yi-Fang Lin, "Circularly Polarized Microstrip Antenna with a Tuning Stub", IEE Electron. Lett., vol.34, No. 9, pp.831-832, April 1998.
103. D. H. Schaubert and F. G. Farrar, "Some Conformal Printed Circuit Antenna Designs", in Proc. Workshop Printed Circuit Antenna Tech., New Mexico State Univ., Las Cruces, pp. 5/1-21, October 1979.
104. C. Wood, "Improved Bandwidth of Microstrip Antenna Using Parasitic Elements", IEE Proc., Pt.H, vol.127, pp.231-234, 1980.
105. C. K. Aanandan and K. G. Nair, "Compact Broadband Microstrip Antenna", IEE Electron. Lett. Vol. 22, No. 20, pp. 1064-1065, 1986.
106. D. R. Poddar, J. S Chatterjee and S. K. Choudhary, "On Some Broad Band Microstrip Resonators", IEEE Trans. Antennas Propogate., vol. AP-31, pp. 193-194, 1983.
107. A. G. Derneryd and I. Karlsson, "Broadband Microstrip Antenna Element and Array", IEEE Trans. Antennas Propogate., vol.AP-24, pp.140-141, 1981.
108. N. Das and J. S. Chatterjee, "Conically Depressed Microstrip Patch Antenna", IEE Proc., Pt.H, vol.130, pp. 193-196, 1983.
109. L. Jeddari, K. Mahdjoubi, C. Terret and J.P. Daniel, "Broadband Conical Microstrip Antenna", Electron. Lett., vol. 21, pp. 896-898, 1985.
110. V. N. Pandharipande and K. G. Verma, "Wide Band Microstrip Patch Array at X-band", J.Inst.Elec.Telecom.Eng., vol.29, pp. 497-500, 1983.

111. P. S. Bhatnagar, J. P. Daniel, K. Mahadjoubi and C. Terret, "Hybrid Edge, Gap and Directly Coupled Triangular Microstrip Antenna", *Electron. Lett.*, vol.22, pp. 853-855, 1986.
112. P. S. Bhatnagar, J. P. Daniel, K. Mahadjoubi and C. Terret, "Experimental Study on Stacked Microstrip Antennas", *Electron. Lett.*, vol.22, pp.864-865, 1985.
113. C. Wood, "Curved Microstrip Lines as Compact Wideband Circularly Polarized Antennas", *IEE J. MOA*, vol.126, pp.5-13, 1979.
114. P. S. Hall, C. Wood and C. Garrek, "Wide Bandwidth Microstrip Antennas for Circuit Integration", *IEE Electron. Lett.*, vol.15, pp. 458-460, 1970.
115. A. Sabban, "A New Broadband Stacked Two Layer antenna", *Dig. Int. Symp. Antennas and Propogat.*, vol.1, pp. 63-66, May 1983.
116. T. Hori and N. Nakagima, "Broad Band Circularly Polarized Array Antenna with Coplanar Feed", *Trans. Inst. Electron. and Commun. Eng., Jpn, Part B*, vol. J 68B, pp. 515-522, 1985.
117. C. J. Prior and P. S. Hall, "Microstrip Disc Antenna with a Short-Circuited Annular Ring", *Electron. Lett.*, vol.21, pp. 719-721, 1985.
118. K. M. Luk, C. L. Mak, Y. L. Chow and K. F. Lee, "Broadband Microstrip Patch Antenna", *IEE Electron. Lett.*, vol. 34, No. 15, pp. 1442-1443, July 1998.

119. M. Deepukumar, J. George, C. K. Aanandan, P. Mohanan and K. G. Nair, "Broadband Dual Frequency Microstrip Antenna", IEE Electron. Lett., vol. 32, No. 17, pp. 1442-1443, August 1996.
120. Yeunjeong Kim, Wansuk Yun and Youngjoong Yoon, "Dual-Frequency and Dual Polarisation Wideband Microstrip Antenna", IEE Electron. Lett., vol. 34, No. 15, pp. 1442-1443, July 1998.
121. W. K. Lo, C. H. Chan and K. M. Luk, "Circularly Polarized Patch Antenna Array Using Proximity-Coupled L-Strip Line Feed", IEE Electron. Lett., vol. 36, No. 14, pp. 1174-1175, July 2000.
122. Chih- Yu Huang, Jian-Yi Wu, Cheng-Fu Yang and Kin Lu Wong, "Gain-Enhanced Compact Broadband Microstrip Antenna", IEE Electron. Lett., vol. 34, No. 2, pp. 138-139, January 1998.
123. Kin-Lu Wong and Jian-Yi Wu, "Bandwidth Enhancement of Circularly Polarised Microstrip Antenna Using Chip Resistor Loading", IEE Electron. Lett., vol. 33, No. 21, pp. 1749-1750, October 1997.
124. Y. X. Guo, K. M. Luk, K.F. Lee and Y.L. Chow, "Double U-Slot Rectangular Patch Antenna", IEE Electron. Lett., vol. 34, No. 19, pp. 1805-1809, September 1998.
125. K. M. Luk, Y. X. Guo, K. F. Lee and Y.L. Chow, "L- Probe Proximity Fed U-Slot Patch Antenna", IEE Electron. Lett., vol. 34, No. 19, pp. 1806-1807, September 1998.
126. R. B. Waterhouse, "Broadband Stacked Shorted Patch", IEE Electron. Lett., vol. 35, No. 2, pp. 138-139, January 1999.

127. K. P. Ray and G. Kumar, "Multi-Frequency and Broadband Hybrid-Coupled Circular Microstrip Antennas", IEE Electron. Lett., vol. 33, No. 6, pp. 437-438, March 1997.
128. Kin-Lu Wong and Jen-Yea Jan, "Broadband Circular Microstrip antenna with Embedded Reactive Loading", IEE Electron. Lett., vol. 34, No. 19, pp. 1804-1805, September 1998.
129. B. L. Ooi and C. L. Lee, "Broadband Air-Filled Stacked U-slot Patch Antenna", IEE Electron. Lett., vol. 35, No. 7, pp. 515-517, April 1999.
130. Chih-Yu Huang, Jian-Yi Wu and Kin-Lu Wong, "Slot-Coupled Microstrip antenna for Broadband Circular Polarisation", IEE Electron. Lett., vol. 34, No. 9, pp. 835-836, April 1998.
131. Kin Lu Wong and Wen Hsiu Hsu 'Broadband Triangular Microstrip Antenna with U-shaped Slot', IEE Electron. Lett., Vol. 33, No. 25, pp. 2085-2086, 1997.
132. Jia-Yi Sze and Kin Lu Wong, 'Broadband Rectangular Microstrip Antenna with pair of toothbrush-shaped slots', IEE Electron. Lett., vol. 34, No. 23, pp. 2186-2187, November 1998.
133. W. C. Chew, "A Broad Band Annular Ring Microstrip Antenna", IEEE Trans. Antennas Propogat., vol.AP-30, pp. 918-922, 1982

INDEX

| | | | |
|-----------------------------|-------------------|-------------------------------------|--------------|
| Agarwal | 20 | Gain | 15,43,63,70 |
| Anechoic Chamber | 37 | Giardiol | 21 |
| Antennas | | Ground Plane | 1,2 |
| Dipole | 1 | Gulton | 19 |
| Loop | 1 | Hammerstad | 20 |
| Microstrip | 1 | Hammer | 21 |
| Printed circuit | 1 | Henderson | 22 |
| Antenna Efficiency | 65,66 | Howell | 1,19 |
| Aperture Coupled Antenna | 8 | IE3D | 63 |
| Araki | 22 | Impedance Bandwidth | 67 |
| Arrow Shaped antenna | 52,53,59 | Incident Power | 65,66 |
| Axial Ratio | 45,77 | Intelligent Vehicle Highway systems | 1 |
| Bahl | 21 | Interference | 108 |
| Bailey | 20 | Isolation | 108,131 |
| Bandwidth | 6, 10,41,52,85,98 | Itoh | 22 |
| Bassinot | 19 | James | 20 |
| Byron | 19 | Kuester | 21 |
| CURVIEW | 45 | Lewin | 19 |
| Carver | 20 | Line Extension factor | 121 |
| Cavity model | 115 | Lo | 20,22 |
| Coffey | 20 | Loss tangent | 10 |
| Coaxial feeding | 53 | MERL Soft | 43 |
| Compactness | 70 | MGRID | 45 |
| Conformal Antennas | 10 | MODUA | 45 |
| Cross Coupling | 108 | Magnetic Current Distribution | 13 |
| Cross Talk | 2,16, 52,108,131 | Menzel | 22 |
| Derneryd | 19 | Microstrip | |
| Deschamps | 1,19 | Patch Antenna | 4,11 |
| Design equations | 59, 115 | Slot Antenna | 11 |
| Dielectric constant | 4 | Travelling Wave Antenna | 11 |
| Dielectric Constant | 4,53 | Munson | 1 |
| Dielectric Substrate | 4 | Microwave Antenna | 6 |
| Dimensional Stability | 10 | Microwave Integrated Circuit | 6 |
| Directivity | 15 | MMIC | 15 |
| Dual frequency | 6,13, 52,53 | Modes of operation | |
| Dual Port Geometry | 16,108,131 | TM_{10} | 13, 14,55,85 |
| Effective Resonating length | 121 | TM_{01} | 13, 14,55,85 |
| Effective permittivity | 121 | TM_{60} | 93,100,138 |
| Electromagnetic Simulation | 15 | TM_{06} | 85,138 |
| Electromagnetic Coupling | 73 | TM_{20} | 13, 14 |
| Embedded Rectangular Slot | 85, 138 | Mode Verification | 135,138 |
| Excitation Techniques | | Mosig | 21 |
| Aperture Coupled feed | 8,9 | Mink | 21 |
| Coaxial feed | 7,9,53 | Munson | 1 |
| Microstrip Feed | 8,9 | Network Analyzer | 37 |
| Proximity Coupled Feed | 8,9,131 | Non Radiating Edge | 138 |
| FDTD | 15 | PATTERN VIEW | 45 |
| FIDELITY | 15 | Paging | 7 |
| Frequency design | 63 | Permittivity | 59 |
| Frequency ratio tuning | 72,86 | Phased Array Radar | 6 |
| Fringe fields | 4.5, 118 | Photo Lithographic Technique | 39 |

| | |
|-------------------------|------------|
| Planar | 1, 2 |
| Printed Structures | |
| Coplanar line | 2, 3 |
| Finline | 2, 3 |
| Inverted line | 2, 3 |
| Microstrip Line | 2, 3 |
| Slot Line | 2, 3 |
| Strip Line | 2, 3 |
| Suspended line | 2, 3 |
| Polarization | |
| Circular | 6,74,77,81 |
| Diversity | 16,74 |
| Linear | 6,74,77,81 |
| Orthogonal | 86 |
| Tracking | 77 |
| Radiation | 4 |
| Radiating edge | 93 |
| Radiation Efficiency | 65,66 |
| Radiation Pattern | 13,45,67 |
| Radiated Power | 65,66 |
| Relative gain | 70 |
| Resonant Frequency | 13,41, 55 |
| Return Loss | 41, 67 |
| Richards | 22 |
| S-Parameter Test Set | 37 |
| Sanford | 19,22 |
| Satellite Communication | 6, 15 |
| Schaubert | 22 |
| Shorting pin | 6 |
| Simulation Packages | |
| Fidelity | 15 |
| IE3D | 45,135 |
| Slanted lengths | 53 |
| Slot loading | 6,85 |
| Stubs | 6 |
| Substrate | 10 |
| Superstrate | 70 |
| VSWR | 67 |
| Waves in Microstrip | |
| Guided Waves | 2, 3 |
| Leaky Waves | 2, 3 |
| Space Waves | 2, 3 |
| Surface Waves | 2, 3 |
| Wilson | 20 |

LIST OF PUBLICATIONS

INTERNATIONAL JOURNALS

1. **M. Paulson**, S.O. Kundukulam, C. K. Aanandan and P. Mohanan, **IEE Electronics Letters**, "Resonance frequencies of compact microstrip antenna", Vol. 37, No. 19, September 2001, pp 1151- 1153.
2. S.O. Kundukulam, **M. Paulson**, C. K. Aanandan, P. Mohanan, and K. Vasudevan, **Microwave and Optical Technology Letters**, "Dual band dual polarized compact microstrip antenna", Vol. 25, No. 5, June 5 2000, pp 328-330
3. **M. Paulson**, S.O. Kundukulam, C. K. Aanandan, P. Mohanan, and K. Vasudevan, **Microwave and Optical Technology Letters**, "Circularly Polarized compact microstrip antenna", Vol. 26, No. 5, September 5 2000, pp 308-309
4. **M. Paulson**, S.O. Kundukulam, C. K. Aanandan and P. Mohanan, **Microwave and Optical Technology Letters**, "A new compact dual-band dual-polarized microstrip antenna", Vol. 29, No. 5, June 5 2001, pp 315-317
5. S.O. Kundukulam, **M. Paulson**, C. K. Aanandan and P. Mohanan, **Microwave and Optical Technology Letters**, "Slot loaded compact microstrip antenna for dual frequency operation", Vol. 31, No. 5, December 5 2001, pp 379-381
6. **M. Paulson**, S.O. Kundukulam, C. K. Aanandan and P. Mohanan, **Microwave and Optical Technology Letters**, "Analysis and design of a dual port compact microstrip antenna", Vol. 32, No. 2, January 20 2002, 125-127
7. Sona O Kundukulam, **Manju Paulson**, C.K. Aanandan and P. Mohanan, **International Journal of RF and Microwave Computer Aided Engineering**, "Analytical Equations for Compact Dual Frequency Microstrip Antenna" (Accepted for Publication)
8. Sona O Kundukulam, **Manju Paulson**, C.K. Aanandan and P. Mohanan, **Microwave and Optical Technology Letters**, "Compact Circular Sided Microstrip Antenna for Circular Polarisation", (Accepted)

INTERNATIONAL SEMINARS/ SYMPOSIA

1. **Manju Paulson**, Sona O Kundukulam, C. K. Aanadan and P. Mohanan, **IEEE AP Symposia 2002**, "Compact Arrow Shaped Antenna with Embedded Rectangular Slot for Dual Frequency Dual Polarisation Operation", June 16th to 21st at Texas, (Accepted)
2. Sona O Kundukulam, **Manju Paulson**, C. K. Aanadan, P. Mohanan and K. Vasudevan, **IEEE AP Symposia 2002**, "A Circular sided compact microstrip antenna", June 16th to 21st at Texas (Accepted)

NATIONAL SEMINARS/ SYMPOSIA

1. **Manju Paulson**, Sona O Kundukulam, C. K. Aanandan and P. Mohanan, "*New Compact microstrip antenna for dual frequency operation*" **Proceedings on National Symposium on Antennas and Propagation (APSYM-2000)**, 6-8 December, Cochin, pp.94-97, 2000.
2. Sona O Kundukulam, **Manju Paulson**, C. K. Aanandan and P. Mohanan, "*Dual frequency dual polarized crescent-shaped microstrip antenna*" **Proceedings on National Symposium on Antennas and Propagation (APSYM-2000)**, 6-8 December, Cochin, pp.90-93, 2000.
3. Sona O Kundukulam, **Manju Paulson**, C. K. Aanandan and P. Mohanan, "*Dual port dual polarized microstrip antenna*" Nov 2-4, **Microwave-2001 Symposium proceedings**, Jaipur, pp 11-13
4. **Manju Paulson**, Sona O Kundukulam, C. K. Aanandan and P. Mohanan, "*Arrow-Shaped Microstrip Antenna for Broadband Operation*" **Proceedings on National Conference on Communication (NCC 2002)**, 25-27 January, Indian Institute of Technology, Bombay, pp 210- 213
5. **Manju Paulson**, Sona O Kundukulam, C. K. Aanandan and P. Mohanan, "*Compact Dual band Microstrip Antenna with slots on its radiating edges*" **Proceedings on Microwave Measurement Techniques and Applications (MMTA 2002)**, 4-6 February, Jawaharlal Nehru University, Delhi, 2002.
6. Sona O Kundukulam, **Manju Paulson**, C. K. Aanandan and P. Mohanan, "*Design and Analysis of Circular sided Microstrip Antenna*" **Proceedings on Microwave Measurement Techniques and Applications (MMTA 2002)**, 4-6 February, Jawaharlal Nehru University, Delhi, 2002.



RESUME OF THE CANDIDATE

MANJU PAULSON

Permanent Address

(W/o) Henry Paul
Panakkal House
P.O. Puthenpalli,
Mammiyur 680 103
Kerala, India

Phone:91 487 554275
Email:manjuhenry@yahoo.com

Present Address

Senior Research Fellow
Department of Electronics
Cochin University of Science and Technology
Cochin 682 022
Kerala, India

Phone:91 484 576418

Objective

*To involve in the **research works in Microwave Electronics** with special interest to microstrip antennas, microwave communication, microwave devices etc.*

*Research and development activities in fields related to **Digital/Microwave Electronics***

EDUCATION

- a) **Ph. D in Microwave Electronics** Thesis submitted in May 2002
- b) **Master of Science in Electronics** Cochin University of Science and Technology (May 1998)
- c) **Bachelor of Science in Physics** Calicut University (June 1995)

COMPUTER PROFICIENCY

Programming Languages Visual Basic, Basic, Foxpro, Visual C++, C++, C, Visual Foxpro, LISP, Matlab

Simulation Softwares IE3D, FIDELITY.

AWARDS OBTAINED

Council of Scientific and Industrial Research, Government of India awarded direct **Senior Research Fellowship** in January 2002